UNIVERSITY OF PÉCS

Doctoral School of Chemistry

Kinetics and Mechanism of the Reactions of Pentathionate Ion by Different Halogen-Containing Oxidizing Agents

Ph.D. dissertation

Li Xu

supervisor:

Dr. Attila Horváth

associate professor

Pécs, 2014

Contents

Chapter 1

Introduction

Polythionates ($S_xO_6^{2-}$, $x \geq 3$), also known as polysulfane disulfonic acids or polysulfane disulfonates, are sulfur-based molecules in which a sulfur chain is terminated at both end by SO_3^- groups.[1–3] These compounds, in particular trithionate, tetrathionate, pentathionate and hexathionate are important intermediates in redox transformation of sulfur containing compounds in several environmentally or industrially important processes and the metabolism of sulfur–oxidizing and sulfur–reducing microorganisms.[4–10] A review[11] and recent advances[12,13] in the sampling and analysis of sulfur-oxygen species including polythionates have facilitated their direct identification and study in many environments. A notable application of polythionates is the formation of copper sulfide, Cu_xS thin film on the polyamide surface, markedly promoting the optoelectrical efficiency of transportation, where polythionate is used as a precursor of polymer sulfurization in acidic conditions as a result of its polysulfur chain.[14,15] In a thermal spring in Yellowstone National Park, Xu *et al.*[9] reported that polythionate was formed via thiosulfate oxidation in presence of pyrite and polythionate decomposes either by reaction with H_2S or through hydrolysis. Takano *et al.*[16] have reported that polythionates were detected within sulfur globules in a crater lake and as part of the structure of microbially formed sulfur globules.[8] Changes in polythionate concentrations by reaction with aqueous H_2S and SO_2 discharged through vents may serve as an indicator of imminent volcanic eruptions.[17]

The oxidation of metal sulfide minerals generates acidic, metal rich fluids. At many locations worldwide, mining of pyrite(FeS_2)-rich deposits has increased oxidative dissolution and led to the formation of environmentally damaging solutions

known as acid mine drainage (AMD).[3] Many researches have indicated that pyritic sulfur may be oxidized through different pathways in the environment and thiosulfate, $S_2O_3^{2-}$, has been proposed to be a leaving group in the procedure of the oxidation.[18–22] Polythionates can then be formed during the subsequent oxidation of thiosulfate. Observation of pyrite oxidation in experimental and natural settings has shown that thiosulfate and polythionates can be determined at neutral pH as well as at lower pHs, but significantly more is produced at neutral pH than at low pH,[7,18,20,23,24] which means that understanding the reactivity of the polythionates may contribute to the understanding of the governing pathways of pyrite oxidation under different conditions.

As we know, cyanidation process was used in leaching of copper, silver, gold and other noble metals from their ores beside the fact that the toxicity of cyanide has long been known. Recently, there are considerable efforts to find alternative and less harmful processes to exchange the cyanidation technology. Thiosulfate solution, as a nontoxic alternative, seems to be a promising opportunity to replace that cyanidation process. The recovery of noble metals using thiosulfate was first proposed early in the 1900s.[25] After late 1970's, an atmospheric ammoniacal thiosulfate leach system to recover gold and silver from copper-bearing metal sulfides concentrates and pressure leach residues was developed.[26,27] Later, it was patented to a conventional thiosulfate process which was carried out under alkaline conditions with employing copper salt as the oxidant and ammonia to stabilize the copper. Numerous studies have been conducted on the thiosulfate-copper-ammonia process and several reviews about it were reported.[28,29] However, a number of problems arose during the procedure of thiosulfatolysis process. One of them is the generation of polythionates from oxidation of thiosulfate by copper(II), which is detrimental to the subsequent metal recovery process with ion-exchange resin. In addition, the ammonia used in alkaline conditions will increase many environmental problems.

Zhang *et al.*[30–32] have investigated the thiosulfate leaching process under neutral or slightly acidic conditions instead of alkaline condition using FeEDTA or oxalate(Fe-OX) as an oxidant. It was found that more polythionates including trithionate, tetrathionate, pentathionate and hexathionate can be produced from the oxidation of thiosulfate as a result of a general rearrangement of polythionates under neutral solutions:[33,34]

$$2\,S_xO_6^{2-} \rightarrow S_{x-1}O_6^{2-} + S_{x+1}O_6^{2-} (x > 3). \tag{1.1}$$

Furthermore this process is catalyzed by thiosulfate:[35–39]

$$S_xO_6^{2-} + S_2O_3^{2-} \rightleftharpoons S_{x+1}O_6^{2-} + SO_3^{2-} (x \geq 3). \tag{1.2}$$

Excess of thiosulfate, therefore, facilitates the formation of higher polythionates under neutral or slightly acidic conditions used for thiosulfate leaching processes. Since adsorption of polythionates on the ion-exchange site of resins becomes stronger as the sulfur chain increases,[40] it is crucial to remove polythionates from the leach prior to the ion-exchange process. A good understanding of kinetics and mechanism of formation and consumption of polythionates is therefore important for controlling the leaching process and for recovery of noble metals.

In an alkaline medium, degradation of polythionates seems to be a promising solution to remove the polythionates from the leaching process. The decomposition of polythionates in alkaline solutions has been studied since the beginning of last century. The researches by Naito *et al.*[41] and Rolia and Chakrabarti[42] have shown that the stability of polythionates in an alkaline medium increases with decreasing length of the sulfur chain. Therefore, the most stable polythionate is trithionate.* In case of trithionate, it is fairly stable toward decomposition under slightly alkaline condition (pH ≤ 9.0). When pH increases (pH ≥ 11), the disproportionation of trithionate proceeds according to the following equation:[41,42]

$$S_3O_6^{2-} + H_2O \longrightarrow S_2O_3^{2-} + SO_4^{2-} + 2\,H^+, \tag{1.3}$$

or at pH > 13,

$$2\,S_3O_6^{2-} + 6\,OH^- \longrightarrow S_2O_3^{2-} + 4\,SO_3^{2-} + 3\,H_2O, \tag{1.4}$$

an alternative route also appears.

The alkaline decomposition of tetrathionate has been investigated for several decades, it has been shown that the decomposition strongly depends on the alkalinity of the solution:[43–47]

pH = 8.9

$$2\,S_4O_6^{2-} \rightarrow S_3O_6^{2-} + S_5O_6^{2-} \tag{1.5}$$

pH = 11.5

$$2\,S_4O_6^{2-} + 6\,OH^- \rightarrow 2\,S_3O_6^{2-} + 5\,S_2O_3^{2-} + 3\,H_2O \tag{1.6}$$

*Actually dithionate is the most stable polythionate, but it is a "dead-compound" towards further oxidations.

Above pH = 12, the overall decomposition can be described by either of the following processes

$$2\,S_4O_6^{2-} + 6\,OH^- \rightarrow 2\,SO_3^{2-} + 3\,S_2O_3^{2-} + 3\,H_2O \tag{1.7}$$

$$4\,S_4O_6^{2-} + 10\,OH^- \rightarrow 2\,SO_4^{2-} + 7\,S_2O_3^{2-} + 5\,H_2O. \tag{1.8}$$

The study by Rolia and Chakrabart[42] in 1982 has shown that at high pH (10–12), the product, thiosulfate ion catalyzes the decomposition of tetrathionate and a rate equation of the consumption of tetrathionate was also proposed. Recent study by Zhang[48] indicated that there is no thiosulfate catalysis and the stoichiometry of the reaction is more complicated that was expected because of formation of sulfide ion during the course of decomposition. In 2004, Breuer and Jeffrey[49] reported that the decomposition was dramatically effected by the ionic strength of the solution and type of buffer used, which may be able to explain the differences in the previous studies. More recently, a comprehensive kinetic and mechanistic study in the pH range of 9.2–12.2 by Varga and Horváth[50] has shown that besides sulfite and sulfate, thiosulfate and trithionate are formed during the alkaline degradation process. The detailed kinetic model proposed by them showed that the product distribution was strongly effected by the pH, initial concentration of tetrathionate and the kinetic traces cannot be evaluated by assuming a single stoichiometry in contrast to the previous studies mentioned above.

Compared to trithionate and tetrathionate, notably less is known about the alkaline degradation of hexathionate and pentathionate. However, the detailed kinetics of decomposition of pentathionate[51] and hexathionate[52] have been investigated by Pan *et al.* by recently available experimental techniques, high–performance liquid chromatography (HPLC) and capillary electrophoresis (CE), and computational techniques based on previous studies on the decomposition of pentathionate[36,53] and reaction of hexathionate with nucleophilic reagents.[37,38] They provided a reasonable explanation about the trends observed in the alkaline decomposition of polythionates. The rate coefficients of the reactions between several nucleophilic agents and polythionates suggested a reasonable correlation against the electron density in the vicinity of the sulfur atom of the sulfur chain to be attacked. A plausible kinetic mechanism was suggested to take their experimental observations into account in which the initiating rate-determining step of the alkaline decomposition of polythionates that proceeds via breakage of the inner sulfur chain between β-

and γ-S atoms by the attack of γ-S of the sulfur chain in polythionates by hydroxide ion.

It is generally well-known that oxidations of thiosulfate ion by different oxidizing agents lead finally to sulfate ion via formation of different sulfur–containing intermediates (mainly polythionates with a considerably long half-lives). These reactions of thiosulfate, for example, with bromate, chlorite, iodate and periodate, exhibit several exotic nonlinear dynamical phenomena such as autocatalysis under batch condition,[54–57] bistability and complex periodic and aperiodic behavior[58–60] in a continuously stirred tank reactor (CSTR), and an appearance of varieties of different reaction-diffusion patterns (chemical waves and chemical reaction fronts) in unstirred system.[61–64] Recent investigations have been shown that not only chemical but also electrochemical oxidation of thiosulfate leads to the formation of higher polythionates.[40,65] Moreover, the kinetic studies of hydrogen peroxide–thiosulfate,[66] chlorite–thiosulfate,[67] and hypochlorous acid–thiosulfate[68] systems have clearly demonstrated that besides sulfate ion, polythionates such as trithionate, tetrathionate and pentathionate are also produced in detectable amounts. These intermediates will further react with the corresponding oxidants (such as chlorite, periodate, iodate *etc.*) and intermediates of corresponding oxidants (like hypochlorous and chlorine dioxide) sometimes displaying fascinating kinetics and may thus contribute to the appearance of a rich variety of kinetic phenomena[54,61–64,69–71] found experimentally in the oxidation of thiosulfate. Therefore, systematic investigation on the kinetics and mechanism of the oxidations of polythionates by different oxidants seems to be expected as a crucial part of the studies of oxidations of thiosulfate. A firm knowledge of the oxidation of polythionates may accelerate further researches on the kinetics and mechanism of oxidation of thiosulfate.

A series of reaction systems has been well-known to exhibit fascinating nonlinear phenomena. One of the well–established systems is chlorite–tetrathionate (CT) reaction, which was first studied by Nagypál and Epstein[72] in 1986 and it was showed that the reaction exhibits supercatalytic effect with respect to hydrogen ion. After observation of the appearance of cellular structures in the unstirred system by Tóth,[73] the CT–reaction has been showed a substantial role in studying several interesting nonlinear phenomena in connection with front propagation such as pattern formation,[74] 2D–front instabilities[75–91] and 3D–front instabilities,[92] spatial bistability,[74,93–95] excitability waves,[74,93,94,96] monostable state[74] and oscilla-

tion[96] by several independent research groups. The majority of these studies have focused on the investigation of the appearance of the front instability as a function of effective diffusion coefficients,[75,76,83] temperature,[83,88] cell orientation or other geometrical parameter,[77,84,89,90] density changes,[81,82,88] initial concentrations,[82,88] external electric field[78,86] and viscosity.[79,87] The kinetic model of CT-reaction was firstly proposed by Nagypál[72] and was almost exclusively used in the majority of those studies mentioned above. However, it was found that the rate coefficient has to be modified significantly with a different overall stoichiometric equation most probably due to the complexity of CT reaction.[97,98] Later in 2006, Horváth[99] *et al.* suggested coexistence of two limiting stoichiometries including one that produces chlorine dioxide and chloride ione and the other that leads to the formation of chlorate and chloride ions as products. They also proposed a detailed kinetic model based on which the supercatalytic effect of hydrogen ion, self-inhibition of chlorite and autocatalytic effect of chloride can be explained. More recently, an improved model[100] with rate equation consisting of two terms including the concentration of hydrogen ion both in the second and third power has been established, which can be used for quantitative explanation of the front propagation in the unstirred chlorite–tetrathionate reaction system. The other systematic searches about kinetics and mechanism of many oxidation reactions of tetrathionate, for example, hypochlorous acid–tetrathionate,[101,102] chlorine dioxide–tetrathionate,[103] iodine–tetrathionate,[104,105] bromine–tetrathionate,[106] iodate–tetrathionate[107]and periodate–tetrathionate,[108] have been also elucidated during last decade.

Compared to tetrathionate, significantly less information is available in the literature about the oxidations of trithionate and pentathionate despite the fact that their similar structures and their behaviors in oxidative chemical reactions may hint as well the appearance of several nonlinear phenomena just as in case of tetrathionate. Only several research articles could be located that explicitly deal with the redox transformation of trithionate. Among them one is about the oxidation of trithionate by ferrate ion studied by Read *et al.*[109,110] and others are about the investigations on the iodine–trithionate,[111] chlorine dioxide–trithionate,[112] hypochlorous–trithionate[113] and chlorite-trithionate[114] reactions reported by Csekő. The latter three reactions, which are the subsystems of the chlorite–trithionate reaction, have been confirmed to be the alternative systems over the CT–reaction for studying spatiotemporal structures in connection with front propagation.

Pentathionate, as one of the important polythionates generated in the oxidation of thiosulfate and other sulfur compounds, reacts further with the oxidants and therefore may play a crucial role in the appearance of exotic nonlinear dynamical phenomena. A good understanding of the oxidation of pentathionate will accelerate the researches of oxidation of other higher polythionates as well as deeper understanding about the oxidation of thiosulfate. Unfortunately, no information has yet been available in the literature about the oxidation of pentathionate except only a single study[109,110] that directly investigates the oxidation of pentathionate by the ferrate ion. On the basis of the above mentioned literatures of the previous studies related to oxidation of thiosulfate, trithionate and tetrathionate, a simple redox reaction of pentathionate with iodine can be a good candidate as a starting point on the studies of redox reaction of pentathionate. Because on the one hand, the reaction can easily be followed by UV–visible spectroscopy; on the other hand, the kinetics of trithionate–iodine[111] and tetrathionate–iodine[104,105] reactions have already been available for comparison. As described above, the reactions of pentathionate with corresponding oxidants such as iodate, periodate, chlorite, hypochlorous and chlorine dioxide *etc.* are also interesting to be investigated. Hereby, I have chosen four kinetics studies on pentathionate–iodine, pentathionate–iodate, pentathionate–periodate and pentathionate–chlorine dioxide as the framework of my Ph.D and the results obtained are presented in this dissertation.

Chapter 2

Experimental Section

2.1 Materials and Buffers

2.1.1 Materials

Potassium pentathionate was first prepared by the reaction of sodium thiosulfate with hydrochloric acid and arsenious oxide followed by ion exchange with a slurry of finely crystalline potassium acetate as described previously.[115] The major reaction taking place during the synthesis can be described by the following equation

$$5Na_2S_2O_3 + 6HCl \overset{As_2O_3}{=} 6NaCl + 2Na_2S_5O_6 + 3H_2O. \quad (2.1)$$

Sulfur precipitate, sulfur dioxide and sulfide (in form of arsenic sulfide) were also produced from side reactions during the process of synthesis, these contaminants, however, can easily be removed from the pentathionate prior to ion exchange. Fortunately, other polythionates (like tetrathionate, hexathionate), are not formed during the synthesis under the circumstances applied, which is an important factor because separation of polythionates meets several difficulties. To confirm the purity of potassium pentathionate, Raman spectroscopy was carried out by a NXR Fourier transform Raman spectrometer. Its exact purity was checked by the following method. A known amount of potassium pentathionate was dissolved in pure distilled water followed by addition of a bromine solution in excess. The reaction mixture was left to stand for at least 5 minutes, which was proven to be enough to oxidize pentathionate into sulfate completely. The excess of bromine was then removed by boiling the solution for a couple of minutes. The hydrogen ion, liberated

by the oxidation of pentathionate by bromine according to the equation:

$$S_5O_6^{2-} + 10Br_2 + 14H_2O = 5SO_4^{2-} + 28H^+ + 20Br^-, \quad (2.2)$$

was determined by titrating the sample against standard sodium hydroxide solution. The purity of the solid potassium pentathionate was found to be better than 97.0% and checked prior to each experiment. No thiosulfate, sulfite and elementary sulfur impurities could be detected up to 2–4 weeks. Because the composition of solid pentathionate[115] is $K_2S_5O_6 \cdot \frac{1}{2} H_2O$, this means that it may contain only a trace amount of sulfate or tetrathionate besides crystalline water. Once the purity of the solid sample was proven to be decreased because of the formation of elementary sulfur and other sulfur species, it was discarded and a new solid potassium pentathionate sample was prepared again.

The chlorine dioxide stock solution was prepared by acidification of the sodium chlorite solution with 50% (v/v) sulfuric acid. Chlorine dioxide evolved was removed with an air stream and dissolved in cold water. The stock solution was kept refrigerated and was protected from light to avoid its photochemical decomposition. Purity of the chlorine dioxide stock solution was checked each day prior to use for chloride, chlorite, and chlorate impurities after purging out its $^{\cdot}ClO_2$ content. None of these impurities could be detected up to a month. All of the other chemicals including iodine, potassium iodate (Reanal), potassium metaperiodate (Reanal), potassium iodide, sodium chloride, acetic acid, sodium acetate, phosphoric acid, sodium dihydrogen phosphate and sodium perchlorate, were of the highest purity commercially available and were used without further purification. The stock solutions were prepared from twice ion-exchanged and double-distilled water. The initial concentration of iodine solution was determined by titration of the stock solutions with standardized thiosulfate and/or spectrophotometrically before each experiment. The concentration of stock chlorine dioxide solution was also determined by standard iodometric method and/or spectrophotometrically before each experiment.

2.1.2 Buffers

- For the iodine–pentathionate and chlorine dioxide–pentathionate reaction systems, the pH of the solutions was maintained in the range of 3.95–5.15

and 4.25–5.45, respectively, by acetic acid/acetate buffer taking the pK_a of acetic acid as 4.55.[116]

- For iodate–pentathionate and periodate–pentathionate reaction systems, phosphoric/dihydrogen phosphate buffer was used to maintain the pH of solutions between 1.30–2.20 and 1.10–2.15 by taking the pK_a of phosphoric acid as 1.80.[116] The initial concentration of dihydrogen phosphate, [$H_2PO_4^-$], was always kept constant at 0.1 M and the desired pH was adjusted by the necessary amount of phosphoric acid in the reaction of iodate–pentathionate and the total amount of phosphoric acid with dihydrogen phosphate was always kept at 0.65 M in the periodate–pentathionate reaction system.

The ionic strength was adjusted to be 0.5 M in all measurements by adding the necessary amount of sodium perchlorate for iodine–pentathionate, iodate–pentathionate and periodate–pentathionate reactions and by the buffer component acetate in chlorine dioxide–pentathionate reaction solution. The temperature of the reaction vessel for all of reactions was always maintained at 25.0 ± 0.1 °C. The initial concentrations of pentathionate ion were varied in the ranges of 0.0293–1.40 mM, 0.054–1.080 mM, 0.10–6.0 mM and 0.25–9.0 mM in the case of iodine–pentathionate, chlorine dioxide–pentathionate, iodate–pentathionate and periodate–pentathionate, respectively. Initial concentrations of oxidants, iodine, chlorine dioxide, iodate and periodate for these four reaction systems were changed in the ranges of 0.063–0.768 mM, 0.238–5.87 mM, 0.25–4.0 mM and 0.667–9.17 mM, respectively. Effect of the initially added iodide ion on the reaction of iodine with pentathionate and effect of the initially added chloride ion on the reaction of chlorine dioxide–pentathionate were also studied on the concentration range between 0–1.897 mM and 0–24.2 mM, respectively. In this experimental setup, these four reactions were individually investigated at 176, 132, 159 and 159 different experimental conditions and some of experiments were also repeated that gave the evidence about the reproducibility of the kinetic curves.

2.2 Methods and Instrumentation

All of the four reactions were followed by a Zeiss S600 diode-array spectrophotometer in the visible range without using the deuterium lamp of the spectropho-

tometer. All the reactions have been carried out in a standard quartz cuvette equipped with a magnetic stirrer and a Teflon cap having 1 cm optical path. The stirring rate was controlled at 750 rpm to provide sufficiently fast mixing of the reactants before initiating reaction. The method of initiating reaction were as follows:

- In case of the iodine–pentathionate and the chlorine dioxide–pentathionate reactions, the buffer components and perchlorate (if necessary) followed by the oxidant (iodine and chlorine dioxide) and if necessary iodide/chloride solution were delivered from a pipet. The spectrum of the solution was always recorded before injection of the pentathionate solution to determine the exact initial concentration of iodine and chlorine dioxide precisely. The reaction was started with the addition of the necessary amount of pentathionate solution from a fast-delivery pipet. It should be note that during the whole course of the experiments, the deuterium lamp of the spectrophotometer was always switched off to eliminate the undesired photochemical decomposition of chlorine dioxide.[130,131]

- In the case of iodate–pentathionate and periodate–pentathionate reactions, the buffer components and sodium perchlorate followed by pentathionate solution were delivered into the cuvette by a pipet, and the iodate/periodate solution was injected finally from a fast delivery pipet. In case of the effect of iodide, the buffer components, sodium perchlorate, pentathionate and iodide were delivered into the cuvette followed by injection of iodate/pentathionate.

2.3 Data Treatment

In the visible range, only iodine and triiodide were found to absorb light, therefore, pentathionate–iodine, pentathionate–iodate and pentathionate–periodate reactions were investigated by monitoring the total amount of iodine and thus the isosbestic point of the iodine–triiodide system, λ = 468 nm (molar absorbances of both species at this wavelength were taken into consideration as $\varepsilon_{I_2} = \varepsilon_{I_3^-} = 750\,M^{-1}cm^{-1}$), was selected to nolinear parameter estimation by the *ChemMech*/*ZiTa* program package[117] developed to fit basically unlimited number of experimental series. For the reaction of pentathionate with chlorine dioxide, because the only absorbing species is chlorine dioxide within the wavelength range studied, λ = 430 nm was chosen

for data evaluation. Molar absorbance of chlorine dioxide was determined to be 155±4 $M^{-1}cm^{-1}$ at this wavelength.

In the reaction of iodine–pentathionate, altogether 23000 experimental points from 176 kinetic runs were used for simultaneous fitting. Originally, each kinetic run contained more than 200 absorbance–time data pairs in the oxidation of pentathionate by chlorine dioxide, iodate and periodate, therefore, it was necessary to reduce the number of time points (40–80) to avoid unnecessary and time-consuming calculations. Essence of this method has already been described elsewhere.[99] Altogether more than 6600 experimental points from 132 kinetic runs of reaction of chlorine dioxide with pentathionate, almost 11000 experimental points from 159 kinetic series of reaction of iodate with pentathionate and around 9425 experimental point from 159 kinetic curves of reaction of periodate with pentathionate were used for the simultaneous evaluation. To obtain the kinetic model and the individually rate coefficients, an absolute fitting procedure has been chosen in iodine–pentathionate and chlorine dioxide–pentathionate, and a relative fitting procedure has been chosen in iodate–pentathionate and periodate–pentathionate to minimize the average deviation between the measured and calculated absorbances. The quantitative criterion for an acceptable fit was that the average deviations for the absolute fit approached 0.006 absorbance units respectively for iodine–pentathionate and chlorine dioxide–pentathionate reactions and the average deviation for the relative fit approached 5.0% respectively for iodate–pentathionate and periodate–pentathionate reactions, which were close to the experimentally achievable limit of error of the spectrophotometer in the visible range.

2.4 Computational Details of Theoretical Calculations for $S_xO_6^{2-}$ and $S_xO_6I^-$ (x = 3–5)

For all the calculations, the PBE0 functional was selected, i.e., the zero–parameter hybrid functional by Adamo and Barone[117] based on the generalized gradient approximation exchange and correlation functionals by Perdew, Burke, and Ernzerhof.[118] For all atoms, the def2-TZVPD triple–ζ basis set with polarization and diffuse basis functions[119] were employed. This model chemistry exhibited a reasonable agreement with the experimental geometrical parameters[120] for all species

of the $S_xO_6^{2-}$ type (x = 3–5). Optimized geometries were identified by the absence of negative eigenvalues in the vibrational frequency analysis. Geometry optimizations were completed with solvent effects taken into account by employing the polarizable continuum model methodology[121] with dielectric constant ε = 78.355 for water. For all of the calculations, the Firefly 7.1.G quantum chemical package[122] was used. Natural bond orbital (NBO) analysis[123] have been performed by the module NBO 5.G implemented in Firefly.

Chapter 3

Result and Discussion

3.1 Oxidation of Pentathionate Ion by Iodine

3.1.1 Stoichiometry

The stoichiometry of the reaction was established by visible spectroscopy from the end of the kinetic measurements in an excess of iodine. Table 3.1 contains the stoichiometric ratio (SR) in excess of iodine defined as $SR = ([T_{I_2}]_0 - [T_{I_2}]_\infty)/[S_5O_6^{2-}]_0$. Here, the $[T_{I_2}] = [I_2] + [I_3^-]$. The calculation of SR indicated that the ratio of iodine and pentathionate is 10, and the only sulfur-containing product of the reaction is the sulfate ion. Therefore, the stoichiometry of this reaction can be expressed as following equation:

$$S_5O_6^{2-} + 10I_2 + 14H_2O = 5SO_4^{2-} + 20I^- + 28H^+. \tag{3.1}$$

3.1.2 Individual Curve Fitting Method

Survey of the experimental curves in the pentathionate–iodine reaction reveals two important characteristics of this system. On the one hand, the decay of iodine is independent of pH within the pH range used in the experiments, as seen in Figure 3.1. The same phenomenon has also been observed in the tetrathionate–iodine[104,105] and trithionate–iodine[111] systems, meaning that this feature is a general

Table 3.1: Measured SR (defined as $([T_{I_2}]_0 - [T_{I_2}]_\infty)/[S_5O_6^{2-}]_0$) in an excess of iodine

$[T_{I_2}]_0$/mM	$[S_5O_6^{2-}]_0$/mM	pH	A_∞ at 468 nm	SR
0.455	0.03	3.95	0.1310	9.42
0.487	0.03	4.25	0.1497	9.66
0.522	0.03	4.55	0.1668	10.08
0.504	0.03	5.15	0.1537	10.06
0.731	0.05	3.95	0.1841	9.79
0.767	0.05	4.25	0.2177	9.62
0.745	0.05	4.55	0.2045	9.53
0.732	0.05	4.85	0.2043	9.27
0.752	0.05	5.15	0.2125	9.45
0.767	0.05	4.25	0.2177	9.62
0.524	0.0293	4.55	0.1705	10.22
Average SR				9.7 ± 0.3

phenomenon of the polythionate–iodine reactions.* On the second hand, Figure 3.2 describes the effect of initially added iodide ion on the consumption of the total amount of iodine. It clearly demonstrates that an increase of initially added iodide ion significantly inhibits the pentathionate–iodine reaction. Therefore, iodide ion acts as an autoinhibitor† of the system because its concentration monotonously increases during the course of reaction. To account for all of these observations, the first effort to evaluate the kinetic curves individually was, therefore, based on the

*It may sound strange for most chemists (especially analytical chemists) at first glance that tetrathionate can be oxidized further by iodine eventually into sulfate. The basic equation of iodometry clearly shows that iodine oxidizes thiosulfate only to tetrathionate. We should emphasize, however, that on the one hand the tetrathionate–iodine reaction is orders of magnitude slower than the corresponding thiosulfate–iodine reaction and on the other hand the former reaction is strongly inhibited by iodide ion.[105] Usually the iodometric titrations are performed under high excess of iodide ion, consequently during the titration process no oxidation of tetrathionate occurs, hence the traditional basic equation of iodometry still stands.

†The autoinhibition is defined as a process where one of the product formed during the course of the reaction slows down the rate of its formation, which is a negative feedback. The species causes this phenomenon is called as an autoinhibitor.

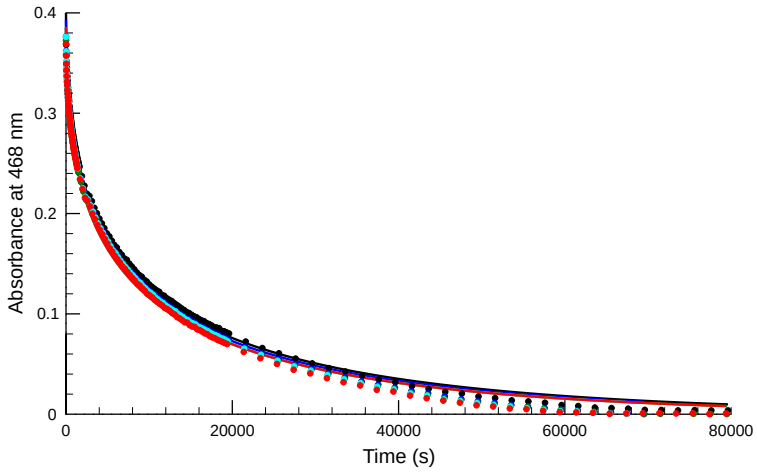

Figure 3.1: Measured (dots) and calculated (solid lines) absorbance–time curves at $[S_5O_6^{2-}]_0$ = 0.201 mM and $[I_2]_0$ = 0.511 mM at different pH in absence of initially added iodide ion. pH = 3.95 (black), 4.25 (blue), 4.55 (green), 4.85 (cyan), 5.15 (red).

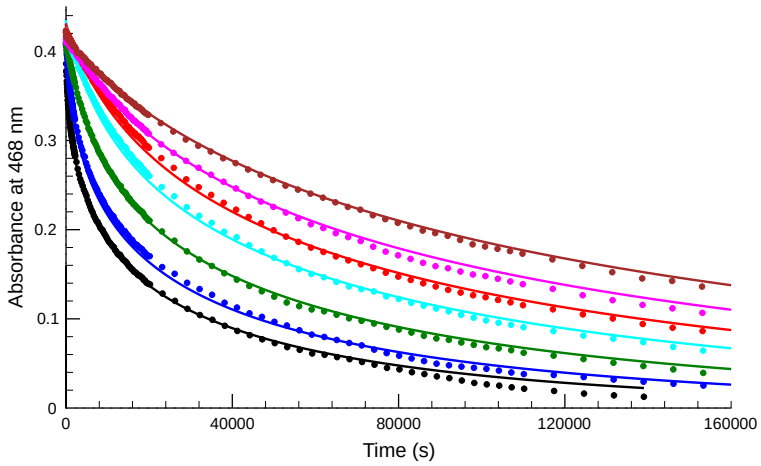

Figure 3.2: Measured (dots) and calculated (solid lines) absorbance–time curves at $[S_5O_6^{2-}]_0$ = 0.11 mM, $[I_2]_0$ = 0.56 mM and pH = 4.55 in presence of initially added iodide ion. $[I^-]_0$/mM = 0.0 (black), 0.101 (blue), 0.399 (green), 0.699 (cyan), 0.998 (red), 1.397 (magenta), 1.796 (brown).

following apparent rate equation:

$$-\frac{1}{10}\cdot\frac{\mathrm{d}[T_{I_2}]}{\mathrm{d}t} = k_{\mathrm{app}}\frac{[S_5O_6^{2-}][T_{I_2}]}{[I^-]}. \tag{3.2}$$

The surprising result of the calculation is that eq. 3.2 is able to fit all of the 176 kinetic curves with k_{app} equals $(3.15 \pm 0.50) \times 10^{-5}$ s^{-1} within an acceptable error. Although we also noticed that k_{app} slightly decreases as the initial concentration of iodide increases. This feature is illustrated in Table 3.2. Later it will be shown that this feature can easily explained by the proposed model.

3.1.3 Proposed Kinetic Model

Because the overall reaction produces relatively huge amount of proton (see: eq. 3.1) the protonation and deprotonation processes of the buffer components would seem to be necessary to follow the slight change of pH during the course of the reaction:

$$CH_3COOH \rightleftharpoons H^+ + CH_3COO^-. \tag{E1}$$

However, as shown above, the pH does not affect the reaction; therefore, this equilibrium was only taken into consideration for the sake of completeness. The first effort to describe all the 176 kinetic curves simultaneously was based on eq. 3.1 being augmented by the well-known triiodide formation equilibrium:

$$I_2 + I^- \rightleftharpoons I_3^- \tag{R1}$$

In this model, the iodide inhibition was taken into consideration simply by the formation of the kinetically inactive triiodide ion and the rate equation of eq. 3.1 was considered to be an overall second–order reaction, having the formal kinetic order of both reactant unity. This kinetic model fits all of the data with an unacceptably high average deviation of 0.046 absorbance units. Therefore, it can be concluded that the inhibition of iodide ion cannot be taken into account only by the formation of triiodide ion. On the basis of the remarkable resemblance of the kinetic behavior of the polythionate–iodine reaction,[104,105,111] a kinetic models R1–R9 similar to the reactions mentioned above was proposed as follows:

$$I_2 + H_2O \rightleftharpoons HOI + I^- + H^+ \tag{R2}$$

$$S_5O_6^{2-} + I_2 \rightleftharpoons S_5O_6I^- + I^- \tag{R3}$$

$$S_5O_6I^- + H_2O \longrightarrow S_3O_3OH^- + S_2O_3I^- + H^+ \tag{R4}$$

$$S_5O_6I^- + I^- \longrightarrow S_2O_3I^- + S_3O_3I^- \tag{R5}$$

Table 3.2: Apparent Rate Coefficients of Representative Examples Determined by the Individual Curve Fitting Method

$[S_5O_6^{2-}]_0$/mM	$[I_2]_0$/mM	$[I^-]_0$/mM	pH	$k_{app} \times 10^5$ s^{-1}
0.03	0.455	0	3.95	3.73
0.06	0.43	0	3.95	3.48
0.121	0.445	0	3.95	3.17
0.251	0.45	0	3.95	3.15
0.5	0.45	0	3.95	3.23
0.8	0.41	0	3.95	3.25
1.401	0.42	0	3.95	3.13
0.05	0.064	0	4.85	3.78
0.05	0.096	0	4.85	3.67
0.05	0.18	0	4.85	3.33
0.05	0.245	0	4.85	3.38
0.05	0.355	0	4.85	3.25
0.05	0.509	0	4.85	3.37
0.05	0.732	0	4.85	3.76
0.061	0.533	0	3.95	3.35
0.061	0.543	0	4.25	3.20
0.061	0.533	0	4.55	3.17
0.061	0.538	0	4.85	3.09
0.061	0.533	0	5.15	3.25
0.489	0.520	0	4.55	3.02
0.489	0.520	0.100	4.55	2.66
0.489	0.520	0.499	4.55	2.54
0.489	0.515	0.999	4.55	2.25
0.489	0.512	1.300	4.55	2.14
0.489	0.515	1.600	4.55	1.95
0.489	0.520	1.897	4.55	1.83

$$S_3O_3OH^- + 3I_2 + 5H_2O \xrightarrow{\text{fast}} 3HSO_3^- + 8H^+ + 6I^- \quad \text{(R6)}$$

$$S_2O_3I^- + I_2 + 3H_2O \xrightarrow{\text{fast}} 2HSO_3^- + 4H^+ + 3I^- \quad \text{(R7)}$$

$$S_3O_3I^- + 3I_2 + 6H_2O \xrightarrow{\text{fast}} 3HSO_3^- + 9H^+ + 7I^- \quad \text{(R8)}$$

$$HSO_3^- + I_2 + H_2O \xrightarrow{\text{fast}} SO_4^{2-} + 2I^- + 3H^+ \quad \text{(R9)}$$

The parameters determined by the simultaneous evaluation of the kinetic curves has been listed in Table 3.3. By the help of the proposed kinetic model, all the 176 kinetic curves can be well described by 0.0048 absorbance unit average deviation (the results are shown Figure 3.1–3.4).

Table 3.3: Fitted and Fixed Rate Coefficients of the Proposed Kinetic Model. No error indicates that the given parameter is fixed during the calculation process

step	rate equation	parameter
R1	$k_{R1}[I_2][I^-]$	5.7×10^{9} $M^{-1}s^{-1}$
	$k_{-R1}[I_3^-]$	8.5×10^{6} s^{-1}
R2	$k_{R2}[I_2]$	5.52×10^{-2} s^{-1}
	$k_{-R2}[I_2]/[H^+]$	1.98×10^{-3} Ms^{-1}
R2′	$k'_{R2}[HOI][H^+][I^-]$	1.023×10^{11} $M^{-2}s^{-1}$
	$k'_{-R2}[HOI][I^-]$	3.67×10^{9} $M^{-1}s^{-1}$
R3	$k_{R3}[S_5O_6^{2-}][I_2]$	10^{1} $M^{-1}s^{-1}$
	$k_{-R3}[S_5O_6I^-][I^-]$	10^{6} $M^{-1}s^{-1}$
R4	$k_{R4}[S_5O_6I^-]$	3.29 ± 0.06 s^{-1}
R5	$k_{R5}[S_5O_6I^-][I^-]$	$310\pm66M^{-1}s^{-1}$
R6	$k_{R6}[S_3O_3OH^-][I_2]$	$>10^{2}$ $M^{-1}s^{-1}$
R7	$k_{R7}[S_2O_3I^-][I_2]$	$>10^{2}$ $M^{-1}s^{-1}$
R8	$k_{R8}[S_3O_3I^-][I_2]$	$>10^{3}$ $M^{-1}s^{-1}$
R9	$k_{R9}[HSO_3^-][I_2]$	3.1×10^{9} $M^{-1}s^{-1}$

Step R1 is the well-known fast equilibrium of the formation of triiodide ion studied by several authors.[124,125] The rate coefficients of the forward and reverse reactions were set to $k_{R1} = 5.7 \times 10^9$ $M^{-1}s^{-1}$ and $k_{R1} = 8.5 \times 10^6$ s^{-1} to give $\log\beta_{I_3^-} = 2.83$, where $\beta_{I_3^-}$ is the formation constant of triiodide ion.[116]

Step R2 is the hydrolytic equilibrium of iodine in an aqueous solution. The rate coefficients of the forward and reverse reactions including the hydroxide-driven pathway were determined previously, therefore, these values were used as fixed ones throughout the whole fitting procedure.[126–128]

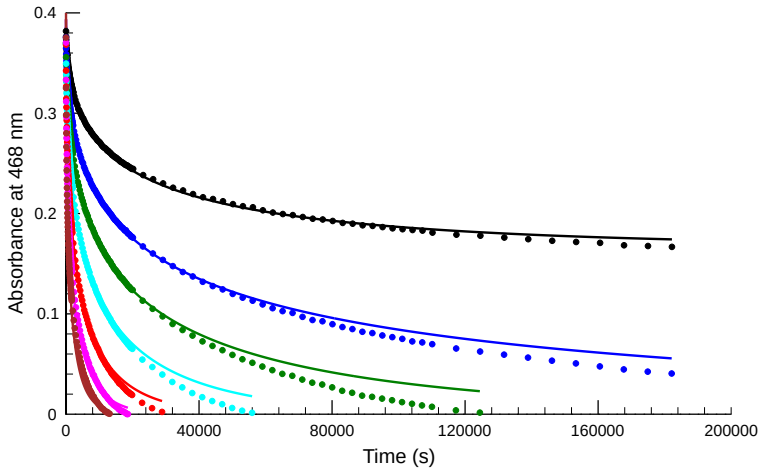

Figure 3.3: Measured (dots) and calculated (solid lines) absorbance–time curves at $[I_2]_0$ = 0.51 mM and pH = 4.55 in absence of initially added iodide ion. $[S_5O_6^{2-}]_0$/mM = 0.03 (black), 0.06 (blue), 0.101 (green), 0.201 (cyan), 0.400 (red), 0.800 (magenta), 1.401 (brown).

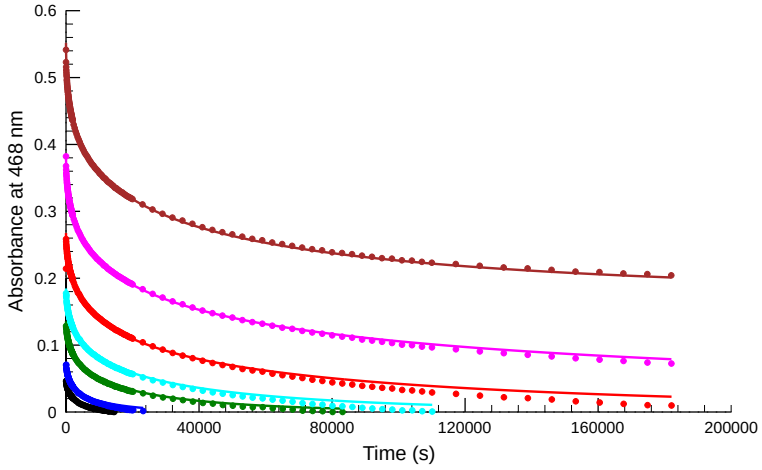

Figure 3.4: Measured (dots) and calculated (solid lines) absorbance–time curves at $[S_5O_6^{2-}]_0$ = 0.05 mM and pH = 4.85 in absence of initially added iodide ion. $[I_2]_0$/mM = 0.064 (black), 0.096 (blue), 0.18 (green), 0.245 (cyan), 0.355 (red), 0.509 (magenta), 0.732 (brown).

Step R3 is a rapid initiating equilibrium between the reactants producing $S_5O_6I^-$ and iodide ion. Later we shall see that the attack of the iodine molecule is likely

to occur on the β or β'-sulfur of pentathionate. The calculation has provided only a higher limit for $K_{R3} = k_{R3}/k_{-R3} = 0.01$; any value lower than that leads to the same average deviation, meaning that this equilibrium is shifted far to the left. To provide a low steady-state concentration for the species $S_5O_6I^-$, the k_{R3} was set as $10\ M^{-1}s^{-1}$ and k_{-R3} was set as a value of $10^6\ M^{-1}s^{-1}$ to provide $K_{R3} = 10^{-5}$ during the calculation process.

Step R4 is one of the possible pathways of $S_5O_6I^-$ to produce additional sulfur-containing short-lived intermediates via the break up of sulfur chain. The solvent water molecule attacks probably the γ-sulfur of the sulfur chain (although an attack on β'-sulfur cannot be ruled out entirely) resulting in $S_3O_3OH^-$ and $S_2O_3I^-$. Because both species are short-lived intermediates, the kinetic measurements do not a provide a solid basis to distinguish between Step R4 and the following reaction:

$$S_5O_6I^- + H_2O \longrightarrow S_3O_3I^- + S_2O_3OH^- + H^+ \tag{3.3}$$

One should keep in mind that iodine in $S_3O_3I^-$ is placed on the inner sulfur and not on the terminal one to be in agreement that iodine attacks the β-sulfur of the sulfur chain. If further reaction of $S_2O_3OH^-$ with iodine considered to be a rapid reaction resulting in the formation hydrogen sulfite as well, Step R4 can easily be replaced by eq. 3.3 kinetically. However, as been shown later, the attack of the oxygen atom of the solvent molecule most likely takes place on the γ-sulfur of $S_5O_6I^-$; therefore, step R4 is rather kept in the final model. If $K_{R3} = 10^{-5}$ is used to provide a low steady-state concentration for $S_5O_6I^-$, then value of $k_{R4} = 3.29 \pm 0.06\ s^{-1}$ can be calculated. The fitting also indicated that k_{R4} and K_{R3} cannot be determined independently due to the strong correlation between these kinetic parameters; only their product could be calculated. Later we shall see that this fact can conveniently be explained by the rate equation obtained from the proposed kinetic model.

Step R5 is the other important conversion reaction of $S_5O_6I^-$ in which iodide ion probably attacks one of the inner sulfur of the sulfur chain resulting in breaking up of sulfur-sulfur bond as well. Such a reaction of the intermediate $S_xO_6I^-$ with iodide ion was already proposed in the tetrathionate–iodine reaction[105] and turns out to be necessary to describe adequately the polythionate–iodine reactions. It was found that the individual rate coefficient of this reaction cannot be determined as well because of the strong correlation between the rate coefficients of k_{R3}, k_{-R3} and k_{R5}; only the product of K_{R3} and k_{R5} can be calculated unambiguously. As a result,

if $K_{R3} = 10^{-5}$ was considered in the calculation process, the $k_{R5} = 310 \pm 66$ $M^{-1}s^{-1}$ can be obtained in the model.

Steps R6 and R8 are fast processes in which the short–lived intermediates $S_3O_3OH^-$, $S_2O_3I^-$ and $S_3O_3I^-$ are oxidized by iodine resulting in hydrogen–sulfite and iodide ion. All of these reactions were found to be rapid processes and only lower limits of k_{R6}, k_{R7} and k_{R8} (indicated in Table 3.3) could be determined from these measurements.

Step R9 is the rapid, essentially diffusion–controlled, reaction of hydrogen sulfite and iodine studied thoroughly by Yiin and Margerum.[129] The value of k_{R9} was determined as 3.1×10^9 $M^{-1}s^{-1}$ in their work for its rate coefficient, and was fixed throughout the whole calculation process.

3.1.4 Formal Kinetics

Because no intermediates were found in a detectable amount during the course of the reaction, a rate equation can easily be deduced from the proposed model. Considering that

$$-\frac{1}{10}\cdot\frac{\mathrm{d}[T_{I_2}]}{\mathrm{d}t} = -\frac{\mathrm{d}[S_5O_6^{2-}]}{\mathrm{d}t} = k_{R3}[S_5O_6^{2-}][I_2] - k_{-R3}[S_5O_6I^-][I^-] \tag{3.4}$$

and

$$-\frac{\mathrm{d}[S_5O_6I^-]}{\mathrm{d}t} = k_{R3}[S_5O_6^{2-}][I_2] - k_{-R3}[S_5O_6I^-][I^-] - k_{R4}[S_5O_6I^-] - k_{R5}[S_5O_6I^-][I^-] \tag{3.5}$$

applying a steady–state approximation for species $S_5O_6I^-$, the following equation can be obtained

$$[S_5O_6I^-] = \frac{k_{R3}[S_5O_6^{2-}][I_2]}{k_{R4} + (k_{-R3} + k_{R5})[I^-]} \tag{3.6}$$

It has to be noted that all the intermediates, including $S_5O_6I^-$, $S_3O_3OH^-$, $S_2O_3I^-$, $S_3O_3I^-$ and HSO_3^- are short-lived intermediates and the steady-state approximation can be applied for them. However, if we define the rate by the consumption of pentathionate, only the steady-state approximation for $S_5O_6I^-$ is necessary to derive the rate equation. If we would like to define the rate of reaction by the consumption of iodine, certainly, the steady-state approximation for all these species are required. Hence, the former equal sign in equation 3.4 hides the steady-state approximations applied for species $S_3O_3OH^-$, $S_2O_3I^-$, $S_3O_3I^-$ and HSO_3^-.

Upon substitution of eq. 3.6 into eq. 3.4, followed by some algebraic manipulation, we can arrive at

$$-\frac{1}{10}\cdot\frac{\mathrm{d}[T_{I_2}]}{\mathrm{d}t}=-\frac{\mathrm{d}[S_5O_6^{2-}]}{\mathrm{d}t}=\frac{(k_{R3}k_{R4}+k_{R3}k_{R5}[I^-])[S_5O_6^{2-}][T_{I_2}]}{k_{R4}+(k_{-R3}+k_{R5}+k_{R4}K_{R1})[I^-]+K_{R1}(k_{-R3}+k_{R5})[I^-]^2} \tag{3.7}$$

where K_{R1} is the formation constant of triiodide. Taking into account that the $k_{-R3} \gg k_{R5} + k_{R4}K_{R1}$ inequality is fulfilled and $k_{-R3}[I^-] \gg k_{R4}$ holds apart from at the very beginning of the reaction, the following equation is obtained:

$$-\frac{1}{10}\cdot\frac{\mathrm{d}[T_{I_2}]}{\mathrm{d}t}=\frac{K_{R3}k_{R4}+K_{R3}k_{R5}[I^-]}{1+K_{R1}[I^-]}\frac{[S_5O_6^{2-}][T_{I_2}]}{[I^-]} \tag{3.8}$$

Comparing eq. 3.7 with eq. 3.2 one can easily see that k_{app} slightly depends on the actual iodide concentration.

$$k_{R3}=\frac{K_{R3}k_{R4}+K_{R3}k_{R5}[I^-]}{1+K_{R1}[I^-]} \tag{3.9}$$

Substituting the rate coefficients determined here at low initial iodide concentration, the value of 3.15×10^{-5} s^{-1} for k_{app} can be calculated, while at high initial iodide concentration, $k_{app} = 0.6 \times 10^{-5}$ s^{-1} can be obtained. Comparing these values with experimentally determined k_{app} values at different initial conditions (see Table 3.2), it is found that the results strongly support the proposed kinetic model as well. This equation also helps to understand why only the products of $K_{R3}k_{R4}$ and $K_{R3}k_{R5}$ can be calculated from the experiments.

3.1.5 General Pathway of the Sulfur-Chain Breakage of Polythionates

Previous studies of trithionate[111] and tetrathionate[104,105] oxidations by iodine along with the study presented here suggest the fact that sulfur-chain breakage of polythionates starts generally with the same equilibrium:

$$S_xO_6^{2-} + I_2 \rightleftharpoons S_xO_6I^- + I^- \tag{3.10}$$

where x = 3, 4 and 5. This equilibrium is shifted far to the left and established rapidly compared to the timescale of the reaction in question. Should these reactions start with I^+, the inhibitory effect of iodide can easily be explained by eq. 3.10. As shown previously,[104,105,111] the kinetically inactive triiodide formation in itself is not able

to explain the inhibitory effect of the iodide ion. From these studies, it was also enlightened that the following rate equation describes well the kinetic curves of all of the polythionates–iodine reactions:

$$v = k_x \frac{[S_xO_6^{2-}][I_2]}{[I^-]} \tag{3.11}$$

where $10^5 \times k_x$ = 82.7, 4.1 and 3.15 s^{-1} in case of trithionate, tetrathionate and pentathionate, respectively. From these values, one can easily calculate that the half-life of the corresponding trithionate–iodine, tetrathionate–iodine and pentathionate–iodine reaction is 840, 16900 and 22000 s, respectively. In other words, it means that longer sulfur-chain of polythionates corresponds to a more sluggish reaction toward iodine. It raises an important question about the attack of iodine on polythionates in a molecular level. Figure 3.5 indicates the calculated structures of polythionates and $S_xO_6I^-$ species. It is seen that among the polythionates the β-sulfur of trithionate has the most negative partial charge (−0.411). Compared to this, the partial charge of the β (and β')-sulfur atom decreases to −0.203 in the case of tetrathionate, but a further increase of the sulfur chain results in a minor change, only to −0.199, for the partial charge of β- and β'-sulfur atoms in the case of pentathionate. Because the β (and β')-sulfur of the polythionate sulfur chain is negatively charged, this site is a possible candidate to be attacked by iodine, furthermore, supports a formal I^+ transfer to the β-sulfur of the polythionate chain. Moreover, the increase of the partial charge of the β-sulfur of $S_xO_6I^-$ compared to those of the corresponding polythionates (0.237, 0.219, and 0.217 electrons for the trithionate, tetrathionate and pentathionate, respectively) may also explain why the trithionate–iodine reaction is faster by more than 1 order of magnitude compared to the tetrathionate–iodine and pentathionate–iodine reactions and why there is not much difference between the rates of the tetrathionate–iodine and pentathionate–iodine reactions. The central kinetic role of the β- and β'-sulfur of the sulfur chain is also supported by the well-known catalytic effect of thiosulfate on the rearrangement of tetrathionate.[39] Once $S_xO_6I^-$ forms, one may easily see that the length of the bond between the α- and β-sulfur atoms increase in each polythionate in the range of 0.152–0.212 Å, facilitating an attack of the solvent molecule to finally break up the sulfur chain. The fate of $S_xO_6I^-$, however, differs in the case of trithionate compared to those of the higher polythionates. In the former case, $S_3O_6I^-$ has two different routes for sulfur–chain breakup: hydrolysis and the reaction of iodine.[111] In the other cases,

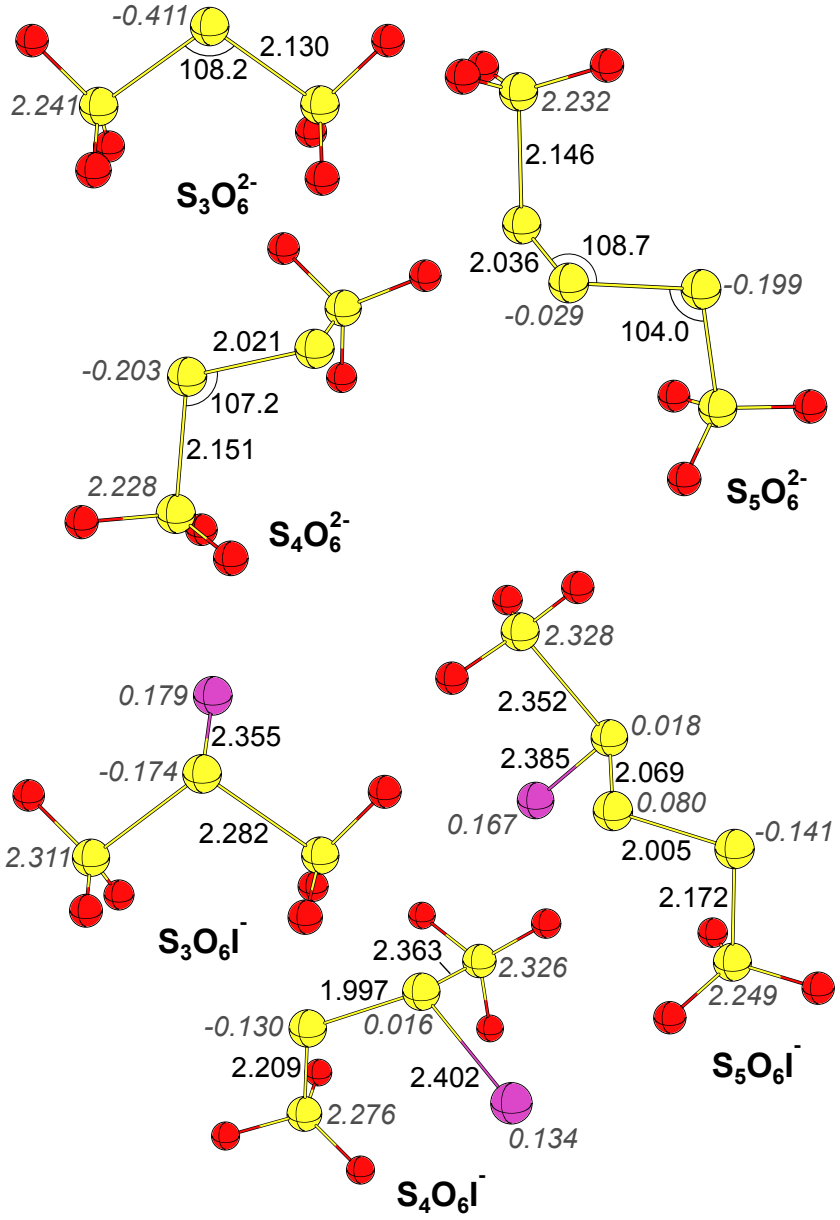

Figure 3.5: Molecular structures of polythionates and $S_xO_6I^-$ species calculated at the PBBEO/TZVPD lever of theory. Bond distances are given in angstroms and bond angles in degrees. Natural charges are written in italics.

however, besides the hydrolysis, the attack of the iodide ion is also a possible route for $S_xO_6I^-$ to be converted. The lack of attack of the iodide ion on $S_3O_6I^-$ may easily be explained by the lack of a sterically not hidden positively charged sulfur atom of the molecule. The present study of the pentathionate–iodine reaction reveals that $S_5O_6I^-$ can also be attacked by the iodide ion to break up the sulfur chain. As

can be seen, the β- and γ-sulfur atoms are partially positively charged parts of the molecule that can be attacked by the electron-rich iodide ion. This further attack (which probably takes place on the γ-sulfur because of its slightly more positive partial charge) increases the length of the β-sulfur–γ-sulfur bond, resulting in its immediate breakup. Once the sulfur chain breaks up, subsequent rapid oxidizing processes eventually lead to the formation of sulfate.

3.2 Reaction of Pentathionate Ion with Iodate Ion

3.2.1 Preliminary Observation

Typical experimental data are illustrated in Figure 3.6 indicating that iodine forms only after a well-defined time lag. In addition to that the absorbance increase

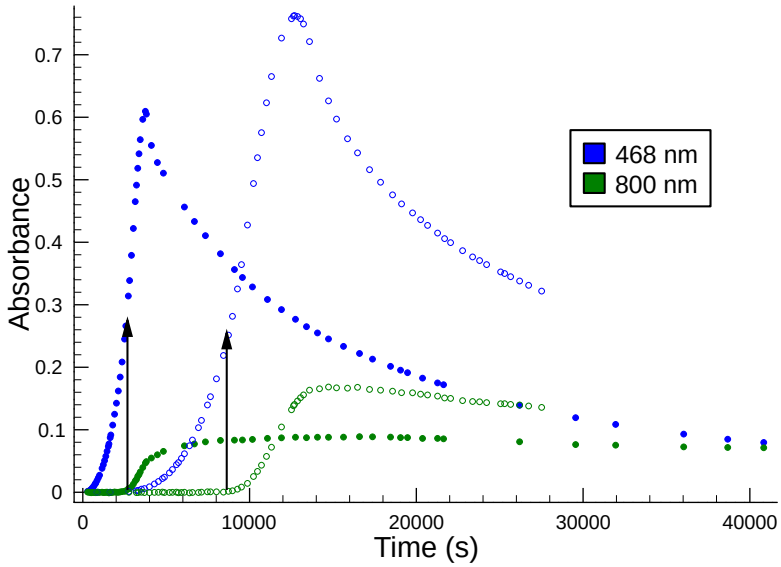

Figure 3.6: Measured absorbance–time series at two different wavelengths. Conditions are as follows: $[S_5O_6^{2-}]_0$ = 1.4 mM; $[IO_3^-]_0$ = 1.5 mM; pH = 1.4 (filled symbols); $[S_5O_6^{2-}]_0$ = 1.0 mM; $[IO_3^-]_0$ = 1.6 mM; pH = 1.8 (empty symbols). Arrows point to the place of truncation.

at 800 nm suggests that a light-scattering species must form during the course of reaction because none of the possible end-products (any sulfur species, iodine and

triiodide) have detectable absorbance at this wavelength.

Moreover after the reaction is completed detectable amount of colloidal sulfur precipitation can be collected from the cuvette. Since a light-scattering species disturbs the quantitative determination of concentration from the measured absorbance at the wavelength range in question, all the absorbance–time curves should be truncated after the appearance of detectable amount of colloidal sulfur for quantitative purposes. Such an example (the place of truncation) is also shown in Figure 3.6. This figure also strengthens the fact that in pentathionate excess the total amount of iodine goes through a maximum. It indirectly proves that the appearance of iodine after a well-defined time-lag is not the consequence of the complete consumption of pentathionate. Later, we shall also see that pentathionate and iodine coexist for a relatively long period of time due to the slow pentathionate–iodine reaction especially when the concentration iodide ion becomes non-negligible. Consequently, in this sense it means that the iodate–pentathionate system cannot be treated as a true Landolt-type clock reaction. In those reactions (for example sulfite–iodate, sulfite–bromate and thiosulfate–iodate) appearance of iodine is the consequence of the complete removal of substrate due to the fact that substrate (sulfite or thiosulfate) instantaneously reacts with iodine.

Furthermore an important observation is yet to be highlighted. As shown in Figure 3.6 the appearance of iodine has a characteristic sigmoidal shape that may either refer to an autocatalytic feature or simply to a delayed consecutive reaction scheme.

Figure 3.7 indicates a series of experiments where the initial concentration of iodide was varied meanwhile the rest of the conditions was kept constant. As seen the time necessary to build up the concentration of iodine is significantly shortened by an initial addition of iodide. Consequently, it is concluded that iodide ion is a real autocatalyst of the reaction. Combining the observed clock behavior with this experimental fact, it is suggested that this reaction should better be classified as an autocatalysis-driven clock reaction.[‡]

[‡]A general concept of the characterization of different types of clock reactions can be summarized as follows: a reaction featuring clock behavior emerged from the concurrent consumption of a substrate and an appearance of a clock species is called as a *substrate-depletive clock reactions*, while a systems featuring a clock behavior emerging from the autocatalytic build-up of the clock species without depleting the substrate is called as an *autocatalysis-driven clock reaction.*

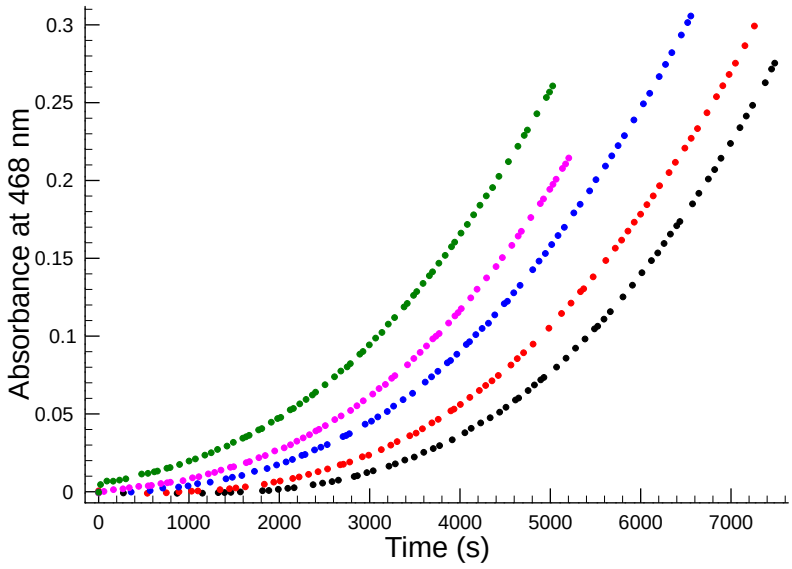

Figure 3.7: Measured absorbance–time series at 468 nm. Conditions are as follows: $[S_5O_6^{2-}]_0$ = 0.6 mM; $[IO_3^-]_0$ = 1.7 mM; pH = 1.8; I = 0.5 M. $[I^-]_0/\mu$M = 0.0 (black); 1.07 (red); 5.33 (blue); 10.0 (magenta); 25.0 (green).

To enlighten further the results presented, it is also important to analyze the dependence of the time lag necessary for the appearance of iodine as a function of the concentration of reactants. For an easy characterization, here t_i defined as a time necessary to reach the absorbance 0.01 absorbance unit at 468 nm, that corresponds to $[I_2] = 1.33 \times 10^{-5}$ M and analyzed the concentration dependence of t_i. The main advantage of this definition is that it can exactly be determined experimentally and no disturbing side reaction (precipitation of sulfur) can be taken into consideration during the analysis.

3.2.2 Concentration Dependence of t_i

Figure 3.8 shows the dependencies of t_i on the concentration of initial pentathionate meanwhile keeping the other conditions constant. One can easily realize that pH clearly affects the influence of the initial pentathionate concentration on the reciprocal of t_i. The log–log plot suggests that the formal kinetic order of pentathionate increases with decreasing pH. Since this value is significantly lower than one within the studied concentration range, it refers to a complex overall affect on

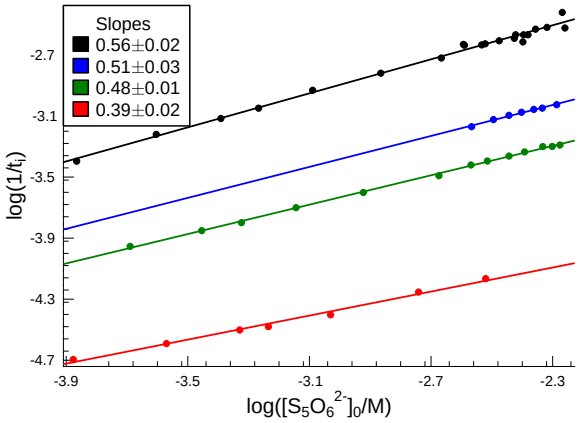

Figure 3.8: Dependence of t_i on the concentration of pentathionate. Conditions are as follows: $[IO_3^-]_0$ = 1.5 mM; pH = 1.43 (black), 1.69 (blue), 1.82 (green), 2.24 (red).

the formation of iodine. A plausible explanation of this phenomenon is that in the beginning stage of the reaction, iodate slowly oxidize pentathionate into sulfate meanwhile it is reduced to iodide ion. Iodide ion reacts further with iodate ion in the well-known Dushman reaction to produce iodine.[132] Then pentathionate slowly reduces iodine (See Chapter 3.1) to reform iodide ion ready to open up a new cycle. This reduction, however, becomes slower as the reaction proceed, because iodide ion formed inhibits the pentathionate–iodine reaction (Results shown in Chapter 3.1). As a result once the concentration of iodide ion reaches a certain value after that point the reaction is mainly governed by the Dushman reaction leaving the initiative pentathionate–iodate reaction to be unessential anymore. Consequently, at higher pHs, the initiative pentathionate–iodate reaction becomes less and less important in controlling the concentration of iodide ion, therefore t_i gradually becomes less dependent on the initial concentration of pentathionate. (It can be understood from the decreasing kinetic order of pentathionate as a function of pH.)

Figure 3.9 indicates the effect of initial concentration of iodate on t_i. It is clearly showed that the formal kinetic order of iodate can be treated as unity. As a natural continuation of the earlier point of view this experimental fact can easily be understood because Dushman reaction is a first order with respect to iodate concentration. So if the formal kinetic order of iodate in the starting pentathionate–iodate reaction is also unity then the overall effect should also give a first order dependence.

Elucidating further the concentration dependence of t_i, Figure 3.10 explains

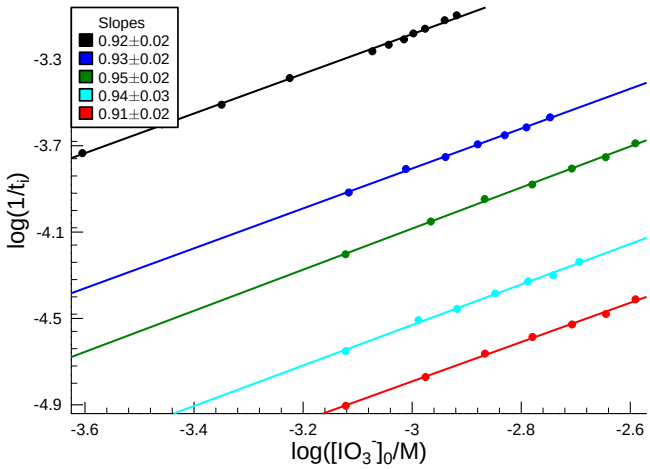

Figure 3.9: Dependence of t_i on the concentration of iodate. Conditions are as follows: $[S_5O_6^{2-}]_0$ = 0.38 mM and pH = 1.43 (black); $[S_5O_6^{2-}]_0$ = 1.0 mM and pH=1.82 (blue); $[S_5O_6^{2-}]_0$ = 0.26 mM and pH = 1.82 (green); $[S_5O_6^{2-}]_0$ = 1.0 mM and pH = 2.24 (cyan); $[S_5O_6^{2-}]_0$ = 0.25 mM and pH = 2.24 (red).

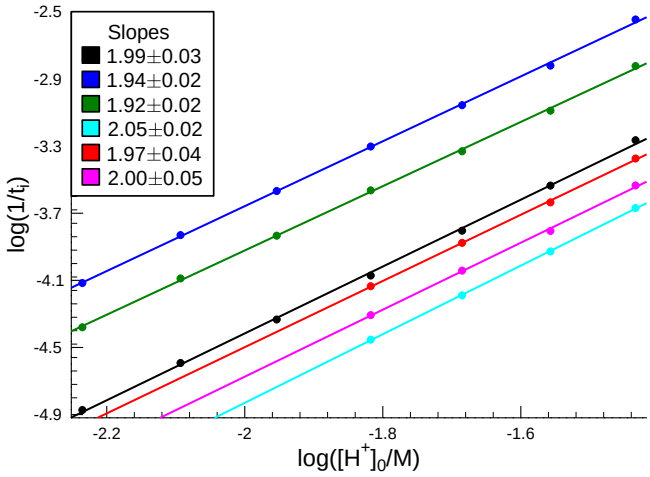

Figure 3.10: Dependence of t_i on the concentration of hydrogen ion. Conditions are as follows: $[IO_3^-]_0$ = 0.75 mM, $[S_5O_6^{2-}]_0$ = 0.5 (black); $[IO_3^-]_0$ = 1.5 mM, $[S_5O_6^{2-}]_0$ = 6.0 (blue); $[IO_3^-]_0$ = 1.5 mM, $[S_5O_6^{2-}]_0$ = 1.5 (green); $[IO_3^-]_0$ = 0.25 mM, $[S_5O_6^{2-}]_0$ = 0.38 (cyan); $[IO_3^-]_0$ = 0.6 mM, $[S_5O_6^{2-}]_0$ = 0.38 (red); $[IO_3^-]_0$ = 0.35 mM, $[S_5O_6^{2-}]_0$ = 0.38 (magenta).

that formal kinetic order of hydrogen ion is definitely two. It further supports the idea that Dushman reaction plays a central role governing the pentathionate–iodate reaction. Later it is shown that the rates of neither the starting nor any additional reaction depend on $[H^+]^2$.

3.2.3 Effect of Buffer Concentration and the Ionic Strength

It is well-known that the rate of Dushman reaction is strongly affected by the ionic strength, the nature of the buffer components and even it depends on the concentration of the buffer components as well.[133] Moreover phosphates can efficiently catalyze the iodate–iodide reaction.[134] It clearly means that if the Dushman reaction, as expected, plays a decisive role in determining the kinetics of the title reaction in pentathionate–iodate reaction system, then both the change of absolute concentration of buffer components at a constant ionic strength and pH as well as that of the ionic strength at a constant buffer composition and pH should have a significant effect on the kinetic runs. Figure 3.11 and 3.12 show the effect of the buffer components and that of the ionic strength, respectively. It is clear, as expected,

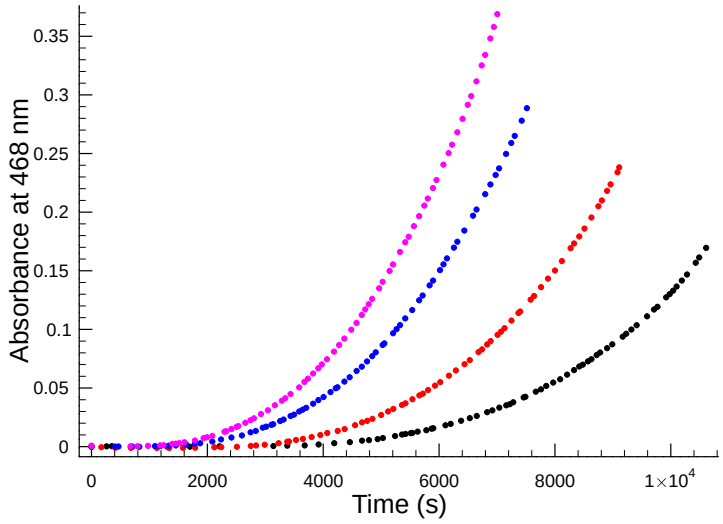

Figure 3.11: Effect of the concentration of buffer components on the formation of iodine. Conditions are as follows: $[IO_3^-]_0$ = 1.7 mM, $[S_5O_6^{2-}]_0$ = 0.6 mM, pH =1.8, I =0.5 M adjusted by the necessary amount of sodium perchlorate. $T_{PO_4^{3-}}$/M = 0.1 (black), 0.35 (red), 0.65 (blue), 0.95 (magenta).

that both of them have a significant accelerating effect on the formation of iodine. These observations therefore further support the general idea proposed above on the mechanism of the pentathionate–iodate reaction.

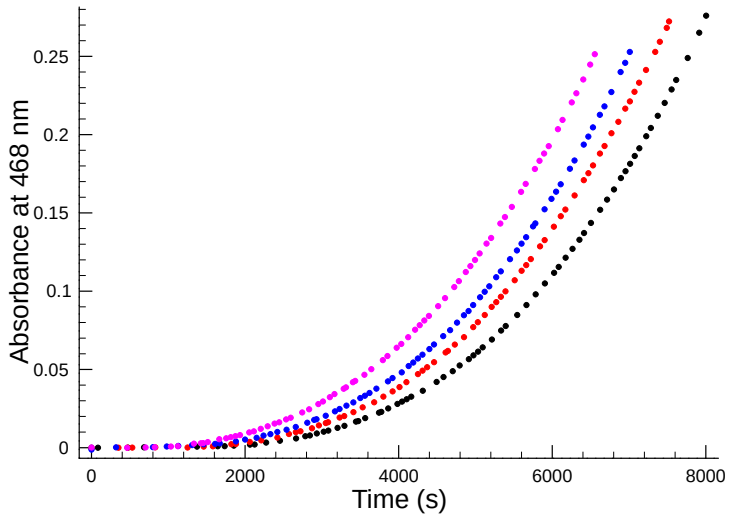

Figure 3.12: Effect of ionic strength on the formation of iodine. Conditions are as follows: $[IO_3^-]_0$ = 1.7 mM, $[S_5O_6^{2-}]_0$ = 0.6 mM, pH =1.8, $T_{PO_4^{3-}}$ =0.65 M. I = 0.334 M (black), 0.5 M (red), 0.7 M (blue), 1.0 M (magenta) adjusted by sodium perchlorate.

3.2.4 Proposed Kinetic Model

To establish the kinetic model of the title reaction for describing quantitatively the measured absorbance–time curves, it is clear that the kinetic model of the pentathionate–iodine reaction and that of Dushman reaction[132,133,135,136] should certainly be included. The species HSO_3^-, $S_2O_3OH^-$, $S_2O_3I^-$, $S_3O_3OH^-$, $S_3O_3I^-$, I_2O_2, HIO_2 and HOI are well-known intermediates of the above mentioned reactions, therefore, all the conceivable mono and bimolecular reactions of these species as well as reactants were taken into consideration during the fitting procedure. As a start the rate equation of all these reactions is supposed to have three terms, the first one was independent of $[H^+]$, the second and the third terms were proportional to $[H^+]$ and $[H^+]^2$, respectively. Those reactions that did not have any effect on the quality of fit have been systematically eliminated, and the final kinetic model is

found as follows:

$$H_3PO_4 \rightleftharpoons H^+ + H_2PO_4^- \tag{E2}$$

$$I_3^- \rightleftharpoons I_2 + I^- \tag{R10}$$

$$I_2 + H_2O \rightleftharpoons HOI + H^+ + I^- \tag{R11}$$

$$S_5O_6^{2-} + I_2 \rightleftharpoons S_5O_6I^- + I^- \tag{R12}$$

$$S_5O_6I^- + H_2O \longrightarrow S_3O_3OH^- + S_2O_3I^- + H^+ \tag{R13}$$

$$S_3O_3OH^- + 3I_2 + 5H_2O \longrightarrow 3HSO_3^- + 6I^- + 8H^+ \tag{R14}$$

$$S_2O_3I^- + I_2 + 3H_2O \longrightarrow 2HSO_3^- + 3I^- + 4H^+ \tag{R15}$$

$$HSO_3^- + I_2 + H_2O \longrightarrow SO_4^{2-} + 2I^- + 3H^+ \tag{R16}$$

$$S_5O_6^{2-} + IO_3^- + 2H_2O \longrightarrow S_3O_3OH^- + 2HSO_3^- + HOI \tag{R17}$$

$$HSO_3^- + IO_3^- \longrightarrow SO_4^{2-} + HIO_2 \tag{R18}$$

$$HIO_2 + I^- + H^+ \longrightarrow 2HOI \tag{R19}$$

$$HSO_3^- + HOI \longrightarrow SO_4^{2-} + I^- + 2H^+ \tag{R20}$$

$$IO_3^- + I^- + 2H^+ \rightleftharpoons I_2O_2 + H_2O \tag{R21}$$

$$H^+ + I^- + I_2O_2 + H_2O \longrightarrow 3HOI \tag{R22}$$

$$I_2O_2 + H_2O \longrightarrow HOI + HIO_2 \tag{R23}$$

Rate coefficients determined by nonlinear simultaneous parameter estimation are illustrated in Table 3.4

The average deviation was found to be 3.7% by a relative fitting procedure. Altogether only four fitted parameters were used, and the rest of the parameters was either fixed or directly taken from previous reports. Figure 3.13–3.15 demonstrate the quality of the fit for representative examples and also support the fact that the proposed kinetic model is working properly under the experimental conditions used here.

As indicated Step E2 is only an auxiliary process, necessary to take the slight pH change into account during the course of reaction. The ratio of rate coefficients of the rapid forward and reverse reactions was adjusted to give the pK_1 of phosphoric acid to be 1.80.[116]

Table 3.4: Fitted and fixed rate coefficients of the proposed kinetic model. No error indicates that the given parameter is fixed during the calculation process.

Step	Rate equation	Parameter value
R10	$k_{R10}[I_3^-]$	8.5×10^6 s^{-1}
	$k_{-R10}[I_2][I^-]$	5.7×10^9 $M^{-1}s^{-1}$
R11	$k_{R11}[I_2]$	0.0552 s^{-1}
	$k_{-R11}[HOI][I^-][H^+]$	1.023×10^{11} $M^{-2}s^{-1}$
R11′	$k'_{R11}[I_2][H^+]^{-1}$	1.98×10^{-3} Ms^{-1}
	$k'_{-R11}[HOI][I^-]$	3.67×10^9 $M^{-1}s^{-1}$
R12	$k_{R12}[S_5O_6^{2-}][I_2]$	10 $M^{-1}s^{-1}$
	$k_{-R12}[S_5O_6I^-][I^-]$	10^6 $M^{-1}s^{-1}$
R13	$k_{R13}[S_5O_6I^-]$	1.63 ± 0.07 s^{-1}
R14	$k_{R14}[S_3O_3OH^-][I_2]$	10^4 $M^{-1}s^{-1}$
R15	$k_{R15}[S_2O_3I^-][I_2]$	10^4 $M^{-1}s^{-1}$
R16	$k_{R16}[HSO_3^-][I_2]$	3×10^9 $M^{-1}s^{-1}$
R17	$k_{R17}[S_5O_6^{2-}][IO_3^-][H^+]$	$(2.05 \pm 0.18) \times 10^{-2}$ $M^{-2}s^{-1}$
R18	$k_{R18}[HSO_3^-][IO_3^-][H^+]$	8800 $M^{-2}s^{-1}$
R18′	$k'_{R18}[HSO_3^-][IO_3^-][H^+]^2$	10^8 $M^{-3}s^{-1}$
R19	$k_{R19}[HIO_2][I^-][H^+]$	10^9 $M^{-2}s^{-1}$
R20	$k_{R20}[HSO_3^-][HOI]$	10^9 $M^{-1}s^{-1}$
R21	$k_{R21}[IO_3^-][I^-][H^+]^2$	10^7 $M^{-3}s^{-1}$
	$k_{-R21}[I_2O_2]$	10^6 s^{-1}
R22	$k_{R22}[I_2O_2][I^-]$	$(1.72 \pm 0.12) \times 10^7$ $M^{-1}s^{-1}$
R23	$k_{R23}[I_2O_2][H^+]$	5770 ± 380 $M^{-1}s^{-1}$

Step R10 is the well-known rapid equilibrium formation of triiodide ion studied by several research groups independently.[124,125] The rate coefficients of the forward and backward reactions were directly taken as 8.5×10^6 s^{-1} and 5.7×10^9 $M^{-1}s^{-1}$, respectively to give the formation constant of triiodide as 2.83.[116]

Step R11 is the iodine hydrolysis studied thoroughly in details by Eigen,[126] Palmer[137] and Lengyel *et. al.*[127] Therefore, the rate coefficients determined by the most recent study[127] was directly adopted and fixed during the calculation procedure.

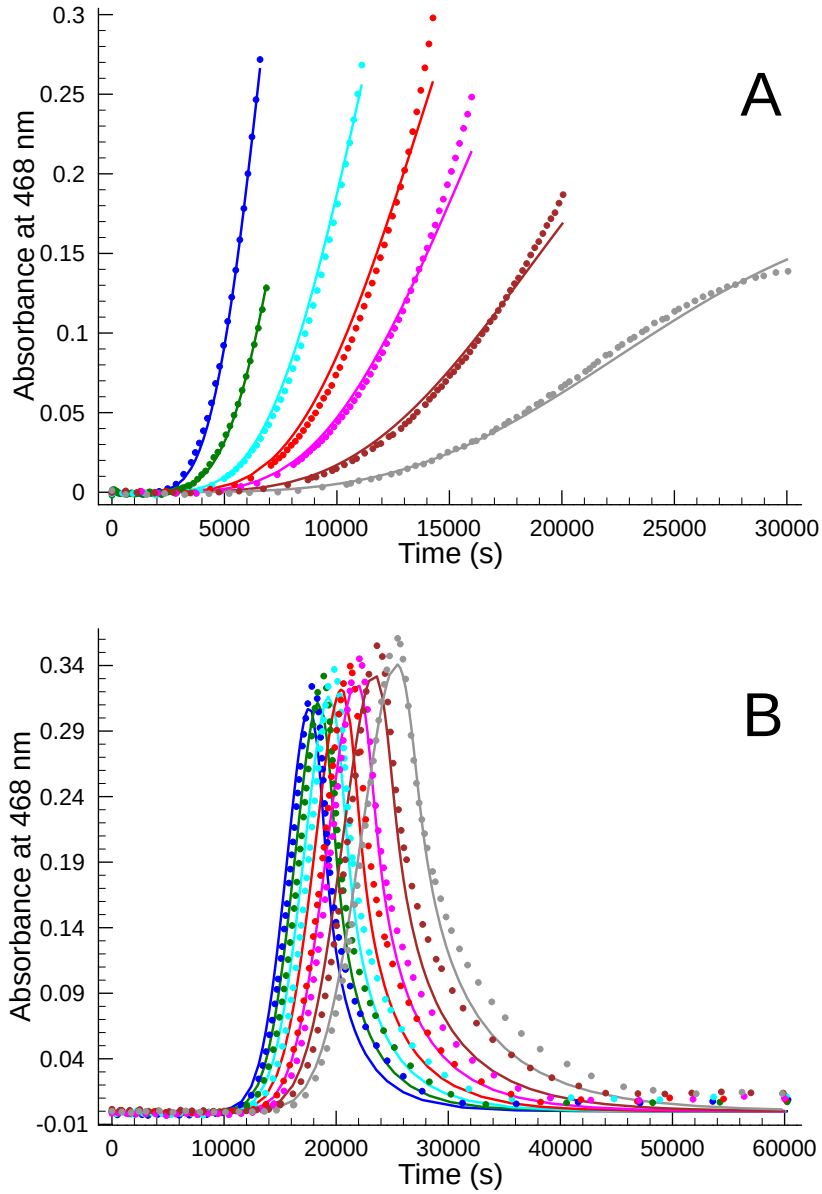

Figure 3.13: Experimental (dots) and fitted (solid lines) absorbance–time curves at 468 nm with respect to changing the concentration of pentathionate. Conditions are as follows: (A) $[IO_3^-]_0$ = 1.5 mM; pH = 1.7; $[S_5O_6^{2-}]_0$/mM = 1.9 (blue); 1.2 (green); 0.72 (cyan); 0.48 (red); 0.35 (magenta); 0.21 (brown); 0.12 (grey). (B) $[IO_3^-]_0$ = 1.5 mM; pH = 2.2; $[S_5O_6^{2-}]_0$/mM = 6.0 (blue); 5.5 (green); 5.0 (cyan); 4.5 (red); 4.0 (magenta); 3.5 (brown); 3.0 (grey).

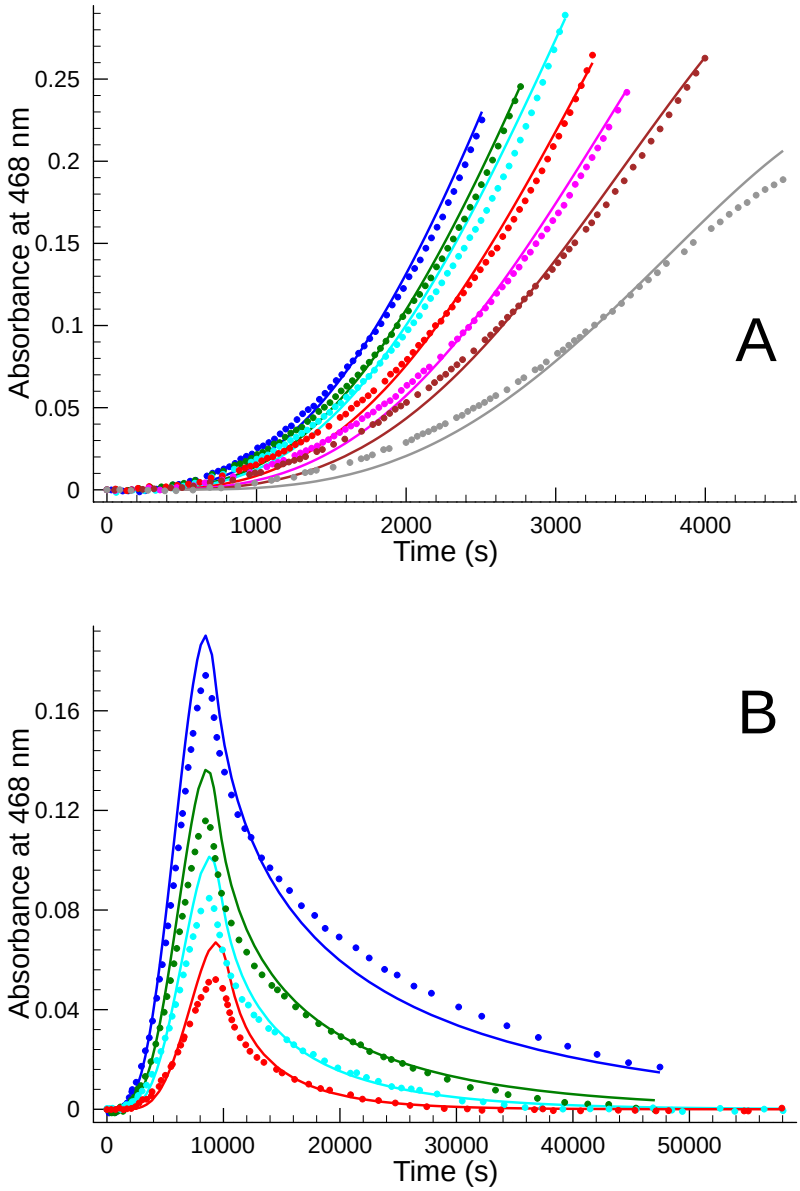

Figure 3.14: Experimental (dots) and fitted (solid lines) absorbance–time curves at 468 nm with respect to changing iodate concentration. Conditions are as follows: (A) $[S_5O_6^{2-}]_0$ = 1.0 mM; pH = 1.3; $[IO_3^-]_0$/mM = 2.0 (blue); 1.8 (green); 1.6 (cyan); 1.4 (red); 1.2 (magenta); 1.0 (brown); 0.75 (grey). (B) $[S_5O_6^{2-}]_0$ = 0.38 mM; pH = 1.4; $[S_5O_6^{2-}]_0$/mM = 0.6 (blue); 0.45 (green); 0.35 (cyan); 0.25 (red).

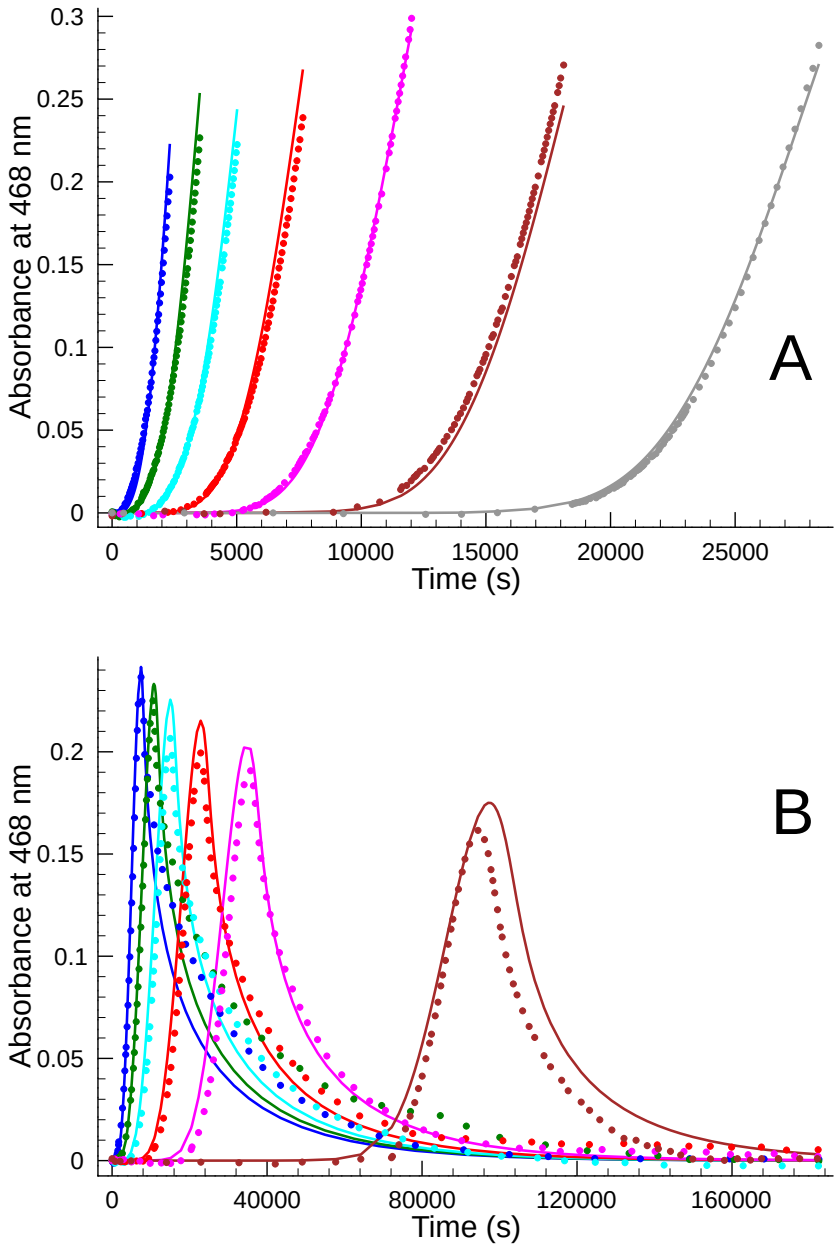

Figure 3.15: Experimental (dots) and fitted (solid lines) absorbance–time curves at 468 nm with respect to changing pH. Conditions are as follows: (A) $[S_5O_6^{2-}]_0$ = 1.5 mM; $[IO_3^-]_0$ = 1.5; pH = 1.3 (blue); 1.45 (green); 1.6 (cyan); 1.75 (red); 1.9 (magenta); 2.0 (brown); 2.2 (grey). (B) $[S_5O_6^{2-}]_0$ = 0.5 mM; $[IO_3^-]_0$ = 0.75 mM; pH = 1.3 (blue); 1.45 (green); 1.6 (cyan); 1.75 (red); 1.9 (magenta); 2.2 (brown).

Steps R12–R15 were directly adopted from the pentathionate–iodine reaction

in which R12 has already been point out to be a rapidly established equilibrium shifted far to the left. Steps R14 and R15 are rapid processes; the absolute values of these rate coefficients cannot be determined from these experiments. Therefore, the rate coefficients of k_{R12}, k_{-R12}, k_{R14} and k_{R15} have been set as 10 $M^{-1}s^{-1}$, 10^6 $M^{-1}s^{-1}$, 10^4 $M^{-1}s^{-1}$ and 10^4 $M^{-1}s^{-1}$, respectively. As a start, the k_{R13} was fixed to be 3.29 s^{-1} as determined in the pentathionate–iodine reaction, but it turned out, as expected, that this parameter can also be determined from the present work. The reason can easily be understood as follows: although at a first glance this reaction may also be treated as a Landolt-type clock reaction, the coexistence of the substrate pentathionate ion and iodine (the species determining the clock behavior) indicates that this reaction should rather belong to a different type of clock reaction. The fact that time scale of the title reaction coincides with that of the pentathionate–iodine reaction, however, provides an opportunity to determine k_{R13} from these studies as well. Here the parameter k_{R13} was found to be 1.63 ± 0.07 s^{-1}, which is in a reasonable agreement with the value obtained in the pentathionate–iodine reaction system.

Step R16 is the well-known fast reaction between HSO_3^- and iodine studied thoroughly by Yiin and Margerum[129] and its coefficient, Therefore, k_{R16}, was fixed as to be 3.1×10^9 $M^{-1}s^{-1}$ during the whole calculation process.

Step R17 is the initiation of the title reaction that essentially breaks up the sulfur chain of pentathionate. As a result, iodate is reduced to hypoiodous acid that is further reduced to iodide by bisulfite. (see: Step R20 later) Eventually this sequence of reaction generates iodide ion, the key species of the system. We found that the rate of the initiating reaction should be linearly proportional to $[H^+]$. It would suggest an apparent contradiction to our experimental findings that $1/t_i$ is proportional to square of H^+. However, this finding can easily be reconciled by the fact that once the concentration of iodide ion reaches a certain value the reaction is not governed anymore by step R17. From that point, as shown previously, the overall effect of the pentathionate–iodine and the Dushman reactions determines the conversion of the title reaction. Because the rate of the Dushman reaction is proportional to the square of $[H^+]$, the overall effect is that $1/t_i$ becomes also proportional to $[H^+]^2$. We have also tried to assign different $[H^+]$-dependencies to the initiating reaction with no success. If the rate of step R17 was considered to be pH-independent or to be dependent on $[H^+]^2$ the average deviation was found to be 9.9% and 14.4%,

respectively, from which we concluded rate of Step R28 has to depend on $[H^+]$.

Step R18 is the initial step of the Landolt reaction generating the intermediate iodous acid. The rate coefficients k_{R18} and k'_{R18} were directly adopted from a previous work and fixed during the calculation process.[138]

Step R19 is the relatively rapid comproportionation of iodous acid and iodide ion to form hypoiodous acid. The rate coefficient of this process was fixed at $k_{R19} = 10^9$ $M^{-2}s^{-1}$ as proposed by Lengyel and his coworkers.[128]

Step R20 is the fast oxidation of bisulfite by hypoiodous acid via a formal oxygen transfer process. The rate coefficient of this reaction cannot be determined directly from our present experiments. Considering that both iodine and hypoiodous acid are very reactive oxidants of S(IV) species, here k_{R20} was chosen to be 10^9 $M^{-1}s^{-1}$, close to that of Step R16.

Step R21 is the well-accepted initiating equilibrium of the Dushman reaction,[132,133] where I_2O_2 is considered to be a steady-state intermediate originally proposed by Bray to explain the complex rate equation of Dushman reaction.[139] Later, an experimental evidence of the formation of $H_2I_2O_3$ was also reported in huge excess of iodate at highly acidic conditions,[140] but I_2O_2 and $H_2I_2O_3$ kinetically are indistinguishable species. So far this equilibrium constant has not been determined, therefore to provide I_2O_2 as a low concentration steady-state intermediate and to establish the equilibrium rapidly under the present time scale, k_{R21} and k_{-R21} were set to be 10^7 $M^{-3}s^{-1}$ and 10^6 s^{-1}, respectively.

Steps R22 and R23 are the main driving force of the Dushman reaction in absence and presence of iodide ion, respectively. It is generally thought that buffer assistance occurs via further reactions of the intermediate I_2O_2.[133] Part of present experiments provided an opportunity to show the effect of buffer components ($H_2PO_4^-$) concentration on the values of k_{R22} and k_{R23}. The results are shown in Figure 3.16. As expected a strong influence is obtained that clearly supports the general idea of the buffer-assisted pathway of reactions of I_2O_2. Survey of the literature implies that this is the first direct experimental evidence that such an effect can uniquely be attributed to a certain part of reaction sequences involved in an overall reaction mechanism obtained from a global simultaneous fit of series of experiments. As can also be seen from Figure 3.16, the practical linear dependence of k_{R22} and k_{R23} on $[H_2PO_4^-]_0$ offers a convenient tool to check the reliability of these rate coefficients obtained from majority of the experiments at $[H_2PO_4^-]_0 = 0.1$ M. At this

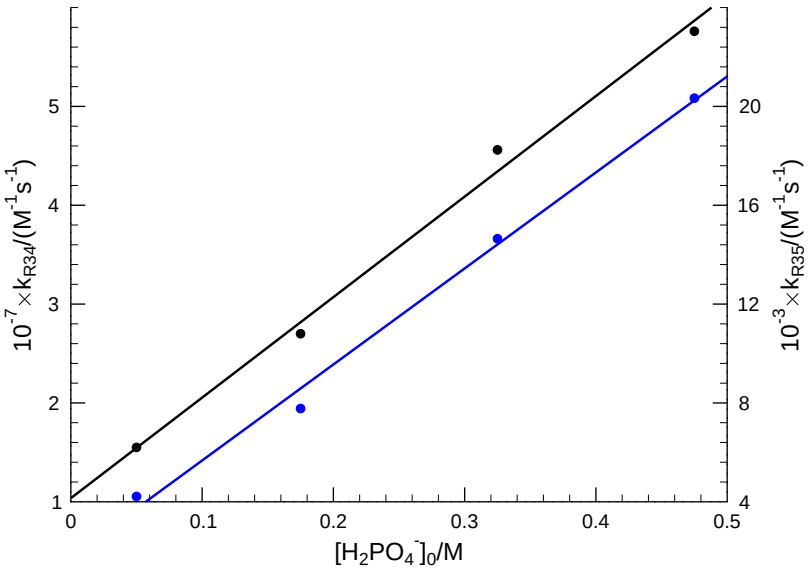

Figure 3.16: Plot of k_{R22} and k_{R23} against the initial concentration of $[H_2PO_4^-]_0$ at I = 0.5 M and pH = 1.80. $[S_5O_6^{2-}]_0$ = 0.6 mM and $[IO_3^-]_0$ = 1.7 mM.

condition, Figure 3.16 provides for $k_{R22} = 2.05 \times 10^7$ $M^{-1}s^{-1}$ and $k_{R23} = 5670$ $M^{-1}s^{-1}$ meaning that both values are in a very good agreement with the corresponding values indicated in Table 3.4. Furthermore, it provides a possibility to compare the rate coefficient of the overall Dushman reaction with $K_{R21}k_{R22} = 2.05 \times 10^8$ $M^{-4}s^{-1}$ which is approximately an order of magnitude lower than found in presence of acetic acid/acetate buffer,[135] but it is in a very good agreement with the value (3.2×10^8 $M^{-4}s^{-1}$) obtained at acetate buffer free conditions.[133]

A word is in order here as well regarding the explanation of the autocatalytic effect of iodide ion. As can be seen sequence of steps R17 and R20 produces iodide ion in a slow process at beginning stage of the reaction resulting in its accumulation. Once its concentration reaches a certain level it ignites the overall Dushman reaction (see: Steps R21–R23) that produces iodine. However at this stage, the concentration of pentathionate is still high enough to reduce completely iodine into iodide ion essentially within no time resulting in a further, but accelerated accumulation of the autocatalyst. This stage lasts until the concentration of pentathionate ion becomes low enough not to remove iodine rapidly anymore. As a result it rings the bell for the clock behavior. Of course this stage is further enhanced by

the fact that increasing iodide ion concentration inhibits the pentathionate–iodine reaction. Moreover, it means that although iodine has already appeared in the solution, pentathionate ion also exists in a detectable amount. Furthermore, even in relative excess of the substrate, iodine persists for a fairly long time but finally depending on the excess of substrate, iodine disappears from the solution. A selected example is indicated in Figure 3.17. In that sense this reaction differs from

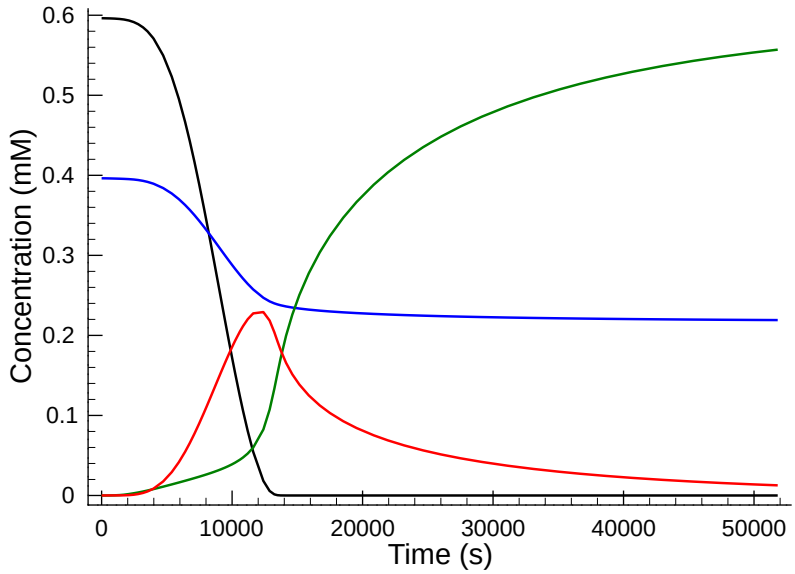

Figure 3.17: Simulated concentration–time curves in pentathionate excess. Conditions are as follows pH = 1.4; $[S_5O_6^{2-}]_0 = 0.4$ mM and $[IO_3^-]_0 = 0.6$ mM. Concentrations of iodine and iodide ion are indicated by red and green color, respectively.

the original Landolt clock-reaction because in that case, iodine cannot appear unless bisulfite is exhausted. Moreover the original Landolt reaction does not exhibit clock behavior if the substrate is in stoichiometric excess. In other words, it means that the so called Landolt-time (the time point of the appearance of iodine) and the time of the complete consumption of the substrate (bisulfite) necessarily coincides in case of the Landolt reaction. In addition to that certain stoichiometric constraints must be held to observe the appearance of iodine. Opposite to this, in case of pentathionate–iodate reaction the time point of appearance of iodine in the solution and the time point of the complete consumption of substrate are distinctly different. Furthermore even in stoichiometric excess of the substrate the

clock species (iodine) appears. It raises an important question whether the title reaction can be classified as a clock reaction or not. It is out of question that the main core of the present reaction and that of the Landolt reaction are the same. It is also clear that the present system also displays clock-behavior, *i.e.* the clock species appears after a well-defined and reproducible time lag. A common sense therefore suggests that it should be designated as a clock reaction. However the main difference, namely the substrate coexists with the clock species for a long period of time, supports that concept that this reaction should rather be classified in a different category of clock reaction. Therefore the Landolt reaction may be classified as the substrate-depletive clock reaction category while the pentathionate–iodate system should be autocatalysis-driven clock reaction category.

Finally we should also mention again that the proposed model has to be extended because it is not able to explain the formation of colloidal sulfur. It is, however, out of the scope of this study, because appearance of colloidal sulfur prevents the quantitative determination of any species by UV-vis spectroscopy. Aforementioned it was enlightened that those parts of the kinetic curves were truncated meaning that there is not enough quantitative experimental information to propose a firmly based route leading to the formation of colloidal sulfur.

3.3 Reaction of Pentathionate Ion with Periodate Ion

3.3.1 Preliminary Observation

As expected an absorbance–time profile similar to the pentathionate–iodate system mentioned above was recorded. Figure 3.18 clearly indicated that iodine is formed only after a fairly long time lag that strongly depends on the initial concentration of the reactants as well as the pH. Another similarity to the pentathionate–iodate system, namely that an absorbance increase at 800 nm, can also be observed. It suggests that a light-scattering species must also be produced during the course of the reaction because none of the possible products has detectable absorbance at this wavelength. Furthermore after completion of the reaction a detectable amount of colloidal sulfur can be collected from the cuvette. It means that an elementary sulfur producing reaction must be involved in the mechanism. Since a light-scattering species disturbs the quantitative absorbance detection, for quantitative simultane-

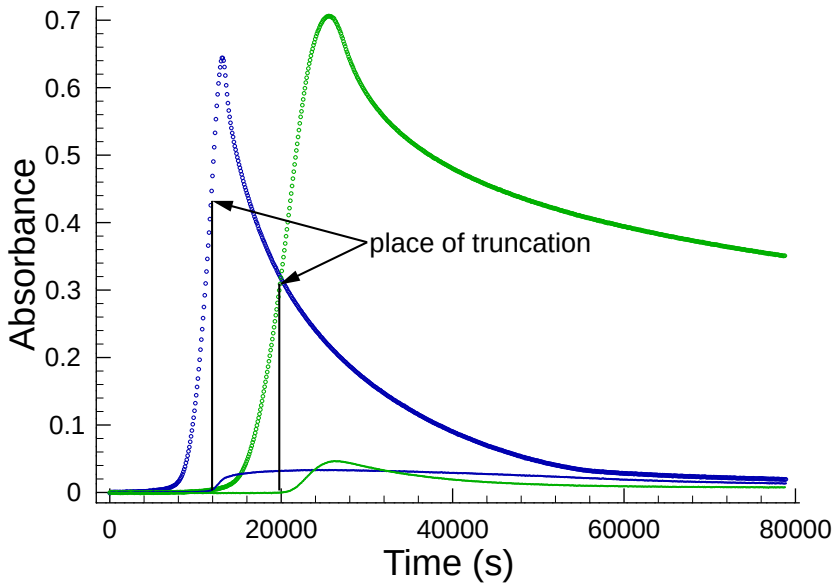

Figure 3.18: Experimental absorbance–time series at two different wavelengths. Conditions are as follows: $[S_5O_6^{2-}]_0 = [IO_4^-]_0 = 2.0$ mM, pH = 1.94 (blue); $[S_5O_6^{2-}]_0 = 0.8$ mM, $[IO_4^-]_0 = 2.0$ mM, pH = 1.94 (green). Empty circles indicates the absorbance measured at 468 nm, while the solid lines represent the measured absorbance at 800 nm.

ous evaluation of the kinetic curves, the kinetic curves should be truncated from the time point, where colloidal sulfur precipitation occurs. Such an example can be seen in Figure 3.18.

Another important observation has to be emphasized as well. In an excess of pentathionate, iodine appears before complete depletion of the substrate pentathionate due to the slow pentathionate–iodine reaction. Of course the concentration of iodine decreases once its production from the sequence of the original reactions ceases and may completely disappear at high excess of pentathionate. In addition to that, initially added trace amount of iodide ion (shown in Figure 3.19) significantly decreases the time necessary for appearance of iodine. Consequently, iodide ion plays a key role in determining the kinetics of the reaction. We shall see later that iodide ion is an autocatalyst of the system therefore the pentathionate–periodate reaction can also be classified as an autocatalysis-driven clock reaction like pentathionate–iodate reaction system.

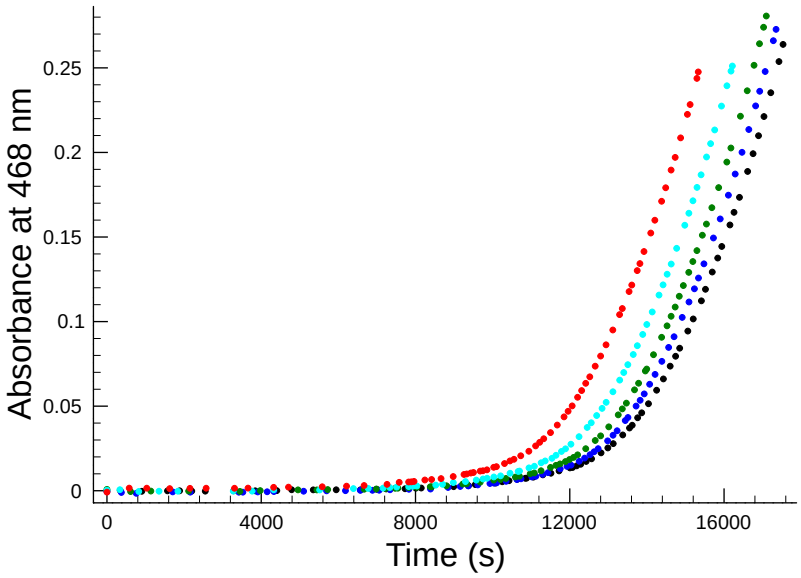

Figure 3.19: Measured absorbance–time series at 468 nm. Conditions are as follows: $[S_5O_6^{2-}]_0$ = 0.6 mM; $[IO_4^-]_0$ = 1.7 mM; pH = 1.8; I=0.5 M. $[I^-]_0/\mu$M = 0.0 (black); 1.07 (blue); 2.67 (green); 5.33 (cyan); 9.78 (red).

The absorbance–time profiles of the measured kinetic curves suggest that initial rate studies are a non-informative way for characterization of the concentration dependence of the reactants. To visualize quantitatively the effect of the reactants and the pH on the reaction, we defined t_i as a time necessary to reach the absorbance 0.01 absorbance unit at 468 nm, that corresponds to $[I_2]$ = 1.33×10^{-5} M and analyzed the concentration dependence of t_i. The main advantage of this definition is that it can exactly be determined experimentally and no disturbing side reaction (precipitation of sulfur) have to be taken into consideration during the analysis.

3.3.2 Concentration Dependence of t_i

Figure 3.20 shows the dependencies of t_i on the concentration of pentathionate meanwhile keeping rest of the conditions constant.

One can easily realize that the pH significantly affects the dependence of concentration of pentathionate on the reciprocal of t_i. The log–log plot suggests that the formal kinetic order of pentathionate increases with increasing of pH which seems to be a completely opposite effect observed experimentally in case of the corre-

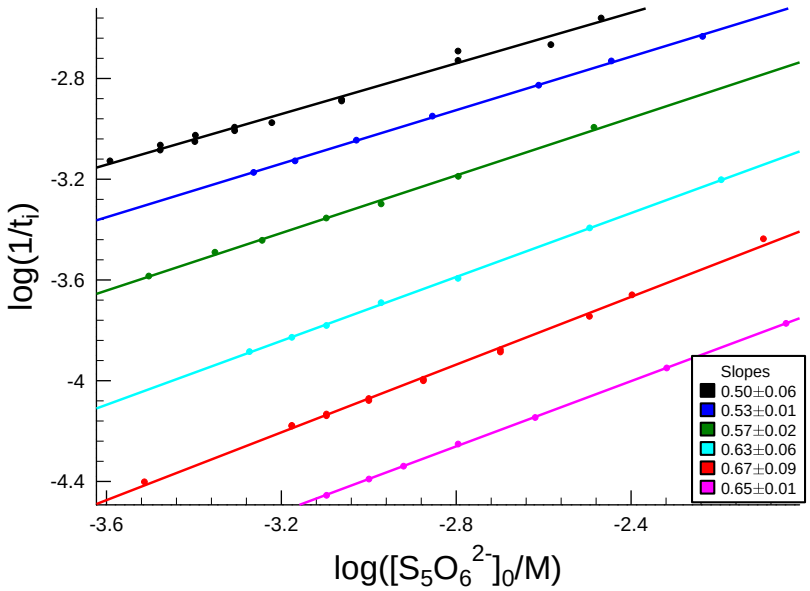

Figure 3.20: Dependence of t_i on the concentration of pentathionate. Conditions are as follows: $[IO_4^-]_0$ = 1.5 mM and pH = 1.1 (black); $[IO_4^-]_0$ = 1.5 mM and pH = 1.31 (blue); $[IO_4^-]_0$ = 2.0 mM and pH = 1.52 (green); $[IO_4^-]_0$ = 2.0 mM and pH = 1.73 (cyan); $[IO_4^-]_0$ = 2.0 mM and pH = 1.93 (red); $[IO_4^-]_0$ = 2.5 mM and pH = 2.15 (magenta).

sponding pentathionate–iodate reaction. Since this value is significantly lower than unity within the concentration range studied, it refers to a complex overall effect on the formation of iodine. A conceivable explanation of this observation is that at higher pHs, mainly the initial step governs the kinetics via the rate-determining step of formation of iodide ion followed by the essentially pH independent processes like the overall pentathionate–iodine and iodide–periodate[141] reactions. Once the pH decreases, the contribution of the Dushman reaction[132] to the overall kinetics becomes more and more pronounced, consequently the effect of the initial pentathionate concentration becomes negligible resulting in decreasing of its formal kinetic order.

Figure 3.21 indicates the dependence of initial periodate concentration on t_i that seems to be again completely different with that observed in the pentathionate–iodate reaction. In case of the pentathionate–iodate reaction the formal kinetic order of iodate was found to be strictly unity corresponding to the fact that the rate of both the initiative pentathionate–iodate and Dushman reactions depends on the

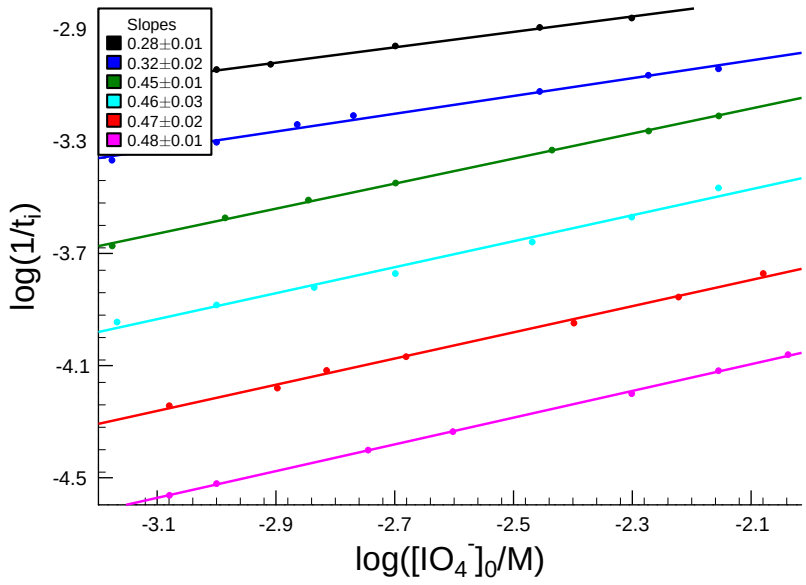

Figure 3.21: Dependence of t_i on the concentration of periodate. Conditions are as follows: $[S_5O_6^{2-}]_0$ = 0.49 mM and pH = 1.1 (black); $[S_5O_6^{2-}]_0$ = 0.55 mM and pH=1.31 (blue); $[S_5O_6^{2-}]_0$ = 0.57 mM and pH = 1.52 (green); $[S_5O_6^{2-}]_0$ = 0.8 mM and pH = 1.73 (cyan); $[S_5O_6^{2-}]_0$ = 1.0 mM and pH = 1.93 (red); $[S_5O_6^{2-}]_0$ = 1.0 mM and pH = 2.15 (magenta).

first power of $[IO_3^-]$. Opposite to that, in the pentathionate–periodate reaction, the formal kinetic order with respect to periodate is significantly lower than unity and it seems to depend on pH. It clearly shows that the lower the pH is, the more the t_i becomes independent of the concentration of periodate. A feasible explanation of this experimental finding is that iodate formed during the course of the iodide–periodate reaction[141] is a key intermediate of the pentathionate–periodate reaction. As the pH decreases, more and more significant contribution from the Dushman reaction and the pentathionate–iodate reaction is expected to occur to the overall kinetics of the parent system. Consequently, the pH-independent iodide–periodate reaction becomes less and less effective to govern the reaction resulting in the cessation of the effect of periodate on t_i.

To further elucidate the concentration dependence of t_i, the effect of pH on the reaction has also been studied. Figure 3.22 explains that the formal kinetic order of hydrogen ion is between 1 and 2 which is also a significant difference

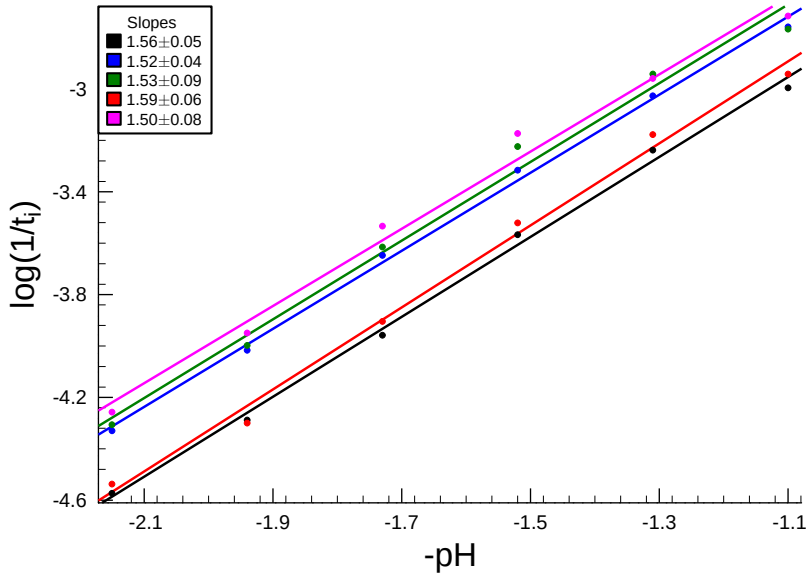

Figure 3.22: Dependence of t_i on the concentration of hydrogen ion. Conditions are as follows: $[IO_4^-]_0$ = 1.5 mM, $[S_5O_6^{2-}]_0$ = 0.5 (black); $[IO_4^-]_0$ = 5.0 mM, $[S_5O_6^{2-}]_0$ = 0.5 (blue); $[IO_4^-]_0$ = 1.5 mM, $[S_5O_6^{2-}]_0$ = 1.5 (green); $[IO_4^-]_0$ = 1.5 mM, $[S_5O_6^{2-}]_0$ = 0.6 (red); $[IO_4^-]_0$ = 5.0 mM, $[S_5O_6^{2-}]_0$ = 0.8 mM (magenta).

compared to that found in the corresponding pentathionate–iodate reaction. This observation can easily be explained because of the consequence of the fact that the overall kinetics of the title reaction is governed by the pentathionate–periodate, pentathionate–iodate, pentathionate–iodine, iodide–periodate and Dushman reactions. Significant differences of pH dependence of these reactions, namely, the pH-independent pentathionate–iodine and iodide–periodate reactions, first order dependence of $[H^+]$ of the initiative step in case of the pentathionate–iodate and pentathionate–periodate reactions, as well as the second-order dependence of the Dushman reaction with respect to H^+ accounts for the complex pH effect found here.

3.3.3 Effect of Buffer Concentration and the Ionic Strength

As mentioned in section 3.2, the Dushman reaction is strongly affected by the ionic strength and catalyzed by phosphates. The pentathionate–iodate reaction is also very sensitive to the concentration of the buffer components and that of the

ionic strength. Therefore, the hypothesis that the pentathionate–iodate and the Dushman reactions play a key role in determining the kinetic behavior of parent system can indirectly be checked via the influence of the ionic strength and the total buffer concentration. Figures 3.23 and 3.24 depict the effect of the buffer components and that of the ionic strength on the kinetic runs, respectively. It is

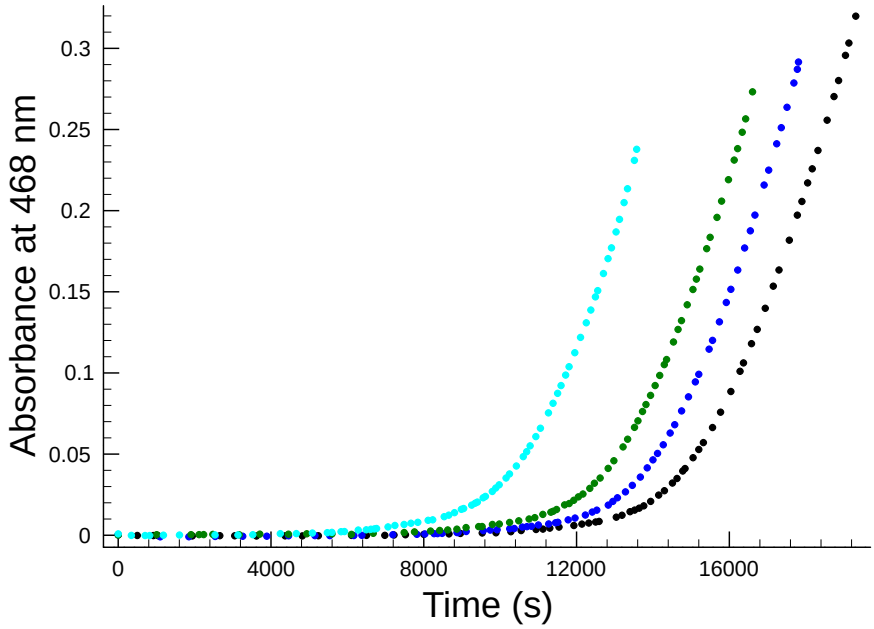

Figure 3.23: Effect of ionic strength on the formation of iodine. Conditions are as follows: $[IO_4^-]_0$ = 1.7 mM, $[S_5O_6^{2-}]_0$ = 0.6 mM, pH = 1.8, $T_{PO_4^{3-}}$ = 0.65 M. I = 0.33 M (black); 0.5 M (blue); 0.7 M (green); 1.0 M (cyan) adjusted by sodium perchlorate.

clear, as anticipated, that both the increase of ionic strength and that of the buffer components concentration have an accelerating effect on the formation of iodine. These observations, therefore, give a further decisive evidence that the main core of the proposed kinetic model has to include both the pentathionate–iodate and Dushman reactions.

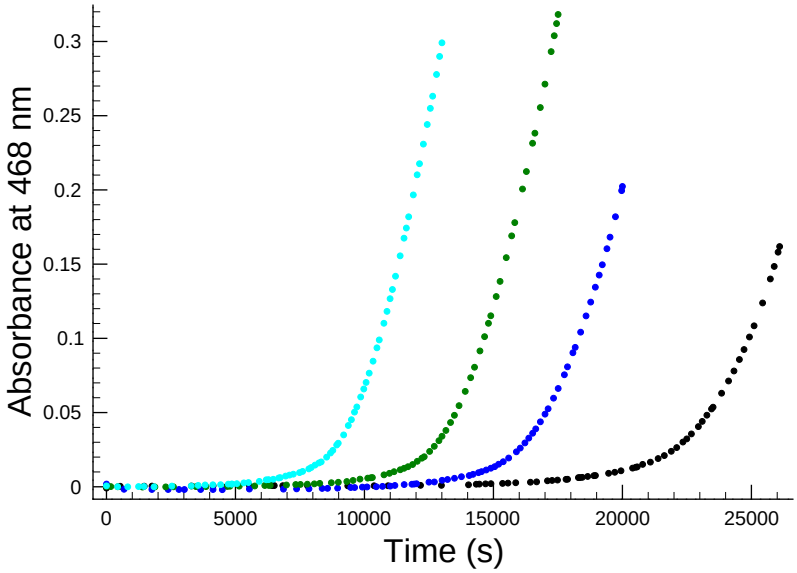

Figure 3.24: Effect of the concentration of buffer components on the formation of iodine. Conditions are as follows: $[IO_3^-]_0$ = 1.7 mM, $[S_5O_6^{2-}]_0$ = 0.6 mM, pH =1.8, I =0.5 M adjusted by the necessary amount of sodium perchlorate. $T_{PO_4^{3-}}$/M = 0.1 (black); 0.35 (blue); 0.65 (green); 0.95 (cyan).

3.3.4 Proposed Kinetic Model

To establish the kinetic model, first the kinetic model of the pentathionate–iodate reaction was completely taken into consideration as described in the previous chapter. This model was then supplemented by the conceivable reactions of periodate with reactants, intermediates and the product iodide ion. As a start the rate equations of all these reactions were supposed to have three therms, namely, the one was independent of pH, the others were proportional to $[H^+]$ and $[H^+]^2$, respectively. Systematic elimination of the reactions which have no any effect on the quality of the fit finally led to the following kinetic model:

$$H_2SO_3 \rightleftharpoons H^+ + HSO_3^- \tag{E3}$$

$$HIO_4 \rightleftharpoons H^+ + IO_4^- \tag{E4}$$

$$I_3^- \rightleftharpoons I_2 + I^- \tag{R24}$$

$$I_2 + H_2O \rightleftharpoons HOI + H^+ + I^- \quad \text{(R25)}$$

$$S_5O_6^{2-} + I_2 \rightleftharpoons S_5O_6I^- + I^- \quad \text{(R26)}$$

$$S_5O_6I^- + H_2O \longrightarrow S_3O_3OH^- + S_2O_3I^- + H^+ \quad \text{(R27)}$$

$$S_3O_3OH^- + 3I_2 + 5H_2O \longrightarrow 3HSO_3^- + 6I^- + 8H^+ \quad \text{(R28)}$$

$$S_2O_3I^- + I_2 + 3H_2O \longrightarrow 2HSO_3^- + 3I^- + 4H^+ \quad \text{(R29)}$$

$$HSO_3^- + I_2 + H_2O \longrightarrow SO_4^{2-} + 2I^- + 3H^+ \quad \text{(R30)}$$

$$S_5O_6^{2-} + IO_3^- + 2H_2O \longrightarrow S_3O_3OH^- + 2HSO_3^- + HOI \quad \text{(R31)}$$

$$HSO_3^- + IO_3^- \longrightarrow SO_4^{2-} + HIO_2 \quad \text{(R32)}$$

$$HIO_2 + I^- + H^+ \longrightarrow 2HOI \quad \text{(R33)}$$

$$HSO_3^- + HOI \longrightarrow SO_4^{2-} + I^- + 2H^+ \quad \text{(R34)}$$

$$IO_3^- + I^- + 2H^+ \rightleftharpoons I_2O_2 + H_2O \quad \text{(R35)}$$

$$H^+ + I^- + I_2O_2 + H_2O \longrightarrow 3HOI \quad \text{(R36)}$$

$$I_2O_2 + H_2O \longrightarrow HOI + HIO_2 \quad \text{(R37)}$$

$$S_2O_3OH^- + IO_3^- + H_2O \longrightarrow HIO_2 + 2HSO_3^- \quad \text{(R38)}$$

$$S_5O_6^{2-} + HIO_4 + H_2O \longrightarrow S_2O_3OH^- + S_3O_3OH^- + IO_3^- + H^+ \quad \text{(R39)}$$

$$I^- + IO_4^- + H^+ \longrightarrow HOI + IO_3^- \quad \text{(R40)}$$

$$I^- + IO_4^- + 2H^+ \longrightarrow 2HIO_2 \quad \text{(R41)}$$

$$IO_4^- + HSO_3^- \longrightarrow SO_4^{2-} + IO_3^- + H^+ \quad \text{(R42)}$$

$$IO_4^- + S_2O_3OH^- + H_2O \longrightarrow HOI + 2SO_4^{2-} + 2H^+ \quad \text{(R43)}$$

$$IO_4^- + S_3O_3OH^- + 2H_2O \longrightarrow H^+ + HOI + 3HSO_3^- \quad \text{(R44)}$$

$$IO_4^- + S_2O_3I^- + H_2O \longrightarrow I_2 + 2SO_4^- + 2H^+ \quad \text{(R45)}$$

$$HIO_4 + S_5O_6I^- + 5H_2O \longrightarrow 6H^+ + 2I^- + 5HSO_3^- \quad \text{(R46)}$$

$$IO_4^- + HIO_2 \longrightarrow 2IO_3^- + H^+ \quad \text{(R47)}$$

Rate coefficients determined by nonlinear simultaneous parameter estimation are illustrated in Table 3.5. The average deviation was found to be 4.9% by a relative fitting procedure. Altogether only 13 fitted parameters were used, and the rest of the parameters was either fixed or directly taken from previous reports.

Table 3.5: Fitted and fixed rate coefficients of the proposed kinetic model. No error indicates that the given parameter is fixed during the calculation process.

Step	Rate equation	Parameter value
R24	$k_{R24}[I_3^-]$	8.5×10^6 s^{-1}
	$k_{-R24}[I_2][I^-]$	5.7×10^9 $M^{-1}s^{-1}$
R25	$k_{R25}[I_2]$	0.0552 s^{-1}
	$k_{-R25}[HOI][I^-][H^+]$	1.023×10^{11} $M^{-2}s^{-1}$
R25′	$k'_{R25}[I_2][H^+]^{-1}$	1.98×10^{-3} Ms^{-1}
	$k'_{-R25}[HOI][I^-]$	3.67×10^9 $M^{-1}s^{-1}$
R26	$k_{R26}[S_5O_6^{2-}][I_2]$	10 $M^{-1}s^{-1}$
	$k_{-R26}[S_5O_6I^-][I^-]$	10^6 $M^{-1}s^{-1}$
R27	$k_{R27}[S_5O_6I^-]$	4.83 ± 0.39 s^{-1}
R28	$k_{R28}[S_3O_3OH^-][I_2]$	10^4 $M^{-1}s^{-1}$
R29	$k_{R29}[S_2O_3I^-][I_2]$	10^4 $M^{-1}s^{-1}$
R30	$k_{R30}[HSO_3^-][I_2]$	3×10^9 $M^{-1}s^{-1}$
R31	$k_{R31}[S_5O_6^{2-}][IO_3^-][H^+]$	0.0205 $M^{-2}s^{-1}$
R32	$k_{R32}[HSO_3^-][IO_3^-][H^+]$	8800 $M^{-2}s^{-1}$
R32′	$k'_{R32}[HSO_3^-][IO_3^-][H^+]^2$	10^8 $M^{-3}s^{-1}$
R33	$k_{R33}[HIO_2][I^-][H^+]$	10^9 $M^{-2}s^{-1}$
R34	$k_{R34}[HSO_3^-][HOI]$	10^9 $M^{-1}s^{-1}$
R35	$k_{R35}[IO_3^-][I^-][H^+]^2$	10^7 $M^{-3}s^{-1}$
	$k_{-R35}[I_2O_2]$	10^6 s^{-1}
R36	$k_{R36}[I_2O_2][I^-]$	$(1.10 \pm 0.11) \times 10^7$ $M^{-1}s^{-1}$
R37	$k_{R37}[I_2O_2][H^+]$	10670 ± 990 $M^{-1}s^{-1}$
R38	$k_{R38}[S_2O_3OH^-][IO_3^-][H^+]$	$(4.60 \pm 0.29) \times 10^4$ $M^{-2}s^{-1}$
R39	$k_{R39}[S_5O_6^{2-}][HIO_4]$	0.0121 ± 0.0022 $M^{-1}s^{-1}$
R40	$k_{R40}[I^-][IO_4^-]$	5.52 ± 0.39 $M^{-1}s^{-1}$
R40′	$k'_{R40}[I^-][HIO_4]$	15.2 ± 0.9 $M^{-1}s^{-1}$
R41	$k_{R41}[I^-][IO_4^-]$	0.792 ± 0.061 $M^{-1}s^{-1}$
R42	$k_{R42}[HSO_3^-][IO_4^-]$	$(1.16 \pm 0.15) \times 10^6$ $M^{-1}s^{-1}$
R43	$k_{R43}[S_2O_3OH^-][HIO_4][H^+]$	95.2 ± 8.9 $M^{-2}s^{-1}$
R44	$k_{R44}[S_3O_3OH^-][IO_4^-]$	0.093 ± 0.008 $M^{-1}s^{-1}$
R45	$k_{R45}[S_2O_3I^-][IO_4^-]$	1.7×10^6 $M^{-1}s^{-1}$
R46	$k_{R46}[S_5O_6I^-][HIO_4]$	2410 ± 185 $M^{-1}s^{-1}$
R47	$k_{R47}[IO_4^-][HIO_2]$	$(5.19 \pm 0.35) \times 10^5$ $M^{-1}s^{-1}$

Figures 3.25–3.27 demonstrate the quality of the fit for representative examples and also support the fact that the proposed kinetic model is working properly under our experimental conditions.

As in pentathionate–iodate reaction system, step E2 is also only an auxiliary process, necessary to take the slight pH change into consideration during the course of reaction. Step E3 and E4 were also included because both HSO_3^- and IO_4^- are protonated within the pH range studied and the reactivity difference of their forms may also have influence on the kinetic runs. The ratio of rate coefficients of the rapid forward and reverse reactions was adjusted to give the corresponding pK_a of phosphoric, sulfurous and periodic acid to be 1.80, 1.85, and 1.64, respectively.[116]

As mentioned previously, steps R24–R37 were directly taken from the section 3.3. Majority of the rate coefficients was fixed during the calculation process except for k_{R27}, k_{R36} and k_{R37}. In case of k_{R27}, k_{R36} and k_{R37} the values calculated here were found to be a reasonable agreement with those that found in pentathionate–iodate and pentathionate–iodine systems. It is, however, worthwhile to note that both k_{R36} and k_{R37} differ by approximately a factor of two from the previously determined ones that can readily be explained by the different experimental circumstances applied. As shown in the pentathionate–iodate reaction, both values are very sensitive to the concentration of the buffer components as they are linearly proportional to $[H_2PO_4^-]$. In contrast to this, the value of k_{R27} was found here to be a notably higher than the values in pentathionate–iodate and pentathionate–iodine systems. It seems to suggest that the pentathionate–iodine reaction must also be sensitive to the quality of the buffer applied as well as the absolute concentration of the buffer components.

Step R38 has already been proposed previously but the rate coefficient k_{R38} was found to be slightly less (approximately 5 times) here compared to a report of a previous study.[56] A feasible explanation of this fact would be the difference between the qualities of the buffer applied giving rise to an appearance of specific catalytic effect of acetate buffer on the $S_2O_3OH^-$–iodate reaction. In lack of pure $S_2O_3OH^-$, however, it can therefore be treated only as a hypothesis.

Step R39 is the initiation of the title reaction to breakup the sulfur chain of pentathionate resulting in the formation of $S_2O_3OH^-$, $S_3O_3OH^-$ and iodate. $S_2O_3OH^-$ and $S_3O_3OH^-$ are intermediates of the reaction to be oxidized further by periodate/periodic acid eventually resulting in the formation of iodide ion in a finite

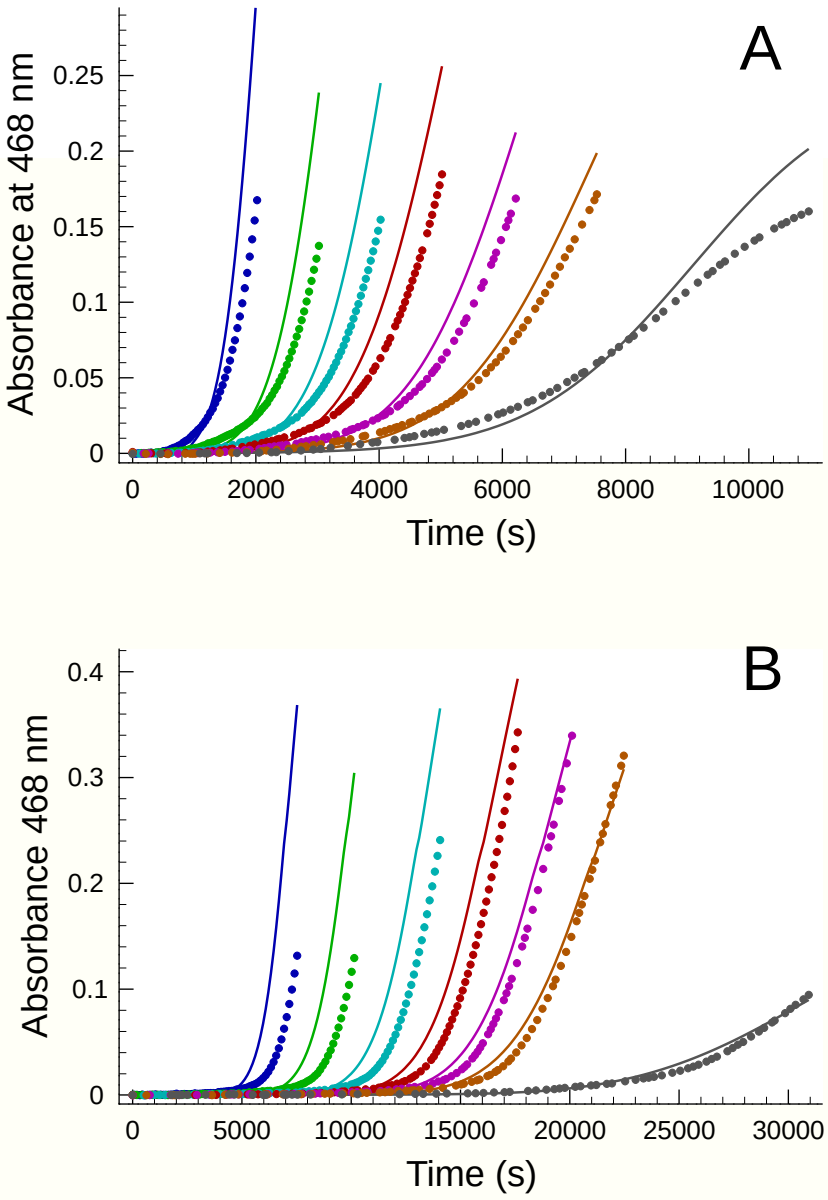

Figure 3.25: Experimental (dots) and fitted (solid lines) absorbance–time curves at 468 nm with respect to changing the concentration of pentathionate. Conditions are as follows: (A) $[IO_4^-]_0$ = 2.0 mM; pH = 1.52; $[S_5O_6^{2-}]_0$/mM = 3.27 (blue); 1.60 (green); 1.07 (cyan); 0.80 (red); 0.57 (magenta); 0.445 (brown); 0.314 (gray). (B) $[IO_4^-]_0$ = 2.0 mM; pH = 1.94; $[S_5O_6^{2-}]_0$/mM = 3.2 (blue); 2.0 (green); 1.33 (cyan); 1.0 (red); 0.80 (magenta); 0.667 (brown); 0.307 (gray).

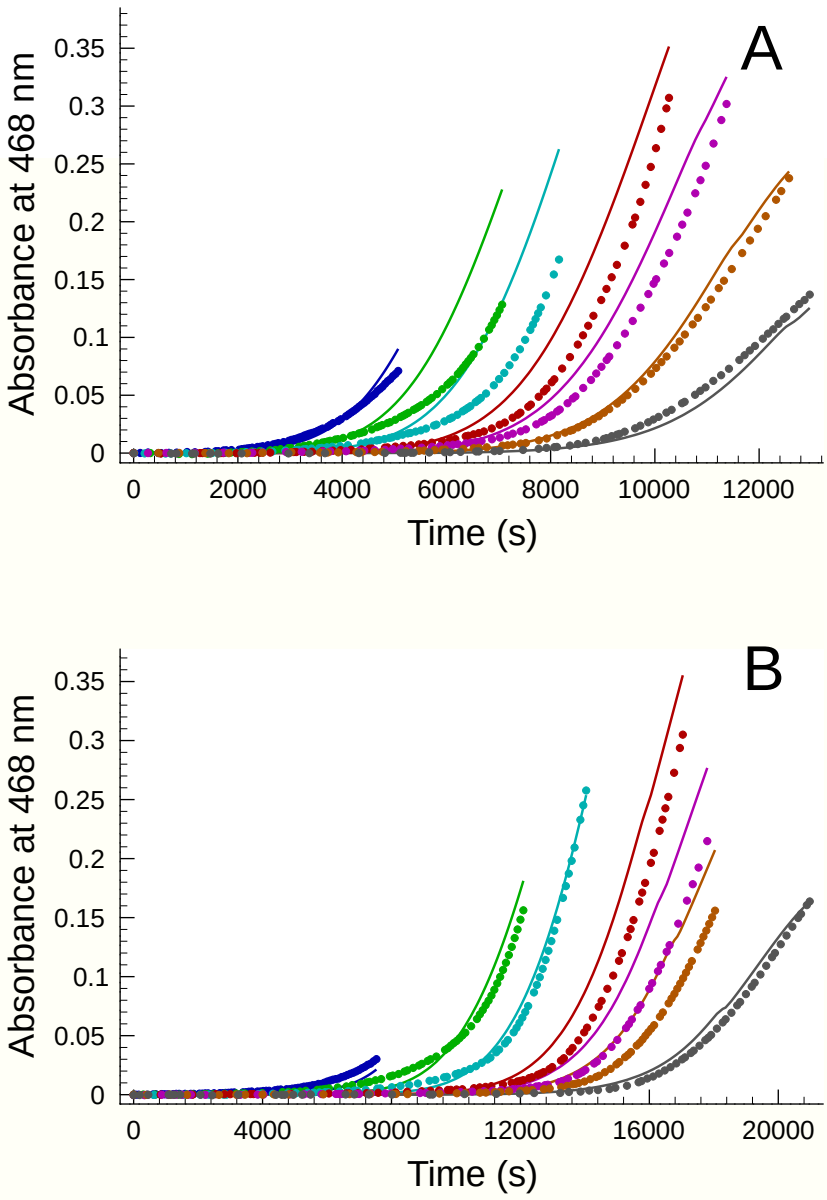

Figure 3.26: Experimental (dots) and fitted (solid lines) absorbance–time curves at 468 nm with respect to changing the concentration of periodate. Conditions are as follows: (A) $[S_5O_6^{2-}]_0$ = 0.8 mM; pH = 1.73; $[IO_4^-]_0$/mM = 7.0 (blue); 5.0 (green); 3.4 (cyan); 2.0 (red); 1.46 (magenta); 1.0 (brown); 0.68 (gray). (B) $[S_5O_6^{2-}]_0$ = 1.0 mM; pH = 1.94; $[IO_4^-]_0$/mM = 8.33 (blue); 6.0 (green); 4.0 (cyan); 2.09 (red); 1.53 (magenta); 1.27 (brown); 0.83 (gray).

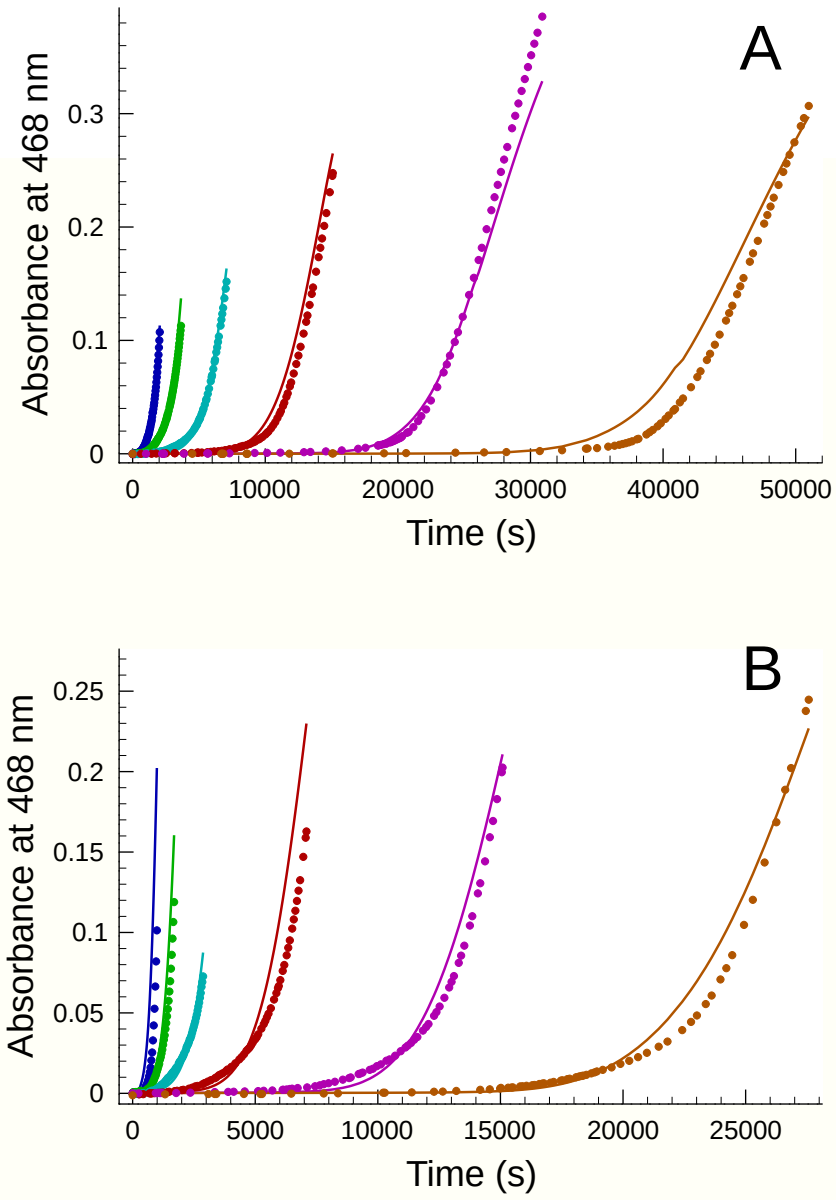

Figure 3.27: Experimental (dots)and fitted (solid lines) absorbance–time curves at 468 nm with respect to changing pH. Conditions are as follows: (A) $[S_5O_6^{2-}]_0$ = 0.5 mM; $[IO_4^-]_0$ = 1.5 mM; pH = 1.1 (blue); 1.31 (green); 1.52 (cyan); 1.73 (red); 1.94 (magenta); 2.15 (brown). (B) $[S_5O_6^{2-}]_0$ = 0.8 mM; $[IO_4^-]_0$ = 5.0 mM; pH = 1.1 (blue); 1.31 (green); 1.52 (cyan); 1.73 (red); 1.94 (magenta); 2.15 (brown).

sequence of reactions. We also found that the periodic acid is more reactiove to break up the sulfur chain, hence the rate of this reaction is proportional to $[HIO_4]$

and the calculated k_{R39} to be 0.0121 ± 0.0022 $M^{-1}s^{-1}$. Both the $[H^+]$- and $[OH^-]$-dependent initial step could be indirectly ruled out based on the simultaneous evaluation of the kinetic curves due to the fact that in these cases significantly higher average deviations could be calculated (6.5% and 7.7%, respectively).

Steps R40–R41 are the well-known oxidation of iodide ion by periodate. It has been well-established that the reaction is governed by two limiting stoichiometries and the rate of formation of iodine is independent of pH.[141] One of the limiting stoichiometry leads exclusively to the formation of iodine (see: the sequence of steps R41, R33 and R25), while the other one produces iodate and iodine (see: the sequence of steps R40 and R25). As seen this feature evidently appears in this present system as well. It is also known that at a strongly acidic condition (below pH = 2) the rate of the iodide–periodate reaction becomes pH-dependent.[142,143] This feature is also reflected in the present model because in step R40 periodate ion and periodic acid are the kinetically active species, respectively (k_{R40} and $k_{R40'}$).

Step R42 is the oxidation of hydrogen sulfite by periodate ion. Unfortunately, no direct research paper has yet been published determining directly the kinetics of this reaction. According to previous study on thiosulfate–periodate,[56] this step is a fast reaction in the time scale of the title reaction. Indeed, it is also found that the value of k_{R42} is $(1.16 \pm 0.15) \times 10^6$ $M^{-1}s^{-1}$ indicating a rapid reaction taking place probably via an oxygen transfer process.

Steps R43 and R44 are further oxidations of the intermediates $S_2O_3OH^-$ and $S_3O_3OH^-$ by periodate ion. Based on the our experiments, both rate coefficients could be determined as indicated in Table 3.5.

Step R45 was also proposed in a previous study of the reaction between thiosulfate and periodate ions. This reaction was found to be a fast second order reaction, therefore we directly adopted its rate coefficient to be $k_{R45} = 1.7 \times 10^6$ $M^{-1}s^{-1}$ from literature.[56]

Step R46 has not been proposed so far. It is well-known that during the reaction of pentathionate and iodine intermediate $S_5O_6I^-$ forms. In an excess of periodate it is also conceivable that periodate can readily oxidize this ion into hydrogen sulfite meanwhile being reduced to iodide ion. We found k_{R46} to be 2410 ± 185 $M^{-1}s^{-1}$.

Step R47 was already proposed in the prevous studies[56,141] and the rate coefficient found here is in a rasonable aggreement with thouse obtained there.

A word is in order here regarding the explanation of the number of parameters

used in the fitting procedure. We have already mentioned that altogether thirteen fitted parameters were used to characterize the experimental curves, which may seem to be an unreasonably large number. Ten of those, however, belong to the reactions that were either directly studied from independent investigations or indirectly proposed as necessary processes to describe the kinetic behavior of a reaction related to the title system. The fixed parameters used here in the fitting procedure were also reported from previous studies. It means that we proposed only 3 new reactions (R39, R44 and R46) and all these reactions are connected to the reactant periodate ion or periodic acid. Among them, of course, step R39 is mandatory because without it no reaction takes place at all, and steps R44 and R46 are reactions of periodate and periodic acid with different intermediates whose reactions are difficult to study individually at all. Removing these two reactions from the model, however, leads to an unacceptably high average deviation with an appearance of systematic errors between the measured and calculated kinetic curves, from which we concluded that these processes play significant roles in determining the formation of iodine. Consequently, we see no option to decrease the number of parameters without preserving the ability of the model to describe quantitatively the experimental curves simultaneously as well as to be in harmony with the models of the related systems.

It should be mentioned that the model presented here is not complete as it is unable to explain the precipitation of sulfur during the course of the reaction. We suggest that

$$S_3O_3OH^- \longrightarrow S_2O_3OH^- + S \tag{3.12}$$

reaction is a conceivable possibility to explain it. Indeed, including this reaction into the model leads to a slightly less average deviation (4.8%). However as we pointed out previously sulfur precipitation prevents the quantitative absorbance determination due to light scattering of the colloid particles, therefore the truncated kinetic curves are non-informative for determining the pathway leading to the formation of sulfur. This led us to conclude that the rate coefficient of eq. 3.12 cannot be determined unambiguously from our experiments.

Finally, we believe that the autocatalytic effect of iodide ion and the clock behavior of the reaction should also be enlightened from this complex model. As can be seen, the initial reaction produces the intermediates $S_2O_3OH^-$, $S_3O_3OH^-$ and iodate ion. Periodate can then further oxidize the former ions (steps R43 and

R44) to produce hypoiodous acid and hydrogen sulfite. These two species react further to give iodide ion via step R34. Once iodide ion is produced, steps R35–R37 and R40–R41 along with steps R25 and R33 lead to the formation of iodine. Iodine is then removed via the pentathionate–iodine reaction to produce iodide ion autocatalytically. As long as the concentration of iodide ion is low, the direct pentathionate–iodate reaction also plays a key role to increase its concentration level. Once the level of iodide ion reaches a certain value pentathionate is not able to eliminate iodine anymore, consequently it rings the bell for the clock behavior. Of course the appearance of iodine is also enhanced by the fact that the pentathionate–iodine reaction is autoinhibitory with respect to iodide ion. From this point, the role of the initial pentathionate–periodate and the pentathionate–iodate reactions is gradually lost, and the periodate–iodide reaction and the Dushman reaction along with the pentathionate–iodine reaction govern mainly the formation and loss of iodine depending on the initial concentration ratio of the reactants. Special kinetic feature of the pentathionate–iodine reaction makes it possible that the clock species iodine and the substrate pentathionate coexist for a relatively long time. It makes a significant difference between the "clock-characteristics" of the title reaction compared to the original Landolt-reaction. This is why we believe that the title reaction is better to be classified as an autocatalysis-driven clock reaction—similarly to the pentathionate–iodate reaction—while the Landolt reaction is a substrate-depletive clock reaction.

We also should have to mention that periodic acid and periodate ion exist in aqueous solution in octahedral (H_5IO_6, $H_4IO_6^-$) and tetrahedral forms (HIO_4, IO_4^-).[153] Based on our experiments, however, it is impossible to differentiate whether the octahedral or the tetrahedral form is more reactive in those reactions where periodate or periodic acid are involved as reactants, because in aqueous solution the concentration ratio of these forms in constant.

$$H_4IO_6^- \overset{K_D}{\rightleftharpoons} IO_4^- + 2H_2O \tag{3.13}$$

This ratio could be shifted experimentally upon an addition of other solvents (for example methanol, ethanole, *etc.*) into pure water, which is out of the scope of this study.

3.4 Oxidation of Pentathionate Ion by Chlorine Dioxide

3.4.1 Stoichiometry

A series of qualitative tests revealed that in excess of chlorine dioxide the only sulfur-containing end product is sulfate. A significant amount of chlorine dioxide is reduced to chloride ion; therefore, the thermodynamically most favorable stoichiometry is

$$S_5O_6^{2-} + 4ClO_2 + 6H_2O = 5SO_4^{2-} + 4Cl^- + 12H^+ \quad (3.14)$$

Table 3.6 contains the stoichiometric ratio (SR) in excess of chlorine dioxide defined as $SR_m = ([ClO_2]_0 - [ClO_2]_\infty)/[S_5O_6^{2-}]_0$.

Table 3.6: Measured (SR_m) and Calculated (SR_c) Defined as $([ClO_2]_0 - [ClO_2]_\infty)/[S_5O_6^{2-}]_0$ in an Excess of Chlorine Dioxide

$[ClO_2]_0$/mM	$[S_5O_6^{2-}]_0$/mM	pH	A_∞ at 430 nm	SR_m	SR_c
1.403	0.22	4.85	0.0136	5.98	6.19
1.428	0.14	4.85	0.063	7.30	7.64
1.410	0.1049	4.85	0.091	7.85	8.10
1.404	0.07944	4.85	0.1124	8.55	8.50
1.345	0.05396	4.85	0.1305	9.32	8.84
1.865	0.3	4.25	0.005	6.11	6.16
1.850	0.3	4.55	0.009	5.97	6.03
1.865	0.3	4.85	0.017	5.85	5.96
1.850	0.3	5.15	0.027	5.59	5.72
1.779	0.3	5.45	0.0281	5.33	5.49
5.888	0.36	4.55	0.513	7.16	6.71
5.496	0.36	4.55	0.457	7.08	6.68
3.876	0.36	4.55	0.2155	6.91	6.54
3.118	0.36	4.55	0.11	6.69	6.47
2.056	0.36	4.55	0.015	5.44	5.61

As can be seen especially at higher chlorine dioxide excess, the stoichiomet-

ric ratio exceeds 4 and reaches almost 10. These measurements clearly hint that chloride is probably not the only chlorine-containing end product. As known from previous studies,[103,112] such a shift in a stoichiometric ratio indicates that a significant amount of chlorate can also be detected among the end products.

Figure 3.28 displays the Raman spectrum purging out the chlorine dioxide excess by N_2 gas. The appearance of characteristics peaks of chlorate at 947, 623 and 484 cm^{-1} clearly supports the fact that chlorate forms in a significant amount

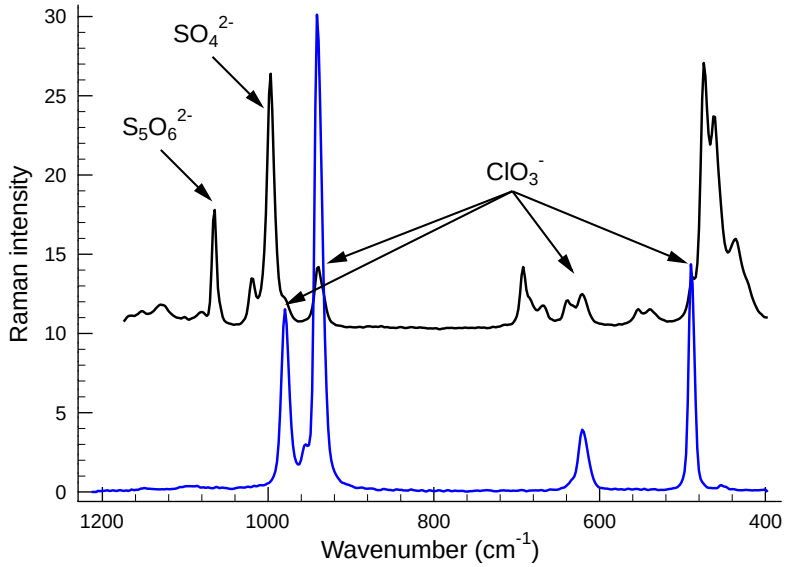

Figure 3.28: Raman spectrum of the end product of the pentathionate–chlorine dioxide reaction compared with spectrum of the sodium chlorate solution. Conditions are as follows: $[S_5O_6^{2-}]_0$ = 6.0 mM and $[ClO_2]_0$ = 12.6 mM.

during the course of reaction. It also means that formally equation

$$6ClO_2 + 3H_2O \;=\; 5ClO_3^- + Cl^- + 6H^+ \tag{3.15}$$

also plays a significant role in determining the stoichiometry of the reaction. At any initial concentration ratio of the reactants an appropriate linear combination of eq. 3.14 and eq. 3.15 properly describes the stoichiometry of the reaction. One may see that the highest SR ratio near 10 can easily be obtained by an algebraic sum of eq. 3.14 and eq. 3.15.

$$S_5O_6^{2-} + 10ClO_2 + 9H_2O \;=\; 5SO_4^{2-} + 5ClO_3^- + 5Cl^- + 18H^+ \tag{3.16}$$

3.4.2 Initial Rate Studies

Figure 3.29 indicates the results of the initial rate studies at a constant initial pentathionate concentration. As can be seen, independently of the pH, the formal kinetic order of chlorine dioxide is markedly higher than unity. Furthermore,

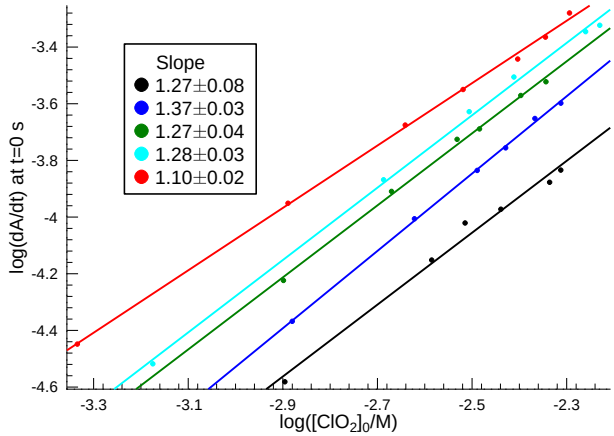

Figure 3.29: Initial rate studies to determine the formal kinetic order of chlorine dioxide at absence of initiallly added chloride ion. Conditions are as follows: $[S_5O_6^{2-}]_0$ = 0.36 mM, pH = 5.45 (black); 5.15 (blue); 4.85 (green); 4.55 (cyan); 4.25 (red).

Figure 3.30 inevitably shows that the formal kinetic order is around 0.5 with respect to hydrogen ion. Although the formal kinetic orders of both chlorine dioxide and hydrogen ion seem to be constant within the concentration range studied, the numbers obtained clearly suggest an appearance of complex kinetics. On the basis of Figure 3.31, this fact can further be supported because the log–log plot of the initial rate–concentration diagram displays a nonlinear relationship, indicating a changing kinetic order of pentathionate. It should be emphasized that this behavior seems to be quite similar to that of the tetrathionate–chlorine.

Figure 3.32 also indicates that initially added chloride ion has a significant catalytic effect on the initial rate of the reaction. Moreover, as can be seen, the formal kinetic order of the chloride ion varies with respect to pH. The lower the pH is, the lower the formal kinetic order of the chloride ion is. This important observation can be explained by the proposed kinetic model later. dioxide reaction.[103]

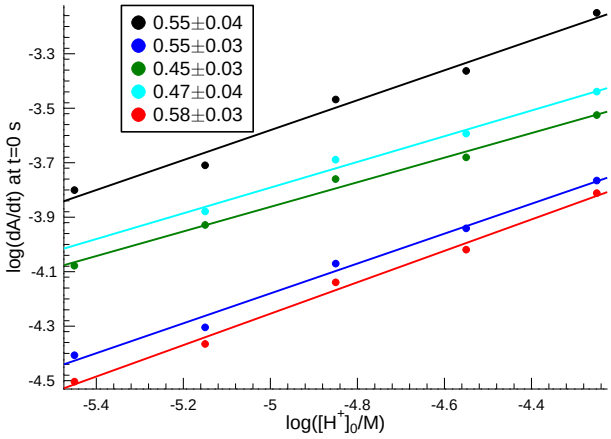

Figure 3.30: Initial rate studies to determine the formal kinetic order of hydrogen ion at absence of initially added chloride ion. Conditions are: $[S_5O_6^{2-}]_0$ = 1.08 mM and $[ClO_2]_0$ = 1.1 mM (black); $[S_5O_6^{2-}]_0$ = 0.3 mM and $[ClO_2]_0$ = 1.86 mM (blue); $[S_5O_6^{2-}]_0$ = 0.3 mM and $[ClO_2]_0$ = 3.23 mM (green); $[S_5O_6^{2-}]_0$ = 0.3 mM and $[ClO_2]_0$ = 3.87 mM (cyan); $[S_5O_6^{2-}]_0$ = 0.36 mM and $[ClO_2]_0$ = 1.42 mM (red).

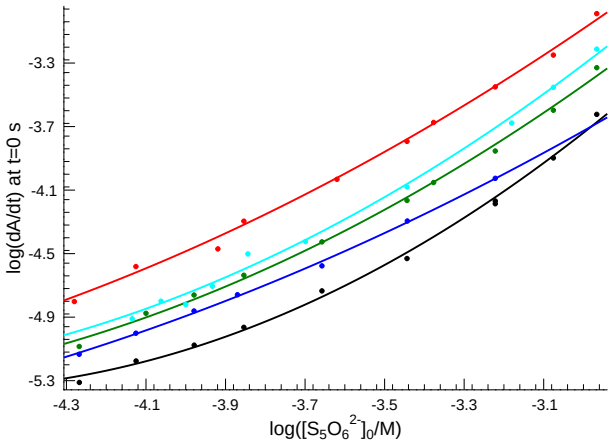

Figure 3.31: Initial rate studies to determine the formal kinetic order of pentathionate ion at absence of initially added chloride ion. The conditions are as follows: $[ClO_2]_0 \approx$ 1.45 mM and pH = 5.45 (black); $ClO_2]_0 \approx$ 1.45 mM and pH = 5.15 (blue); $[ClO_2]_0 \approx$ 1.41 mM and pH = 4.85 (green); $[ClO_2]_0 \approx$ 1.2 mM and pH = 4.55 (cyan); $[ClO_2]_0 \approx$ 1.41 mM and pH = 4.25 (red).

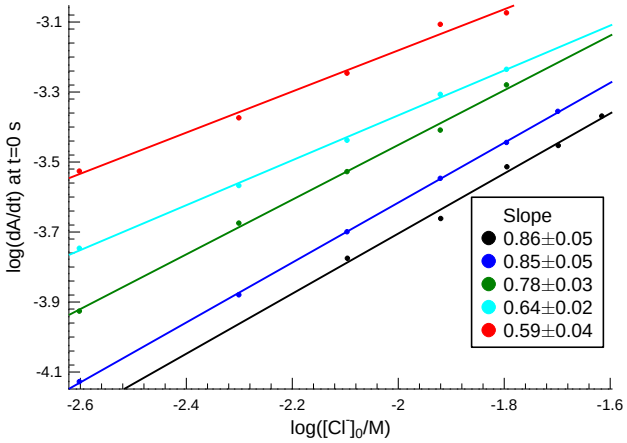

Figure 3.32: Initial rate studies to determine the formal kinetic order of initially added chloride ion. In all these experiments $[S_5O_6^{2-}]_0$ = 0.36 mM was kept constant. Conditions are as follows: $[ClO_2]_0 \approx 1.43$ mM and pH = 5.45 (black); $[ClO_2]_0 \approx 1.41$ mM and pH = 5.15 (blue); $[ClO_2]_0 \approx 1.44$ mM and pH = 4.85 (green); $[ClO_2]_0 \approx 1.4$ mM and pH = 4.55 (cyan); $[ClO_2]_0 \approx 1.42$ mM and pH = 4.25 (red).

3.4.3 Proposed Kinetic Model

To setup the kinetic model, the following species should be taken into account according to the measurements: the reactants (pentathionate and chlorine dioxide), the products (sulfate, chlorate and chloride), and some intermediates like short-lived radicals ($S_5O_6ClO_2^{2-}$, ClO and $S_5O_6^-$) and nonradical species ($S_5O_7^{2-}$, Cl_2O_3, Cl_2O_2, $S_5O_8^{2-}$, $S_5O_9^{2-}$, $S_5O_{10}^{2-}$ and chlorite ion). The chlorine-containing compounds are well-accepted species from the oxidation chemistry of chlorine species. The sulfur-containing radicals are proposed on the basis of the previous studies of polythionate–chlorine dioxide reaction.[103,112] The essence of the method with which we arrived at the best-fitted kinetic model has already been published elsewhere[99] and has been successfully applied in several different cases. As a start, all the conceivable species should be considered to be possibly involved in the kinetic model. Then all mono- and bimolecular reactions of the species are initially added to the model as well as their H^+- and Cl^--catalyzed pathways. Properly setting the initial values of the rate parameters the fitting procedure was started. The reactions considered to be unnecessary (vanishingly low rate parameters were obtained by the fitting procedure) have been removed stepwise. After lengthy and

time-consuming but straightforward elimination of these initial reactions we finally obtained the following kinetic model:

$$S_5O_6^{2-} + ClO_2 \rightleftharpoons S_5O_6ClO_2^{2-} \quad \text{(R48)}$$

$$S_5O_6ClO_2^{2-} \longrightarrow S_5O_6^{-} + ClO_2^{-} \quad \text{(R49)}$$

$$S_5O_6ClO_2^{2-} \longrightarrow S_5O_7^{2-} + ClO \quad \text{(R50)}$$

$$S_5O_6ClO_2^{2-} + ClO_2 \longrightarrow S_5O_7^{2-} + Cl_2O_3 \quad \text{(R51)}$$

$$S_5O_7^{2-} + Cl_2O_3 \longrightarrow S_5O_8^{2-} + Cl_2O_2 \quad \text{(R52)}$$

$$S_5O_6^{-} + ClO_2 + H_2O \longrightarrow S_5O_9^{2-} + Cl^{-} + 2H^{+} \quad \text{(R53)}$$

$$S_5O_9^{2-} + 2ClO_2 + H_2O \longrightarrow S_5O_{10}^{2-} + 2ClO_2^{-} + 2H^{+} \quad \text{(R54)}$$

$$ClO + ClO_2 \longrightarrow Cl_2O_3 \quad \text{(R55)}$$

$$S_5O_8^{2-} + 8ClO_2 + 4H_2O \longrightarrow 5SO_4^{2-} + 4Cl_2O_2 + 8H^{+} \quad \text{(R56)}$$

$$S_5O_{10}^{2-} + 3ClO_2^{-} + 4H_2O \longrightarrow 5SO_4^{2-} + 3Cl^{-} + 8H^{+} \quad \text{(R57)}$$

$$Cl_2O_2 + H_2O \longrightarrow ClO_3^{-} + Cl^{-} + 2H^{+} \quad \text{(R58)}$$

Rate coefficients determined by nonlinear simultaneous parameter estimation are indicated in Table 3.7

The average deviation was found to be 0.0063 absorbance unit by an absolute fitting procedure. Altogether only six fitted parameters were used and the rest of the parameters were either fixed or directly taken from previous reports to fit 6565 points of 132 absorbance–time curves. Figures 3.33–3.36 demonstrate the quality of the fit for representative examples and also support the fact that proposed kinetic model is working properly under the experimental conditions used in this work.

Step R48 is the equilibrium formation of the adduct $S_5O_6ClO_2^{2-}$. This process is a complete analogy of both the tetrathionate–chlorine dioxide[103] and trithionate–chlorine dioxide[112] reactions. As we shall see later, the equilibrium constant $K_{R48} = k_{R48}/k_{-R48}$ can not be determined from these experiments (see Formal Kinetics); therefore, an arbitrarily small value ($K_{R48} = 0.1\ M^{-1}$) was chosen to keep the concentration of $S_5O_6ClO_2^{2-}$ low enough. In other words, only the product of K_{R48} with k_{R49}, k'_{R49}, k''_{R49}, k_{R50} and k'_{R50} can be calculated from the experiments here. This is also reflected in the overall rate equation derived (see later).

Table 3.7: Fitted and Fixed Rate Coefficients of the Proposed Kinetic Model. No error indicates that the parameter is fixed during the calculation process

step	rate equation	parameter value
R48	$k_{R48}[S_5O_6^{2-}][ClO_2]$	1000 $M^{-1}s^{-1}$
	$k_{-R48}[S_5O_6ClO_2^{2-}]$	10^4 s^{-1}
R49	$k_{R49}[S_5O_6ClO_2^{2-}][Cl^-]$	389 ± 6 $M^{-1}s^{-1}$
	$k'_{R49}[S_5O_6ClO_2^{2-}][Cl^-][H^+]$	$(4.53 \pm 0.07) \times 10^7$ $M^{-2}s^{-1}$
	$k''_{R49}[S_5O_6ClO_2^{2-}][S_5O_6^{2-}][H^+]$	$(1.29 \pm 0.02) \times 10^8$ $M^{-2}s^{-1}$
R50	$k_{R50}[S_5O_6ClO_2^{2-}]$	$(2.23 \pm 0.04) \times 10^{-1}$ s^{-1}
	$k'_{R50}[S_5O_6ClO_2^{2-}][H^+]$	$(3.35 \pm 0.02) \times 10^4$ $M^{-1}s^{-1}$
R51	$k_{R51}[S_5O_6ClO_2^{2-}][ClO_2]$	90.3 ± 1.4 $M^{-1}s^{-1}$
R52	$k_{R52}[S_5O_7^{2-}][Cl_2O_3]$	$\geq 10^5$ $M^{-1}s^{-1}$
R53	$k_{R53}[S_5O_6^-][ClO_2]$	$\geq 10^3$ $M^{-1}s^{-1}$
R54	$k_{R54}[S_5O_9^{2-}][ClO_2]$	$\geq 10^3$ $M^{-1}s^{-1}$
R55	$k_{R55}[ClO_2][ClO]$	$\geq 10^6$ $M^{-1}s^{-1}$
R56	$k_{R56}[S_5O_8^{2-}][ClO_2]$	$\geq 10^2$ $M^{-1}s^{-1}$
R57	$k_{R57}[S_5O_{10}^{2-}][ClO_2^-]$	$\geq 10^2$ $M^{-1}s^{-1}$
R58	$k_{R58}[Cl_2O_2]$	≥ 10 s^{-1}

Step R49 is the decomposition of the adduct $S_5O_6ClO_2^{2-}$ producing pentathionate radical and chlorite ion as a result of a formal electron transfer reaction between the reactants. As one can see, this process was found to be catalyzed by chloride ion, hydrogen ion and the reactant pentathionate. Here we provide an indirect evidence which supports that all of these possibilities are necessary to describe all kinetic data obtained at the experimental conditions simultaneously. Stepwise elimination of k_{R49}, k'_{R49} and k''_{R49} leads to the average deviation of 0.0087, 0.0105 and 0.0123 absorbance unit, respectively, with the remaining five parameters. Evidently, in all cases the average deviation increased more than 30% meaning that all these parameters are necessary to describe the kinetic data. Furthermore, the pentathionate-catalyzed decomposition of $S_5O_6ClO_2^{2-}$ can easily be explained by the following sequence of reactions:

$$S_5O_6^{2-} + S_5O_6ClO_2^{2-} \longrightarrow (S_5O_6)_2ClO_2^{4-} \tag{3.17}$$

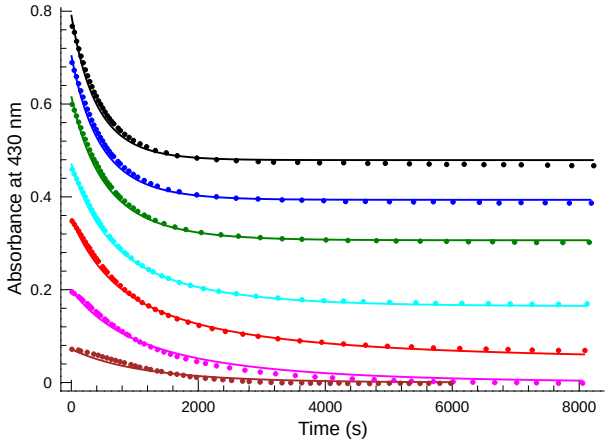

Figure 3.33: Measured (filled circles) and calculated (solid lines) absorbance–time curves in the absence of initially added chloride ion at a constant pentathionate concentration and pH. Conditions are as follows: pH = 4.25, $[S_5O_6^{2-}]_0$ = 0.3 mM, $[ClO_2]_0$/mM = 5.08 (black); 4.25 (blue); 3.95 (green); 3.03 (cyan); 2.28 (red); 1.29 (magenta); 0.46 (brown).

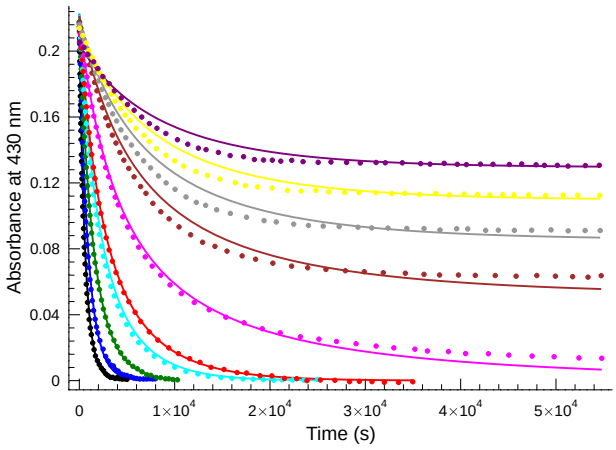

Figure 3.34: Measured (filled circles) and calculated (solid lines) absorbance–time curves in the absence of initially added chloride ion at a constant chlorine dioxide concentration and pH. Experimental conditions are: pH = 4.85, $[ClO_2]_0 \approx 1.42$ mM, $[S_5O_6^{2-}]_0$/mM = 1.08 (black); 0.84 (blue); 0.6 (green); 0.42 (cyan); 0.36 (red); 0.22 (magenta); 0.14 (brown); 0.105 (gray); 0.079 (yellow); 0.054 (purple).

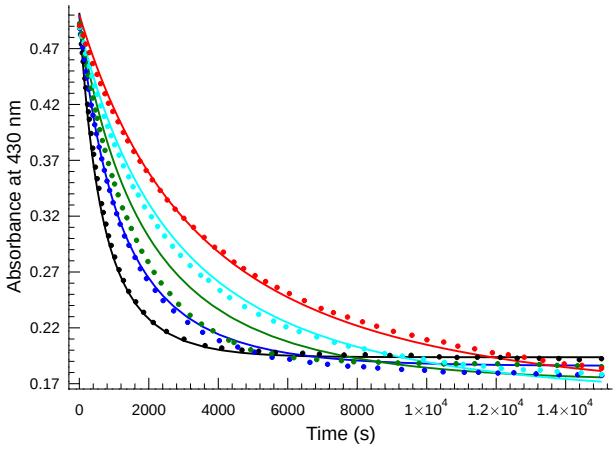

Figure 3.35: Measured (filled circles) and calculated (solid lines) absorbance–time curves in the absence of initially added chloride ion at constant chlorine dioxide and pentathionate concentrations. Conditions are as follows: $[S_5O_6^{2-}]_0$ = 0.36, $[ClO_2]_0 \approx$ 3.23 mM, pH = 4.25 (black); 4.55 (blue); 4.85 (green); 5.15 (cyan); 5.45 (red).

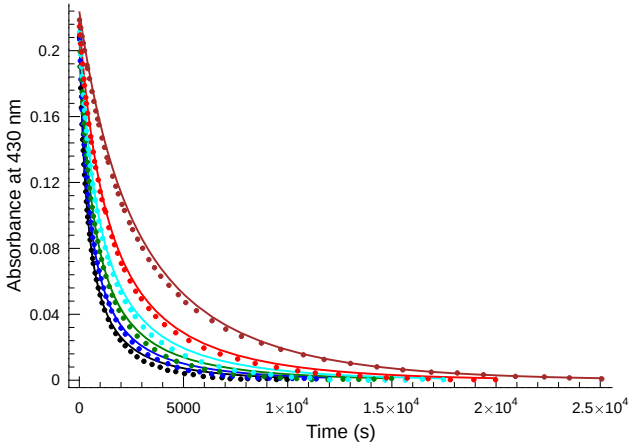

Figure 3.36: Measured (filled circles) and calculated (solid lines) absorbance–time curves in the presence of initially added chloride ion at constant chlorine dioxide and pentathionate concentrations and pH. Conditions are as follows: $[ClO_2]_0 \approx$ 1.44 mM, $[S_5O_6^{2-}]_0$ = 0.36 mM, pH = 4.85, $[Cl^-]$/mM = 16.0 (black), 12.0 (blue), 8.0 (green), 5.0 (cyan), 2.5 (red), 0.0 (brown).

$$(S_5O_6)_2ClO_2^{4-} \longrightarrow S_5O_6^{2-} + S_5O_6^- + ClO_2^- \quad (3.18)$$

This kind of behavior seems to be also general because the same catalytic effect of polythionate was also observed in the case of the tetrathionate–chlorine dioxide reaction.[103]

Step R50 is an alternative route of decomposition of $S_5O_6ClO_2^{2-}$ leading to the formation of short-lived intermediates $S_5O_7^{2-}$ and ClO radical. Eventually, combination of step R48 with step R50 means a formal oxygen transfer between the reactants. Role of steps R49 and R50 can easily be understood because they provide a possibility for shifting the stoichiometry of the reaction from eq. 3.14 and eq. 3.16. As can be seen, besides the normal first-order decomposition, this step is also catalyzed by hydrogen ion. Elimination of k_{R50} or k'_{R50} from the proposed kinetic model is failed. These calculations have revealed that the average deviation increased to 0.0084 and 0.0208 absorbance unit in the case of elimination of k_{R50} and k'_{R50}, respectively. From this it is again concluded that these parameters are also necessary to describe the observed kinetic behavior simultaneously.

Step R51 is the other rate determining reaction between $S_5O_6ClO_2^{2-}$ and chlorine dioxide. Similar reaction was also found to be necessary in the case of the trithionate–chlorine dioxide reaction.[112] This process is responsible for obtaining a higher than unity formal kinetic order with respect to chlorine dioxide. To further confirm the role of this step, it was also eliminated from the proposed model, but a high increase in the average deviation (0.0082 absorbance unit) was obtained, which means that this step must be included in the model.

Rate coefficients of steps R52–R58 cannot be determined from the experiments; only their lower limits can be calculated. These lower limits are indicated in Table 3.7, it should be emphasized that any higher values of these parameters lead to the same final results. As an example, the rate coefficient of step R55, the reaction between ClO and ClO_2^-, is very close to the diffusion-controlled limit.[154] To drive the stoichiometry of the reaction in the proper direction, step R55 should be kept so rapid that the reaction between ClO and ClO_2^- cannot be competitive. This criterion is fulfilled when $k_{R55} \geq 10^6$ $M^{-1}s^{-1}$ stands, as indicated by the calculations; therefore, this value is given in Table 3.7. As a result, it means that steps R52–R58 are only necessary to complete the stoichiometry of the reaction. As can be seen, the sequence of steps R48, R49, R53, R54 and R57 leads to the stoichiometry represented by eq. 3.14 whereas that of steps R48, R50, R51, R52, R55, R56 and R58 leads to the

stoichiometry represented by eq. 3.16. It is also interesting to compare the role of these pathways with the stoichiometric results indicated in Table 3.6. As can be seen, not only the increase of chlorine dioxide excess shifts the stoichiometry of the reaction toward eq. 3.16 but also decrease of pH does. This fact can be explained by the fine balance of steps R49, R50 and R51 at the given experimental conditions. Furthermore, a crucial test about the comparison of calculated SR values from the proposed model with the measured ones has also been performed. Although the measured and calculated SR values slightly differ from each other, their trends with changing pH and chlorine dioxide excess perfectly agree, indicating that the efficiency of the proposed kinetic model was well-justified.

Another important consequence of the short-lived intermediates and their fast reactions has to be emphasized. The reaction in the present case is driven by the short-lived intermediates indicated above. However, they are only feasible possibilities but not the only ones. Any other short-lived intermediates formed in the rate determining steps and their further reactions would lead to the same final result if they are driven so as to fulfill the necessary requirement of the changing stoichiometry mentioned above. Consequently, the proposed kinetic model is only a reasonable but not the only one for the explanation of the experimental data.

Finally, it should be emphasized that hydrogen and chloride ions may both act as autocatalyst because they are products and they also accelerate the rate of reaction. Under the experimental condition presented, however, the characteristic S-shaped type of kinetic curves was not observed. The autocatalytic feature of the hydrogen ion is completely suppressed by application of buffer; therefore, its appearance is not anticipated. However, the autocatalytic effect of chloride ion may be enlarged where the characteristic S-shaped kinetic curves appear, but so far all of our efforts have failed to find such conditions. The reason may be explained by the fact that the effect of chloride ion can only be anticipated at higher pHs, but at these conditions pentathionate is not stable anymore due to its well-known alkaline decomposition.[51,53]

3.4.4 Formal Kinetics

It has been shown that no long-lived intermediates formed in detectable amounts during the course of reaction. Therefore a formal rate equation can be derived

from the proposed mechanism. Applying steady-state approximation for species $S_5O_6ClO_2^{2-}$ leads to the following expression:

$$[S_5O_6ClO_2^{2-}] = k_{R48}[S_5O_6^{2-}][ClO_2] \div \{k_{-R48} + (k_{R49} + k'_{R49}[H^+])[Cl^-] + k''_{R49}[H^+][S_5O_6^{2-}] + k_{R50} + k'_{R50}[H^+] + k_{R51}[ClO_2]\} \quad (3.19)$$

According to the proposed model the consumption of chlorine dioxide can be expressed as

$$-\frac{d[ClO_2]}{dt} = k_{R48}[S_5O_6^{2-}][ClO_2] - k_{-R48}[S_5O_6ClO_2^{2-}] + k_{R51}[S_5O_6ClO_2^{2-}][ClO_2] + k_{R53}[S_5O_6^-][ClO_2] + 2k_{R54}[S_5O_9^{2-}][ClO_2] + k_{R55}[ClO][ClO_2] + 8k_{R56}[S_5O_8^{2-}][ClO_2] \quad (3.20)$$

The steady-state concentrations of short-lived intermediates like $S_5O_6^-$, $S_5O_9^{2-}$, ClO and $S_5O_8^{2-}$ can also be obtained relatively easily. Substituting them into eq. 3.20 followed by some straightforward algebraic manipulations finally leads to the following equation:

$$-\frac{d[ClO_2]}{dt} = k_{R48}[S_5O_6^{2-}][ClO_2] - [S_5O_6ClO_2^{2-}]\{k_{-R48} - 3((k_{R49} + k'_{R49}[H^+])[Cl^-] + k_{R49}[H^+][S_5O_6^{2-}]) - 9(k_{R50} + k'_{R50}[H^+]) - 9k_{R51}[ClO_2]\} \quad (3.21)$$

Substituting eq. 3.19 into eq. 3.21 followed by some simplifications we arrive at the expression of

$$-\frac{d[ClO_2]}{dt} = k_{R48}[S_5O_6^{2-}][ClO_2]\{(4((k_{R49} + k'_{R49}[H^+])[Cl^-] + k''_{R49}[H^+][S_5O_6^{2-}]) + 10((k_{R50} + k'_{R50}[H^+]) + k_{R51}[ClO_2])\} \div \{k_{-R48} + (k_{R49} + k'_{R49}[H^+])[Cl^-] + k''_{R49}[H^+][S_5O_6^{2-}] + (k_{R50} + k'_{R50}[H^+]) + k_{R51}[ClO_2]\} \quad (3.22)$$

Taking into account that $k_{-R48} \gg (k_{R49} + k'_{R49}[H^+])[Cl^-] + k''_{R49}[H^+][S_5O_6^{2-}] + k_{R50} + k'_{R50}[H^+] + k_{R51}[ClO_2]$ inequality is fulfilled under our experimental condition we finally obtain a relatively simple rate equation:

$$-\frac{d[ClO_2]}{dt} = K_{R48}\{[S_5O_6^{2-}][ClO_2](4(k_{R49}[Cl^-] + k'_{R49}[H^+][Cl^-] + k''_{R49}[H^+][S_5O_6^{2-}]) + 10(k_{R50} + k'_{R50}[H^+])) + 10k_{R51}[S_5O_6^{2-}][ClO_2]^2\} \quad (3.23)$$

where $K_{R48} = k_{R48}/k_{-R48}$. Eq. 3.23 clearly shows that the equilibrium constant of K_{R48} cannot be determined from our measurements, only the products of K_{R48} and

the corresponding rate coefficient can be obtained. Moreover the non-unity formal kinetic orders of the reactants as well as that of hydrogen and chloride ions can also be understood. Derivation of the formal rate equation has a series consequence, namely although the reaction is driven via short-lived intermediates like $S_5O_7^{2-}$, $S_5O_8^{2-}$, $S_5O_9^{2-}$ and $S_5O_{10}^{2-}$ this is not the only possibility. Any other sequences of reaction having the same rate determining step but containing other sets of conceivable intermediates that may lead to the same stoichiometries can equally well describe our data, therefore the proposed kinetic model can only be treated as a reasonable feasibility.

Conclusion

The basic work of my Ph. D. dissertation mainly contains the investigation of several redox reactions of pentathionate ion including pentathionate–iodine, pentathionate–iodate, pentathionate–periodate and pentathionate–chlorine dioxide, reaction systems by conventional UV–vis spectroscopy monitoring the absorbance at the visible wavelength range. These researches may provide a better understanding and insight into the nature of the sulfur-chain-breaking reactions of pentathionate that may be helpful as a guide in unraveling more complex oxidation reactions of pentathionate as well as in further investigating the oxidation of thiosulfate. The main results obtained in this work can be summarized as follows.

The pentathionate–iodine reaction has been studied at $T = 25.0 \pm 0.1$ °C and at an ionic strength of 0.5 M in both the absence and presence of an initially added iodide ion at the pH range of 3.95–5.15. It is the first trial to describe the kinetics and mechanism of the pentathionate–iodine reaction. As shown, it is demonstrated that the reaction is independent of pH within the pH range studied and exhibits strong iodide autoinhibition that emerges from the initiating equilibrium between the reactants, resulting in the formation of $S_5O_6I^-$ and iodide ion. As pointed out throughout a comparison of the studies of trithionate–iodine and tetrathionate–iodine as well, this phenomenon seems to be general among the sulfur-chain-breaking reaction of polythionate with a mild oxidizing agent such as iodine. A 9-step kinetic model proposed here can well be used to explain all observations of the measurements.

Based on the investigation of pentathionate–iodine reaction, the pentathionate–iodate and pentathionate–periodate reactions have been studied by monitoring the formation of the total amount of iodine at 468 nm in the presence of phosphoric acid/dihydrogen phosphate buffer. According to the observations, we found that the pentathionate–iodine and pentathionate–iodate reactions can be treated as the

subsystems of pentathionate–periodate reaction. However, the kinetic behaviors of pentathionate–iodate is significantly different with that of pentathionate–periodate reaction. In case of the pentathionate–iodate reaction, the inverse of time necessary to produce a certain amount of iodine is linearly proportional to the initial concentration of iodate ion and the square of the hydrogen ion concentration, while in case of pentathionate–periodate, the formal kinetic order of periodate is significantly lower than unity and that of hydrogen ion is between 1 and 2. It is found that the reciprocal of the time necessary to produce a certain amount of iodine depends complexly with respect to the concentration of pentathionate and pH clearly affects the dependencies both in the pentathionate–iodate and pentathionate–periodate reactions but the effects are opposite: the formal kinetic order of pentathionate increases with decreasing pH in case of the pentathionate–iodate reaction while increases with increasing pH in case of the pentathionate–periodate reaction. These observations and the differences can be well described by the proposed kinetic model. We have also shown that both of the reactions are a clock reaction as the clock species iodine appears after a well-defined reproducible time lag depending on the initial concentration range of the reactants, which resembles on the classical Landolt reaction. There are, however, notably significant differences between these systems: a) the time point when iodine appears in the solution may significantly be different from the time point when substrate pentathionate is consumed in case of pentathionate–iodate and pentathionate–periodate reactions, whereas these time points are the same in case of the Landolt reaction, b) a feature of the appearance and the lack of appearance of the clock species in excess of substrate. In other words, the substrate pentathionate and iodine coexist for a relatively long period of time even in a relative pentathionate excess in cases of both reactions. To take the similarities and also the differences into account, we suggest a distinct category within the generally used term of "clock reactions", where the pentathionate–iodate and pentathionate–periodate reactions may rather belong: the category of autocatalysis-driven clock reactions. Meanwhile the hydrogen-sulfite–iodate reaction is better to be assigned to the category of substrate-depletive clock reactions. It has to be mentioned that experimental evidence shows the sulfur precipitation cannot be avoided at the final stage of both pentathionate–iodate and pentathionate–periodate reactions. It might also be taken into consideration with an addition of eq. 3.12 meaning that both proposed models should be extended to describe the kinetic feature of the

title reaction at longer timescales.

In case of the pentathionate–chlorine dioxide reaction, the measurements were carried at slightly acidic medium by monitoring the absorbance at 430 nm. The result shows that this reaction has several similarities as well as differences with the relevant trithionate–chlorine dioxide and tetrathionate–chlorine dioxide reactions. Raman spectrum of the end products of a reaction solution has clearly shown that pentathionate was oxidized to sulfate, but chlorate is also a marginal product of the reaction besides the chloride ion. Two limiting stoichiometries exist and the initial conditions such as the concentration of the reactants, chloride ion and pH shifts the balance between them. In that sense the polythionate–chlorine dioxide reactions do not differ from each other. Moreover, it is also interesting to note that the otherwise sluggish chloride ion was found to have an accelerating effect on the rate of all the polythionate–chlorine dioxide reactions indicating a general phenomenon. The most pronounced effect can, however, be measured in case of the pentathionate–chlorine dioxide reaction due to the highest formal kinetic order of chloride ion found. On the basis of the initial rate studies, we have noticed significant differences in the formal kinetic order of the reactants. In the trithionate–chlorine dioxide and tetrathionate–chlorine dioxide reactions, the formal kinetic order of at least one reactant is unity, while in case of the pentathionate–chlorine dioxide reaction neither of the formal kinetic order of the reactants as well as that of H^+ was found to be an integer number. It clearly suggests a more complex kinetic behavior with increasing length of the sulfur chain. An 11-step kinetic model was proposed to explain the phenomena observed during the course of experiments and a relatively simple rate equation can be derived from the kinetic model presented. However, it has to be mentioned that the model consisting of the given short-lived intermediates is not the only possibility to describe the measured kinetic curves. Any other sequences of reaction having the same rate determining step but containing other sets of conceivable intermediates that may lead to the same limiting stoichiometries can equally well describe the present kinetic runs, therefore, the proposed kinetic model can only be treated as a reasonable feasibility.

Finally it looks to be worth mentioning some future perspectives of the present works.

- The studies of pentathionate–iodine reaction supports an additional information about the similar phenomena of redox reactions of polythionate (such

as a general pathway of sulfur-chain-breakage of polythionate and iodide inhibition), which may inspire some further theoretical investigations of redox reactions of higher polythionates to obtain deeper insight into the nature of sulfur-chain-breaking reactions of polythionates. Moreover, in the one hand, the pentathionate–chlorine dioxide may be treated as a subsystem of pentathionate–chlorite reaction which is also worth studying as a subsystem of thiosulfate–chlorite reaction. This is similar to trithionate–chlorine dioxide and tetrathionate–chlorine dioxide reactions treating as subsystems of trithionate–chlorite and tetrathionate–chlorite reactions, respectively. In the other hand, understanding the reaction of polythionates with chlorine dioxide and/or chlorite more thoroughly may contribute to better descriptions of nonlinear exotic phenomena of oxidation of thiosulfate with chlorite.

- The pentathionate–iodate and pentathionate–periodate reactions are defined as "autocatalysis-driven clock reactions" and Landolt reaction is suggested to be classified as "substrate-depletive clock reactions". Therefore, we would like to mention the facts that precise clarification of a definition of the term "clock reaction" as well as reclassification of these systems is eagerly expected. Even nowadays, more than 130 years after the original discovery of clock behavior, an induction time is unintentionally used to identify a reaction to be a "clock reaction", a "Landolt-type reaction" and "autocatalytic" in a growing number of publication in leading scientific journals.[144–147] This fact has just recently been noticed by Lente *et. al.* who made a clear distinction between the different types of reactions exhibiting an induction period.[148] As a result their main point is that an appearance of an induction period does not necessarily mean "clock" behavior. Our example clearly shows that some, but not all, autocatalytic reactions may be classified as "autocatalysis-driven clock reactions". Thorough survey of the literature revealed that a couple of different systems exists remarkably resembling on our present systems such as the thiocyanate–iodate,[149] aminoiminomethanesulfinic acid–iodate,[150] 2-aminoethanethiolsulfuric acid–iodate[151] and dimethylaminoiminomethanesulfinic acid–iodate[152] reactions. Realizing the major difference between their clock behaviors compared to that of the original Landolt reaction has, however, remained unnoticed so far. We hope that our suggestion here may pave

the way to clarify the meaning of the generally used term "clock reaction".

- The autocatalysis-driven clock reactions (such as the pentathionate–iodate and pentathionate–periodate reaction) may be used in studying spatiotemporal phenomena. As seen these systems are painfully slow reactions above pH = 3, therefore strongly acidic condition is a necessary requirement for a possible production of spatiotemporal structures. At this condition the key to control the reaction is the concentration level of the autocatalyst iodide ion. It straightforwardly means that the main driving force of the reaction is rather the autocatalytic buildup of iodide ion than that of the increase of H^+ observed in the original Landolt reaction. Since the diffusion constant of iodide ion is significantly lower compared to that of hydrogen ion, it may provide an inherent control for a slower diffusion of the autocatalyst. It may therefore be anticipated that several different spatiotemporal structures might be observed without binding part of autocatalyst reversibly of irreversibly to decrease its mobility.

Bibliography

[1] P. C. Christidis; P. J. Rentyeperis, Experimental charge density in polythionate anions: II. X-ray study of the electron density distribution in potassium tetrathionate, *Z. Kristallogr.,* **1989,** *188,* 31-42.

[2] P. C. Christidis; P. J. Rentyeperis, Experimental charge density in polythionate anions: I. X-ray study of the electron density distribution in potassium trithionate, *Z. Kristallogr.,* **1985,** *173,* 59-74.

[3] G. K. Druschel; R. J. Hamers; J. F. Banfield, Kinetics and mechanism of polythionate oxidation to sulfate at low pH by O_2 and Fe^{3+}, *Geochim. Cosmochim. Acta.,* **2003,** *67,* 4457-4469.

[4] L. A. Chambers; P. A. Trudinger, Microbiological fractionation of stable sulfur isotopes: a review and critique, *Geomicrobiol. J.,* **1979,** *1,* 249-293.

[5] I. Suzuki, Oxidation of inorganic sulfur compounds: chemical and enzymatic reactions, *Can. J. Microbiol.,* **1998,** *45,* 97-105.

[6] B. Takano; Q. Zheng; S. Ohsawa, A telemetering system for monitoring aqueous polythionates in an active crater lake, *J. Volcanol. Geoth. Res.,* **2000,** *97,* 397-406.

[7] A. Schippers; W. Sand, Bacterial leaching of metal sulfides proceeds by two indirect mechanisms via thiosulfate or via polysulfides and sulfur, *Appl. Environ. Microb.,* **1999,** *65,* 319-321.

[8] R. Steudel; G. Holdt; T. Göbel; W. Hazeu, Chromatographic separation of higher polythionates and their dection in cultures of thiobacillus ferrooxidans, *Angew. Chem. Int. Ed. Engl.,* **1987,** *26,* 151-153.

[9] Y. Xu; M. A. A. Schoonen; D. K. Nordstrom; K. M. Cunningham; J. W. Ball, Sulfur geochemistry of hydrothermal waters in Yellowstone National Park, Wyoming, USA. II. formation and decomposition of thiosulfate and polythionate in Cinder Pool, *J. Volcanol. Geoth. Res.,* **2000,** *97,* 407-423.

[10] D. P. Kelly, Thermodynamic aspects of energy conservation by chemolithotrophic sulfur bacteria in relation to the sulfur oxidation pathways, *Arch. Microbiol.,* **1999**, *171,* 219-229.

[11] J. W. O'Reilly; G. W. Dicinoski; M. J. Shaw; P. R. Haddad, Chromatographic and electrophoretic separation of inorganic sulfur and sulfur-oxygen species, *Anal. Chim. Acta,* **2001,** *432,* 165-192.

[12] G. K. Druschel; M. A. A. Schoonen; D. K. Nordstrom; J. W. Ball; Y. Xu; C. A. Cohn, Sulfur geochemistry of hydrothermal waters in Yellowstone National Park, Wyoming, USA. III. An anion-exchange resin technique for sampling and preservation of sulfoxyanions in natural waters, *Geochem. Trans.,* **2003,** *4,* 12-19.

[13] K. J. Umiker; M. J. Morra; I. F. Cheng, Aqueous sulfur species determination using differential pulse polarography, *Microchem. J.,* **2002,** *73,* 287-297.

[14] V. Janickis; R. Maciulevičiusė; R. Ivanauskas; I. Ancutienė, Chemical deposition of copper sulfide films in the surface of polyamide by the use of higher polythionic acids, *Clloid. Polym. Sci.,* **2003,** *281,* 84-89.

[15] R. N. Bhattacharya; H. Wiesner; T. A. Berens; R. J. Matson; J. Keane; K. Ramanathan; A. Swartzlander; A. Mason; R. N. Noufi, 12.3% efficient $CuIn_{1-x}Ga_xSe_2$-based device from electrodeposited precursor, *J. Electrochem. Soc.,* **1997,** *144,* 1376-1379.

[16] B. Takano; H. Saitoh; E. Takano, geochemical implications of subaqueous molten sulfur at Yugama crater lake, Kusatsu-Shirane volcano, Japan, *Geochem. J.,* **1994,** *28,* 199-216.

[17] B. Takano, Correlation of volcanic activity with sulfur oxyanion speciation in a crater lake, *Science,* **1987,** *235,* 1633-1635.

[18] M. B. Golehaber, Experimental study of metastable sulfur oxyanion formation during pyrite oxidation at pH 6-9 and 30°C. *Am. J. Sci.,* **1983,** *283,* 193-217.

[19] H. W. Nesbitt; G. M. Bancroft; A. R. Pratt; M. J. Scaint, Sulfur and iron surface states on fractured pyrite surfaces, *Am. Min.,* **1998,** *83,* 1067-1076.

[20] C. O. Moses; D. K. Nordstrom; J. S. Herman; A. L. Mills, Aqueous pyrite oxidation by dissolved oxygen and by ferric iron, *Geochim. Cosmochim. Acta,* **1987,** *51,* 1561-1571.

[21] A. Schippers; P. Jozsa; W. Sand, Sulfur chemistry in bacterial leaching of pyrite, *Appl. Environ. Microbiol.,* **1996,** *62,* 3424-3431.

[22] B. Hu, Chemical and structural study at the interface between metal sulfides and acids,Ph.D. thesis, University of Wisconsin, **2002.**

[23] A. Schippers; T. Rohwerder; W. Sand, Intermediary sulfur compounds in pyrite oxidation: Implication for bioleaching and biodepyritization of coal, *Appl. Microbiol. Biot.,* **1999,** *52,* 104-110.

[24] B. Elberling; A Schippers; W. Sand, Bacterial and chemical oxidation of pyritic mine tailings at low temperatures, *J. Contam. Hydrol.,* **2000,** *41,* 225-238.

[25] H. A. White, The solubility of gold in thiosulfates and thiocyanates, *J. South. Afr. Inst. Min. Mentall.,* **1905,** *5,* 109-111.

[26] R. M. Berezowsky; L. S. Gormely, Recovery of predious metals from metal sulfides, *US patent4,070,182,* **1978,** *january 24*.

[27] R. M. G. S Berezowsky; V. B. Sefton, Recovery of gold and silver from oxidation leach residues by ammoniacal thiosulfate leaching, *108th AIME Annual, Meeting, New Orlean,* **1979,** *TMS, Warrendale, PA, February 18-22*.

[28] E. Molleman; D. Dreisinger, The treatment of copper-gold ores by ammonium thiosulfate leaching, *Hydrometallurgy,* **2002,** *66,* 1-21.

[29] M. G. Aylmore; D. M. Muir, Thiosulfate leaching of gold–a review, *Miner. Eng.,* **2001,** *14,* 135-174.

[30] H. Zhang, Improved thiosulphate leach process, **2005,** International Patent Publication: WO 2005/017215 A1.

[31] H. Zhang; M. J. Nicol; W. P. Staunton, *Treatment of gold ores;* G. Deschenes, D. Hodouin, L. Lorenzen, Eds.; Canadian Institute of Mining, Metallurgy and Petroleum: Montreal, **2005**, pp 243-257.

[32] I. Chandra; M. I. Jeffrey, A fundamental study of ferric oxalate for dissolving gold in thiosulfate solutions, *Hydrometallurgy,* **2005,** *77,* 191-201.

[33] B. Takano; K. Watanuki, Quenching and liquid chromatographic determination of polythionates in natural water, *Talanta,* **1988,** *35,* 847-854.

[34] R. Steudel; G. Holdt,Ion-pair chromatographic separation of polythionates $S_nO_6^{2-}$ with up to thirteen sulphur atoms, *J. Chromatogr.,* **1986,** *361,* 379-384.

[35] H. Zhang; M. I. Jeffrey, A kinetic study of rearrangement and degradation reactions of tetrathionate and trithionate in near-neutral solutions, *Inorg. Chem.,* **2010,** *49,* 10273-10282.

[36] M. Goehring; W. Helbing; I. Appel, Ueber die sulfoxylsäure. III. Die spontane zersetzung von polythionatlösungen, *Z. Anorg. Chem.,* **1947,** *254,* 185-200.

[37] O. Foss, Displacement equlibria and catalysis on thiosulphate, Xanthates and dithiocarbamates of divalent sulphur, Selenium and Tellurium, *Acta Chem. Scand.,* **1949,** *3,* 1385-1399.

[38] O. Foss, Remarks on the reactivities of the penta- and hexathionate ions, *Acta Chem. Scand.,* **1958,** *12,* 959-966.

[39] A. Fava; S. Bresadola, Kinetics of the catalytic rearrangement of tetrathionate, *J. Am. Chem. Soc.,* **1955,** *77,* 5792-5794.

[40] M. I. Jeffrey; S. D. Brunt, The quantification of thiosulfate and polythionates in gold leach solutions and on anion exchange resins, *Hydrometallurgy,* **2007,** *89,* 52-62.

[41] K. Naito; H. Hayata; M. Mochizuki, The reactions of polythionates: kinetics of the cleavage of trithionate ion in aqueous solutions, *J. Inorg. Nucl. Chem.,* **1975,** *37,* 1453-1457.

[42] E. Rolia; C. L. Chakrabarti, Kinetics of decomposition of tetrathionate, trithionate, and thiosulfate in alkaline media, *Environ. Sci. Technol.,* **1982,** *16,* 852-857.

[43] K. Naito; M. C. Shieh; T. Okabe, Chemical behaviour of low valence sulfur compounds. V. decomposition and oxidation of tetrathionate in aqueous ammonia solution, *Bull. Chem. Soc. Jpn.,* **1970,** *43,* 1372-1376.

[44] A. Kurtenacker; M. Kaufmann, Zur Kenntnis der Polythionate. I. Die zersetzung der polythionate in Wäßriger Lösung, *Z. Anorg. Chem.,* **1925,** *148,* 43–57.

[45] A. Kurtenacker; M. Kaufmann, Zur kenntnis der polythionate IV. Die einwirkung von lauge auf die polythionate, *Z. Anorg. Chem.,* **1925,** *148,* 369-381.

[46] A. Kurtenacker; A. Mutschin; F. Stastny, Über die selbstzersetzung von polythionatlösungen, *Z. Anorg. Chem.,* **1935,** *224,* 399-419.

[47] M. Goehring, Die chemie der polythiosäuren, *Fortschr. Chem. Forsch.,* **1952,** *2,* 444-482.

[48] H. Zhang; D. B. Dreisinger, The kinetics for the decomposition of tetrathionate in alkaline solutions, *Hydrometallurgy,* **2002,** *66,* 59-65.

[49] P. L. Breuer; M. I. Jeffrey, The effect of ionic strength and buffer choice on the decompostion of tetrathionate in alkaline solutions, *Hydrometallurgy,* **2004,** *72,* 335-338.

[50] D. Varga; A. K. Horváth, Kinetics and mechanism of the decomposition of tetrathionate ion in alkaline medium, *Inorg. Chem.,* **2007,** *46,* 7654-7661.

[51] C. Pan; W. Wang; A. K. Horváth; J. Xie; Y. Lu; Z. Wang; C. Ji; Q. Gao, Kinetics and mechanism of alkaline decomposition of the pentathionate ion by the simultaneous tracking of different sulfur species by high-performance liquid chromatography, *Inorg. Chem.,* **2011,** *50,* 9670-9677.

[52] C. Pan; Y. Liu; A. K. Horváth; Z. Wang; Y. Hu; C. Ji; Y. Zhao; Q. Gao, Kinetics and mechanism of the alkaline decomposition of hexathionate ion, *Inorg. Chem.,* **2013,** *117,* 2924-2931.

[53] J. A. Christiansen; W. Drost-Hansen; A. Nielsen, The Kinetics of decomposition of potassium pentathionate in alkaline solution, *Acta Chem. Scand.,* **1952,** *6,* 333-340.

[54] M. Orbán; D. P. Kepper; I. R. Epstein, An iodine–free chlorite–based oscillator: The chlorite-thiosulfate reaction in a continuous flow stirred tank reactor, *J. Phys. Chem.,* **1982,** *86,* 431-433.

[55] D. Varga; I. Nagypál; A. K. Horváth, Complex kinetics of a landolt-type reaction: The later phase of the thiosulfate-iodate reaction, *J. Phys. Chem. A,* **2010,** *114,* 5752-5758.

[56] E. Rauscher; G. Csekő; A. K. Horváth, On the complexity of kinetics and the mechanism of the thiosulfate-periodate reaction, *Inorg. Chem.,* **2011,** *50,* 5793-5802.

[57] W. Zhen; Q. Gao; C. Pan; Y. Zhao; A. K. Horváth, Bisulfite–driven autocatalysis in the bromate–thiosulfate reaction in a slightly acidic medium, *Inorg. Chem.,* **2012,** *51,* 12062-12064.

[58] M. Orbán; I. R. Epstein, Complex periodic and aperiodic oscillation in the chlorite–thiosulfate reaction, *J. Phys. Chem.,* **1982,** *86,* 3907-3910.

[59] J. Maselko; I. R. Epstein, Chemical chaos in the chlorite–thiosulfate reaction, *J. Phys. Chem.,* **1984,** *80,* 3175-3178.

[60] G. R'abai; M. T. Beck; K. Kustin; I. R. Epstein, Sustained and damped pH oscillation in the periodate–thiosulfate reaction in a continuous–flow stirred tank reactor, *J. Phys. Chem.,* **1989,** *93,* 2853-2858.

[61] I. Nagypál; G. Bazsa; I. R. Epstein, Gravity–induced anisotropies in chemical waves, *J. Am. Chem. Soc.,* **1986,** *108,* 3635-3640.

[62] L. Szirovicza; I. Nagypál; I. Bárdi, Propagating reaction front in frozen fhase, *Int. J. Chem. Kinet.,* **1991,** *23,* 99-101.

[63] V. V. Zhivotniko; I. V. Koptyug; R. Z. Sagdeev, Temperature changes visualization during chemical wave propagation, *J. Phys. Chem. A,* **2007,** *111,* 4122-4124.

[64] I. V. Koptyug; V. V. Zhivotniko; R. Z. Sagdeev, Advection of chemical reaction fronts in a porous medium, *J. Phys. Chem. B,* **2008,** *112,* 1170-1176.

[65] Z. Du; Q. Gao; J. Feng; Y. Lu; J. Wang, Dyanmic instabilities and mechanism of the electrochemical oxidation of thiosulfate, *J. Phys. Chem. B,* **2006,** *110,* 26098-26104.

[66] Y. Lu; Q. Gao; L. Xu; Y. Zhao; I. R. Epstein, Oxygen–sulfur species distribution and kinetic analysis in the hydrogen peroxide–thiosulfate system, *Inorg. Chem.,* **2010,** *49,* 6026-6034.

[67] L. Xu; A. K. Horváth; Y. Hu; C. Ji; Y. Zhao; Q. Gao, High performance liquid chromatography study on the kinetics and mechanism of chlorite–thiosulfate reaction in slightly alkaline medium, *J. Phys. Chem. A,* **2011,** *115,* 1853-1860.

[68] D. Varga; A. K. Horváth; I. Nagyál, Unexpected formation of higher polythionates in the oxidation of thiosulfate by hypochlorous acid in a slightly acidic medium, *J. Phys. Chem. B,* **2006,** *110,* 2467-2470.

[69] L. Yuan; Q. Gao; Y. Zhao; X. Tang; I. R. Epstein, Temperature–induced bifurcations in the Cu(II)–catalyzed and catalyst–free hydrogen peroxide–thiosulfate oscillating reaction, *J. Phys. Chem. A,* **2010,** *114,* 7014-7020.

[70] K. Kurin–Csörgei; M. Orbán; G. Rábai; I. R. Epstein, Model for the oscillatory reaction between hydrogen peroxide and thiosulfate catalysed by copper(II) ions, *J. Chem. Soc., Faraday Trans.* **1996,** *92,* 2851-2855.

[71] G. Rábai; I. Hanazaki, Chaotic pH oscillations in the hydrogen peroxide–thiosulfate–sulfite flow System, *J. Phys. Chem. A,* **1999,** *103,* 7268-7273.

[72] I. Nagypál; I. R. Epstein, Fluctuations and stirring rate effects in the chlorite–Thiosulfate Reaction, *J. Phys. Chem.,* **1986,** *90,* 6285-6292.

[73] Á. Tóth; I. Lagzi; D. Horváth, Pattern formation in reaction–diffusion systems: Cellular acidity fronts, *J. Phys. Chem.,* **1996,** *100,* 14838-14839.

[74] F. Gauffre; V. Labrot; J. Boissonade; P. De Kepper; E. Dulos, Reaction–diffusion patterns of the chlorite–tetrathionate system in a conical geometry, *J. Phys. Chem. A,* **2003,** *107,* 4452-4456.

[75] M. Fuentes; M. N. Kuperman; P. D. Kepper, Propagation and interaction of cellular fronts in a closed system, *J. Phys. Chem. A,* **2001,** *105,* 6769-6774.

[76] D. Horváth; Á. Tóth, Diffusion–driven front instabilities in the chlorite–tetrathionate reaction, *J. Chem. Phys.,* **1998,** *22,* 1447-1451.

[77] D. Horváth; S. Tóth; Á. Tóth, Periodic heterogeneity-driven resonance amplification in density fingering, *Phys. Rev. Lett.,* **2006,** *97,* 194501(1-4).

[78] Z. Virányi; D. Horváth; Á. Tóth, Migration-driven instability in the chlorite-tetrathionate reaction, *J. Phys. Chem. A,* **2006,** *110,* 3614-3618.

[79] T. Rica; D. Horváth; Á. Tóth, Viscosity-change-induced density fingering in polyelectrolytes, *J. Phys. Chem. B,* **2008,** *112,* 14593-14596.

[80] D. A. Vasquez; A. D. Wit, Dispersion relations for the convective instability of an acidity front in Hele-Shaw cells, *J. Chem. Phys.,* **2004,** *121,* 935-941.

[81] D. Lima; A. D'Onofrio; A. D. Wit, Nonlinear fingering dynamics of reaction–diffusion acidity fronts: self–similar scaling and Influence of differential diffusion, *J. Chem. Phys.,* **2006,** *124,* 014509(1-10).

[82] T. Bánsági Jr.; D. Horváth; Á. Tóth, Multicomponent convection in the chlorite–tetrathionate reaction, *Chem. Phys. Lett.,* **2004,** *384,* 153-156.

[83] E. Jakab; D. Horváth; Á. Tóth, Temperature-controlled cellular fronts, *Phys. Chem. Chem. Phys.,* **2002,** *4,* 1307-1309.

[84] D. Horváth; T. Bánsági Jr.; Á. Tóth, Orientation dependent density fingering in an acidity front, *J. Chem. Phys.,* **2002,** *117,* 4399-4402.

[85] Z. Virányi; A. Szommer; Á. Tóth; D. Horváth, Lateral instability controlled by constant electric field in an acid-catalyzed reaction, *Phys. Chem. Chem. Phys.,* **2004,** *6,* 3396-3401.

[86] Z. Virányi; A. Szommer; Á. Tóth; D. Horváth, Lateral instability induced by an inhomogeneous electric field, *Chem. Phys. Lett.,* **2005,** *401,* 575-578.

[87] T. Rica; D. Horváth; Á. Tóth, Density fingering in acidity fronts: effect of viscosity, *Chem. Phys. Lett.,* **2005,** *408,* 422-425.

[88] T. Tóth; D. Horváth; Á. Tóth, Thermal effects in the density fingering of th chlorite–tetrathionate reaction, *Chem. Phys. Lett.,* **2007,** *442,* 289-292.

[89] T. Tóth; D. Horváth; Á. Tóth, Density fingering in spatially modulated Hele–Shaw cells, *J. Chem. Phys.,* **2007,** *127,* 234506.

[90] T. Tóth; D. Horváth; Á. Tóth, Scaling law of stable single cells in density fingering of chemical fronts, *J. Chem. Phys.,* **2008,** *128,* 144509.

[91] T. Tóth; D. Horváth; Á. Tóth, Convective instabilites in horizontally propagating vertical chemical fronts, *Phys. Rev. E,* **2009,** *79,* 016216.

[92] Á. Tóth; B. Veisz; D. Horváth, Diffusion–driven front instability in a three–dimensional medium, *J. Phys. Chem. A,* **1998,** *102,* 5157-5159.

[93] I. Szalai; F. Gauffre; V. Labrot; J. Boissonade; P. De Kepper, Spatial bistability in a pH autocatalytic system: from long to short range activation, *J. Phys. Chem. A,* **2005,** *109,* 7843-7849.

[94] D. E. Strier; J. Boissonade, Spatial bistability and excitability in the chlorite–tetrathionate reaction in cylindrical and conical geometries, *Phys. Rev. E,* **2004,** *70,* 016210(1-7).

[95] J. Boissonade; E. Dulos; F. Gauffre; M. N. Kuperman; P. D. Kepper, Spatial bistability and waves in a reaction with acid autocatalysis, *Faraday Discuss,* **2001,** *120,* 353-361.

[96] M. Fuentes; M. N. Kuperman; J. Boissonade; E. Dulos; F. Gauffre; P. D. Kepper, Dynamics effects induced by long range activation in a nonequilibrium reaction–diffusion system, *Phys. Rev. E,* **2002,** *66,* 056205.

[97] A. K. Horváth; I. Nagypál; G. Peintler; I. R. Epstein, Autocatalysis and self–inhibition: coupled kinetic phenomena in the chlorite–tetrathionate reaction, *J. Am. Chem. Soc.,* **2004**, *126,* 6246-6247.

[98] A. K. Horváth, A three–variable model for the explanation of the ''supercatalytic' effect of hydrogen ion in the chlorite–tetrathionate reaction, *J. Phys. Chem. A,* **2005**, *109,* 5124-5128.

[99] A. K. Horváth; I. Nagypál; I. R. Epstein, Three autocatalysts and self–inhibition in a single reaction: a detailed mechanism of the chlorite–tetrathionate reaction, *Inorg. Chem.*, **2006**, *45*, 9877-9833.

[100] G. Peintler; G. Csekő; A. Petz; A. K. Horvath, An Improved Chemical Model for the Quantitative Description of the Front Propagation in the Tetrathionate–Chlorite Reaction, *Phys. Chem. Chem. Phys.*, **2010**, *12*, 2356-2364.

[101] A. K. Horváth; I. Nagypál, Kinetics and mechanism of the reaction between hypochlorous acid and tetrathionate ion, *Int. J. Chem. Kinet.*, **2000**, *32*, 395-402.

[102] D. Varga; A. K. Horváth, Revisiting the kinetics and mechanism of the tetrathionate–hypochlorous acid reaction in nearly neutral medium, *J. Phy. Chem. A*, **2009**, *113*, 13907-13912.

[103] A. K. Horváth; I. Nagypál; I. R. Epstein, Kinetics and mechanism of the chlorine dioxide–tetrathionate reaction, *J. Phys. Chem. A*, **2003**, *107*, 10063-10068.

[104] A. Awtrey; R. E. Connick, Rate law and mechanism of the reaction of iodine with tetrathionate ion, *J. Am. Chem. Soc.*, **1951**, *73*, 4546-4549.

[105] A. Kerek; A. K. Horváth, Kinetics and mechanism of the oxidation of tetrathionate by iodine in a slightly acidic medium, *J. Phys. Chem. A*, **2007**, *111*, 4235-4241.

[106] D. Varga; A. K. Horváth, Simultaneous evaluation of different types of kinetic traces of a complex system: kinetics and mechanism of the tetrathionate–bromine reaction, *J. Phys. Chem. A*, **2009**, *113*, 9988-9996.

[107] T. Koh; M. Yajima, Spectrophotometric determination of tetrathionate by its oxidation with iodate, *Bull. Chem. Soc. Jpn.*, **1991**, *64*, 1854-1858.

[108] Á. Filáry; A. K. Horváth, Photochemically induced catalysis of iodide ion and iodine in the tetrathionate–periodate reaction, *Phys. Chem. Chem. Phys.*, **2010**, *12*, 6742-6749.

[109] J. F. Read; S. A. Bewick; S. C. Donaher; M. D. Watson, The kinetics and mechanism of the oxidation of inorganic oxysulfur compounds by potassium

ferrate. Part III–trithionate and pentathionate ions, *Inorg. React. Mech.,* **2005**, *5,* 281-304.

[110] J. F. Read; S. A. Bewick, The kinetics and mechanism of the oxidation of inorganic oxysulfur compounds by potassium ferrate. Part IV–A theoretical analysis of four models proposed to explain some of the unusual results for trithionate, tetrathionate and pentathionate ions, *Inorg. React. Mech.,* **2005**, *5,* 305-330.

[111] G. Csekő; A. K. Horváth, Non–triiodide based autoinhibition by iodide ion in the trithionate–iodine reaction, *J. Phys. Chem. A,* **2010**, *114,* 6521-6526.

[112] G. Csekő; A. K. Horváth, Kinetics and mechanism of the chlorine dioxide–trithionate reaction, *J. Phys. Chem. A,* **2012**, *116,* 2911-2919.

[113] G. Csekő; E. Rauscher; A. K. Horváth, Kinetics and mechanism of the hypochlorous acid–trithionate reaction, *J. Phys. Chem. A,* **2013**, *117,* 8836-8842.

[114] G. Csekő; L. Ren; Y. Liu; Q. Gao; A. K. Horváth, A new system for studying spatial front instabilities: the supercatalytic chlorite–trithionate reaction, *J. Phys. Chem. A,* **2014**, *118,* 815-821.

[115] D. P. Kelly; A. P. Wood, Synthesis and determination of thiosulfate and polythionates, *Methods Enzymol.,* **1994,** *243,* 475-501.

[116] *IUPAC Stability Constant Database;* Royal Society of Chemistry: London, **1992-1997**.

[117] G. Peintler, *ZiTa, version 2.1–5.0; A comprhensive program package for fitting parameters of chemical reaction mechanism;* Attila József University: Szeged, Hungary, **1989-2001**, www.staff.u-szeged.hu/ peintler/download/chemmech/zitainst.

[118] C. Adamo; V. Barone, Toward reliable density functional methods without adjustable parameters: the PBEO model , *J. Chem. Phys.,* **1999,** *110,* 6158-6170.

[119] J. P. Perdew; K. Burke; M. Ernzerhof, Generalized gradient approximation made simple, *Phys. Rev. Lett.,* **1996,** *77,* 3865-3868.

[120] D. Rappoport; F. Furche, Property-optimized Gaussian basis sets for molecular response calculations, *J. Chem. Phys.*, **2010,** *133,* 134105-134115.

[121] N. N. Greenwood; A. Earnshaw, *Chemistry of the Elements,* 2nd ed.; Butterworth–Heinemann: New York, **1997**.

[122] J. Tomasi; M. Persico, Molecular interactions in solution: an overview of methods based on continuous distributions of the solvent, *Chem. Rev.,* **1994,** *94,* 2027-2094.

[123] A. A. Granovsky, *Firefly,* version 7.1.G, http://classic.chem.msu.su/gran/firefly/index.html.

[124] D. H. Turner; G. W. Flynn; N. Sutin; J. V. Beitz, Laser raman temperature-jump study of the kinetics of the triiodide equilibrium. Relaxation times in the 10^{-8}–10^{-7} second stage, *J. Am. Chem. Soc.,* **1972,** *94,* 1554-1559.

[125] M. Ruasse; J. Aubard; B. Galland; A. Adenier, Kinetic study of the fast halogen-trihalide ion equilibria in protic media by the Raman-laser temperature-jump technique. A non-diffusion-controlled ion-molecule reaction, *J. Phys. Chem.,* **1986,** *90,* 4382-4388.

[126] M. Eigen; K. Kustin, The kinetics of halogen hydrolysis, *J. Am. Chem. Soc.,* **1962,** *84,* 1355-1361.

[127] I. Lengyel; I. R. Epstein; K. Kustin, Kinetics of iodine hydrolysis, *Inorg. Chem.,* **1993,** *32,* 5880-5882.

[128] I. Lengyel; K. Kustin; I. R. Epstein, Rate constants for reactions between iodine- and chlorine-containing species: a detailed mechanism of the chlorine dioxide/chlorite–iodide reaction, *J. Am. Chem. Soc.,* **1996,** *118,* 3708-3719.

[129] B. S. Yiin; D. W. Margerum, Nonmetal redox kinetics: reactions of iodine and triiodide with sulfite and hydrogen sulfite and the hydrolysis of iodosulfate, *Inorg. Chem.,* **1990,** *29,* 1559-1564.

[130] D. M. Stanbury; J. N. Figlar, Vanishingly slow kinetics of the ClO_2/Cl^- reaction: its questionable significance in nonlinear chlorite reactions, *Coord. Chem. Rev.,* **1999,** *187,* 223-232.

[131] A. K. Horváth; I. Nagypál; G. Peintler; I. R. Epstein; K. Kustin, Kinetics and mechanism of the decomposition of chlorous Acid, *J. Phys. Chem. A,* **2003,** *107,* 6966-6973.

[132] S. Dushman, The rate of the reaction between iodic and hydriodic acids, *J. Phys. Chem.*, **1903,** *8,* 453-482.

[133] G. Schmitz, Kinetics and mechanism of the iodate–iodide reaction and other related reaction, *Phys. Chem. Chem. Phys.*, **1999,** *1,* 1909-1914.

[134] A. F. M. Barton; G. A. Wright, Kinetics of the iodate–iodide reaction: catalysis by carboxylate and phosphate ions, *J. Chem. Soc. A,* **1968,** 2096-2103.

[135] G. Csekő; D. Varga; A. K. Horváth; I. Nagypál , Simultaneous investigation of the Landolt and Dushman reactions, *J. Phys. Chem.,* **2008,** *112,* 5954-5959.

[136] A. K. Horváth; I. Nagypál; G. Csekő, Theoretical investigation on the concentration dependence of the Landolt time, *J. Phys. Chem.,* **2008,** *112,* 7868-7872.

[137] D. A. Palmer; R. van Eldik, Spectral characterization and kinetics of formation of hypoiodous acid in aqueous solution, *Inorg. Chem.,* **1986,** *25,* 928-931.

[138] A. K. Horváth, Revised explanation of the pH oscillations in the iodate–thiosulfate–sulfite system, *J. Phys. Chem. A,* **2008,** *112,* 3935-3942.

[139] W. C. Bray, An oxide of iodine, I_2O_2. An intermediate compound, *J. Am. Chem. Soc.*, **1930,** *52,* 3580-3586.

[140] J. A. B. Agreda; R. J. Field; N. J. Lyons, Kinetic evidence for accumulation of stoichiometrically significant amounts of $H_2I_2O_3$ during the reaction of I^- with IO_3^-, *J. Phys. Chem. A,* **2000,** *104,* 5269-5274.

[141] A. K. Horváth, Pitfall of an initial rate study: on the kinetics and mechanism of the reaction of periodate with iodide ions in a slightly acidic medium, *J. Phys. Chem. A,* **2007,** *111,* 890-896.

[142] E. Abel; R. Siebenschein, Ermittlung zeitlich unzuganlicher reaktionskinetik durch reaktionsverteilung, *Z. Phys. Chem.*, **1927,** *130,* 631-657.

[143] A. Indeli; F. Ferranti; F. Secco, A kinetic study of the reaction of periodate with iodide ions, *J. Phys. Chem.,* **1966,** *70,* 631-636.

[144] R. N. Bose; N. Rajasekar; D. M. Thomson; E. S. Gould, Electron transfer. 78. Reduction of carboxylato-bound chromium(V) with bisulfite. A "clock reaction" involving chromium(IV), *Inorg. Chem.,* **1986,** *25,* 3349-3353.

[145] J. H. Merkin; A. J. Poole; S. K. Scott; J. D. B. Smith; B. W. Thomson, Analysis of the bromate–ferroin clock reaction, *J. Math. Chem.,* **1996,** *19,* 15-32.

[146] S. J. Preece; J. Billingham; A. C. King, Chemical clock reactions: the effect of precursor consumption, *J. Math. Chem.,* **1999,** *26,* 47-73.

[147] A. P. Oliveira; R. B. Faria, The chlorate–iodine clock reaction, *J. Am. Chem. Soc.,* **2005,** *127,* 18022-18023.

[148] G. Lente; G. Bazsa; I. Fábián, What is and what isn't a clock reaction?, *New J. Chem.,* **2007,** *31,* 1707-1707.

[149] R. H. Simoyi; M. Manyonda; J. Masere; M. Mtambo; I. Ncube; H. Patel; I. R. Epstein; K. Kustin, Kinetics and mechanism of the oxidation of thiocyanate by iodate, *J. Phys. Chem.,* **1991,** *95,* 770-774.

[150] E. Mambo; R. H. Simoyi, Kinetics and mechanism of the complex oxidation of aminoiminomethanesulfinic acid by iodate in acidic medium, *J. Phys. Chem.,* **1993,** *97,* 13662-13667.

[151] C. Mundoma; R. H. Simoyi, Oxyhalogen–sulfur chemistry. Oxidation of 2-aminoethanethiolsulfuric acid by iodate in acidic medium, *J. Chem. Soc. Faraday Trans.,* **1997,** *93,* 1543-1550.

[152] A. Otoikhian; R. H. Simoyi, Oxidation of a dimethylthiourea metabolite by iodine and acidified iodate: N,N′-dimethylaminoiminomethanesulfinic Acid(1), *Chem. Res. Toxicol.,* **2005,** *18,* 1167-1177.

[153] C. E. Crouthamel; A. M. Hayes; D. S. Martin, Ionization and hydration equilibria of periodic acid, *J. Am. Chem. Soc.,* **1951,** *73,* 82-87.

[154] Z. B. Alfassi; R. E. Huie; S. Mosseri; P. Neta, Kinetics of one-electron oxidation by the ClO radical, *Radiat. Phys. Chem.,* **1988,** *32,* 85-88.

Publications, Presentation

I. Publications forming the basic of Ph.D. dissertation:

1. **L. Xu,** Gy. Csekő, T. Kégl, A. K. Horváth: General Pathway of Sulfur-Chain Breakage of Polythionates by Iodine Confirmed by the Kinetics and Mechanism of the Pentathionate–Iodine Reaction. *Inorg. Chem.,* **2012,** *51,* 7837-7843. **IF: 4.593**

2. **L. Xu,** Gy. Csekő, A. Petz, A. K. Horváth: Kinetics and Mechanism of the Oxidation of Pentathionate Ion by Chlorine Dioxide in a Slightly Acidic Medium. *J. Phys. Chem. A,* **2014,** *118,* 1293-1299. **IF: 2.775**

3. **L. Xu,** A. K. Horváth: A Possible Candidate To Be Classified as an Autocatalysis-Driven Clock Reaction: Kinetics of the Pentathionate–Iodate Reaction. *J. Phys. Chem. A,* **2014,** *118,* 6171-6180. **IF: 2.775**

4. **L. Xu,** A. K. Horváth: An Autocatalysis-Driven Clock Reaction II: Kinetics of the Pentathionate–Periodate Reaction. *J. Phys. Chem. A,* **2014,** *118,* accepted for publication, DOI: 10.1021/jp507925e. **IF: 2.775**

II. Other publications:

1. X. F. Hu, J. X. Xie, **L. Xu,** H. M. Liu, X. L. Lv, Q. Y. Gao: Deposition Dynamics of Sulfur in the Electrochemical Oxidation of Sulfide on Pt Electrode. *Sciencepaper Online,* **2009,** *4,* 453-458. **IF: 0.000**

2. **L. Xu,** J. H. Zheng, Y. Hu, Y. C. Lu, Q. Y. Gao: Separation and Analysis of Chlorite and Sulfur Oxyanions in Mixture Using High Performance Liquid Chromatography. *Chinese J. Anal. Chem.,* **2010,** *4,* 537-541. **IF: 0.790**

3. Y. C. Lu, Q. Y. Gao, **L. Xu,** Y. M. Zhao, I. R. Epstein: Oxygen-Sulfur Species Distribution and Kinetic Analysis in the Hydrogen Peroxide–Thiosulfate System. *Inorg. Chem.,* **2010,** *49,* 6026-6034. **IF: 4.325**

4. **L. Xu,** A. K. Horváth, Y. Hu, C. Ji, Y. M. Zhao, Q. Y. Gao: High Performance Liquid Chromatography Study on the Kinetics and Mechanism of Chlorite–Thiosulfate Reaction in Slightly Alkaline Medium. *J. Phys. Chem. A,* **2011,** *115,* 1853-1860. **IF: 2.946**

5. Y. Hu, J. M. Feng, Y. W. Li, Y. Y. Sun, **L. Xu,** Y. M. Zhao, Q. Y. Gao: Kinetic Study on Hydrolysis and Oxidation of Formamidine Disulfide in Acidic Solutions. *Sci. Chin. Chem.,* **2012,** *55,* 235-241. **IF: 1.330**

6. Csekő Gy., **Xu L.,** Horváth A. K.:A kénlánc oxidációjának kinetikája a politionát–jód reakciókban. *Magyar Kémiai Folyóirat,* **2013,** *119,* 88-92. **IF: 0.000**

III. Presentation:

1. **L. Xu,** Gy. Csekő, A. K. Horváth: Kinetics and mechanism of the pentathionate–iodine reaction. CECE 2013 10^{th} International Interdisciplinary Meeting on Bioanalysis, Pécs, 2013. April 25-27.

Acknowledgement

In academic, first and foremost, I would like to gratefully and sincerely thank Dr. Attila Horváth, my supervisor, for his guidance, support and encouragement during the doctoral studies. He taught me not only to be an experimentalist, but also to be an independent thinker. On the duration of the doctoral learning, he gave me every opportunity to develop my own individuality for my research and studies including the development of the experimental techniques, ability to think independently and experience in the theoretical chemical kinetic fitting and he always helped me to tide over the tough time. For everything you have done for me, I thank you by my heart.

My special thank goes as well to professor László Kollár, head of the Department of Inorganic Chemistry and professor Ferenc Kilár, the leader of the Doctoral School of Chemistry. They always supported me as a Ph.D. student.

I would also like to give my thank to my colleague, Csekő György, for his valuable advice during experimental measurements, and for his help on preparation of chemicals and for all his help enthusiasm during my doctoral journey. Also I am thankful for his careful review of my thesis and valuable comments of my dissertation.

I wish to express my sincere thanks to Dr. Andrea Petz for her friendly help and supporting in her field of Raman spectroscopy. I am thankful for her great help in my research of Raman measurements.

I am also thankful for the financial support from the China Scholarship Council.

Finally, I would like to thank all members in the Department of Inorganic Chemisty, who have helped me directly or indirectly during my doctoral program.